

A plume tectonics model for the Tharsis province, Mars

Daniel Mège and Philippe Masson

Laboratoire de Géologie Dynamique de la Terre et des Planètes (URA CNRS D1369), Université Paris-Sud, bâtiment 509, 91405 Orsay Cedex, France

Received for publication 30 July 1996

Abstract. Morphological and structural data from the whole Tharsis province suggest that a number of shallow grabens radially oriented about the Tharsis bulge on Mars are underlain by dykes, which define giant radiating swarms similar to, e.g. the Mackenzie dyke swarm of the Canadian shield. Mechanisms for graben formation are proposed, and the depth, width, and height of the associated dykes are estimated. Structural mapping leads to define successive stages of dyke emplacement, and provide stress-trajectory maps that indicate a steady source of the regional stress during the whole history of the Tharsis province. A new tectonic model of Tharsis is presented, based on an analogy with dyke swarms on the Earth that form inside hot spots. This model successfully matches the following features: (1) the geometry of the South Tharsis Ridge Belt, which may have been a consequence of the compressional stress field at the boundary between the uplifted and non-uplifted areas in the upper part of the lithosphere at the onset of hot spot activity; (2) extensive lava flooding, interpreted as a consequence of the high thermal anomaly at the onset of plume (hot spot) activity; (3) wrinkle ridge geometry in the Tharsis hemisphere, the formation of which is interpreted as a consequence of buoyant subsidence of the brittle crust in response to the lava load; (4) Valles Marineris limited stretching by preliminary passive rifting, and uplift, viewed as a necessary consequence of adiabatic mantle decompression induced by stretching. The geometrical analysis of dyke swarms suggests the existence of a large, Tharsis-independent extensional state of stress during all the period of tectonic activity, in which the minimum compressive stress is roughly N-S oriented. Although magmatism must have loaded the lithosphere significantly after the plume activity ceased and be responsible for additional surface deformations, there is no requirement for further loading stress to explain

surficial features. Comparison with succession of magmatic and tectonic events related to hot spots on the Earth suggests that the total time required to produce all the surface deformation observed in the Tharsis province over the last 3.8 Ga does probably not exceed 10 or 15 Ma. Copyright © 1996 Elsevier Science Ltd

1. Introduction

The stresses in the Martian crust in the Tharsis province (Fig. 1) have been much investigated during the past 15 years (see reviews in Banerdt *et al.*, 1992; Mège and Masson, 1996a). Topography and gravity data were used as a basis for elastic stress models, which indicate that loading forces are capable of predicting numerous tectonic structures associated with Tharsis (Banerdt *et al.*, 1982, 1992; Sleep and Phillips, 1985; Tanaka *et al.*, 1991). The agreement between the models and observations is however still imperfect (Banerdt *et al.*, 1982; Schultz, 1985; Watters, 1993; Mège and Masson, 1996a), maybe because modelling has not taken a number of rock mechanics laws into account (Golombek, 1985; Schultz and Zuber, 1992, 1994; McGovern and Solomon, 1993).

Among the most used structural constraints on theoretical modelling of lithosphere support and related state of stress are series of grabens radial about Tharsis (Carr, 1974; Frey, 1979a; Wise *et al.*, 1979; Plescia and Saunders, 1982; Scott and Dohm, 1990a,b; Tanaka and Dohm, 1993). Tanaka *et al.* (1991) noted that the regularity of graben widths is a powerful argument in favour of the interpretation of dykes underneath the grabens. However, when dykes are lacking, displacement on a single normal fault generates an area of provisionally compressional stress in the surroundings of the lower part of faults (e.g. Price and Cosgrove, 1990, pp. 186–189). The state of stress in the surroundings of the fault favours the initiation of a conjugate fault at a constant distance from the first one (Melosh and Williams, 1989). More sig-

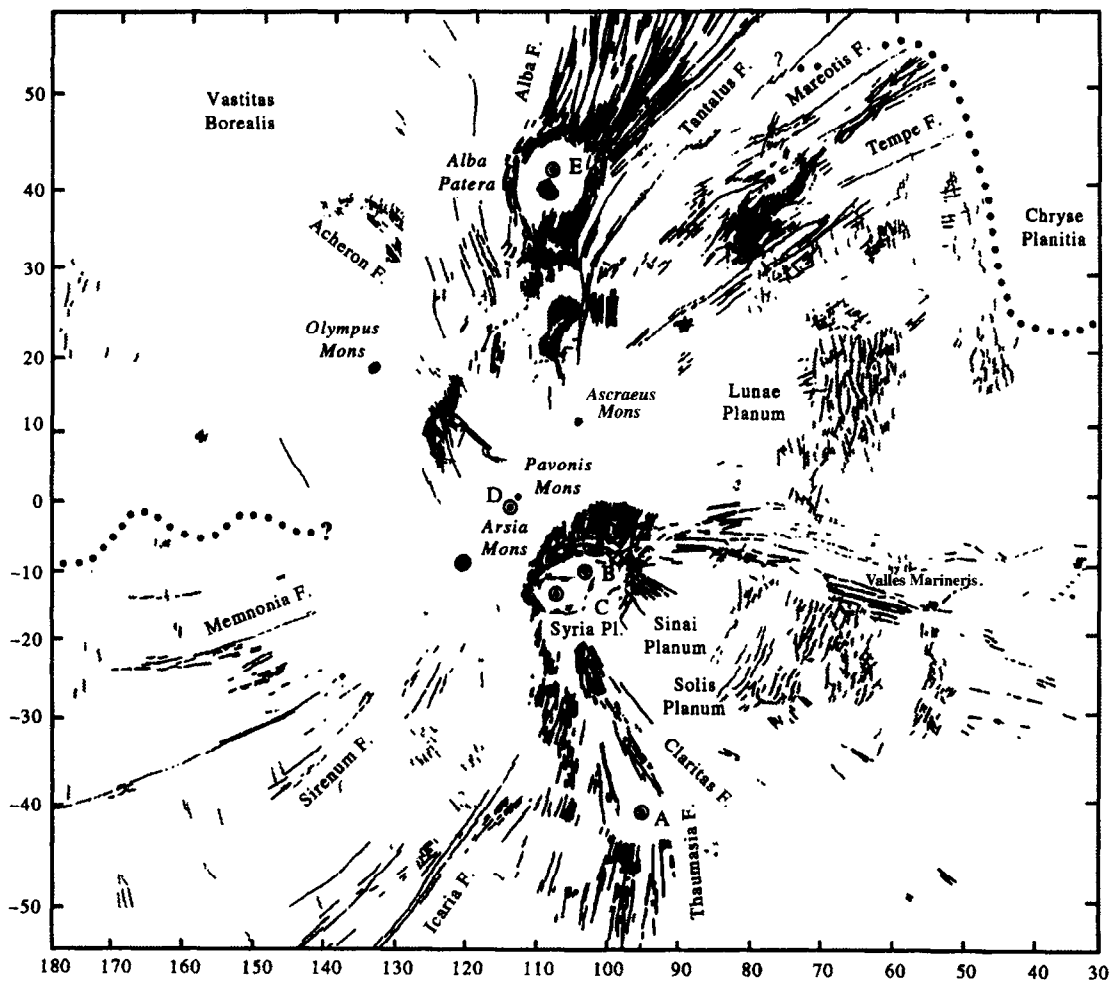


Fig. 1. Simplified structural map of the Tharsis province, displaying the location of Valles Marineris, the main radial pattern sets, the wrinkle ridges (grey patterns, from Watters, 1993), and the calderas of Olympus Mons, Alba Patera, and the Tharsis Montes. Approximate location of the centres of the magma chambers responsible for dyke swarm injection, deduced from the geometry of the swarms and topographic data (U.S.G.S., 1991): A: Solis Planum; B, C: successive stages for Syria Planum, from deflation-related patterns according to chronological relationships in Tanaka and Davis (1988); D: Tharsis (location subject to large uncertainty); E: Alba Patera

nificant characteristics of the Tharsis radial grabens are (1) continuous extensional tectonic patterns over thousands of kilometres radially around a dome, and (2) no displacement gradients along the boundary fault as a function of distance to the fault centre (e.g. Walsh and Watterson, 1989), as observed in most extensional systems on the Earth. These striking characteristics suggest that the mechanism of graben formation has something unusual, that dyke emplacement underneath may help understanding.

This paper uses morphostructural data to propose that many grabens formed more or less directly in response to dyke emplacement, confirming previous suggestions in the Alba Patera (Tanaka and Golombek, 1989) and Tempe Terra (Davis *et al.*, 1995) regions. Dyke emplacement was also suggested by Tanaka *et al.* (1991) as a possible widespread mechanism for radial graben formation over the Tharsis province, but no evidence for this mechanism has been reported except in the Alba Patera and Tempe Terra regions.

Here we present both geomorphological and structural evidence of dykes throughout the Tharsis province (Section 2). The possible mechanisms of graben formation in relation to dyke emplacement are then discussed (Section 3), some of them allowing to deduce some of the characteristics of the dykes (Section 4). Giant radiating dyke swarms are reliable indicators of broad-scale stress trajectories. Consequently, structural mapping in the Tharsis region can directly provide reliable stress-trajectory maps (Section 5), which are used to define a plume tectonics model (Section 6) whose validity is demonstrated by the successful prediction of Valles Marineris formation, wrinkle ridge formation in the Tharsis hemisphere, and the formation of the South Tharsis Ridge Belt. It is also in agreement with most magmatic observations. "Plume tectonics" refers to the definition given by Hill *et al.* (1992), i.e. "the entire process of thermal and structural working above mantle plumes". The model does not require the help of loading stress to explain the Tharsis structural record. It is therefore very different from the detached

crustal cap model by Tanaka *et al.* (1991), both of them are compared and discussed in Section 7.

2. Morphologic and structural evidence of dykes

This section considers both the radial patterns around Tharsis and the elliptical fault network around Syria Planum (Fig. 1). The radial structures around the Tharsis centre are usually called *grabens*, despite that many of them do not display any evidence of faulting. We show that radial-pattern analysis indicates dyke propagation, which contributed to graben formation, subsurface water destabilization, mass wasting processes, and collapse features. Numerous images were analysed in order to emphasize that the processes discussed are likely to be the same ones (sometimes at different evolution levels) in the whole Tharsis region. Examples are taken from Alba Fossae, Tantalus Fossae, Ceraunius Fossae, Mareotis Fossae, Tempe Fossae, Valles Marineris, Noctis Labyrinthus, Claritas Fossae, and Memnonia Fossae. We distinguish between *simple grabens*, whose morphology is primarily guided by tectonics, and *pitted troughs*, displaying pits, pit chains, and coalescing pits. Tectonic structures are frequent around the pitted trough; conversely *linear troughs*, commonly “U”-shaped in cross-section, are normally not surrounded by tectonic structures. This classification, based on a work by Mège (1994), has several features in common with that independently suggested by Davis *et al.* (1995) in Tempe Terra.

2.1. Simple grabens

Simple grabens are as long as 3000 km, commonly 5 km wide, and less than 200 m deep (e.g. U.S.G.S., 1980). The boundary faults dip 60°–70° in the Noctis Labyrinthus/Valles Marineris area (Davis and Golombek, 1990). Grabens have commonly an *en échelon* arrangement, and systematic right stepping in the northeastern region (between Alba Patera and Lunae Planum, Figs 1 and 15c) suggests fracture propagation under varying horizontal stress trajectories (e.g. Pollard, 1987). Grabens have often been affected by further mass wasting processes. However, when they are well preserved (e.g. *a*, Fig. 2), as far as image resolution can suggest, they merely consist of two main boundary faults. This characteristics is important when separating the simple grabens from the other radiating patterns, of greater structural complexity.

2.2. Pitted troughs

A wide range of morphologies exists in the Tempe and Mareotis regions (Fig. 2); some are also common in the other radially fractured regions. These features include pits, pit chains, and coalescing pits. Two kinds of pits are observed: those with conical shape (e.g. Fig. 3) and those with flat, shallow and smooth floor (M on Fig. 6).

Some pit chains are preferentially located on the graben boundary faults (e.g. on T1's northern boundary fault on

Fig. 8), whereas others occur close to the graben centre (e.g. Figs 4 and 6). Some pits follow linear trends that differ up to 15° from the graben trends (e.g. in the middle of area on Fig. 5 a pit chain formed inside a graben, near fault 1, and follows a boundary fault southward, near fault 3). Other pits are not located within grabens (e.g. the pit chains at the bottom of Fig. 4a and on the upper right corner of Fig. 19). These observations indicate that pit formation is probably not the result of graben formation; instead both features should result from the same cause. Graben geometry is more complex where the grabens display inner pits. Below are reported some observations in Figs 4–8 that help understand the links between grabens and pits.

- Most simple grabens have straight boundary faults. The occurrence of pits can be correlated with curved boundary faults (features 1). Additional faults, close to, and often connected with the boundary faults, are also observed. They form nested grabens and present strong similarities to rotational faults separating tilted blocks resulting from limited gravitational sliding.
- Other faults parallel with the boundary faults occur *within* the grabens to their centre (features 2). These faults are generally rectilinear, in contrast with the boundary faults.
- Avoid shallow secondary troughs, partially or fully developed, form within some grabens (features 3). In some cases they occupy the whole graben width. If the inner troughs are bounded by normal faults origin, they increase the vertical offset of the graben boundary faults (features 4).

2.3. Linear troughs

2.3.1. *Linear troughs resulting from pit evolution.* Some linear troughs may result from coalescing pits, as suggested on Figs 2 (radial pattern *b* and small arrows), 5 (north of fault 1) and 6 (near fault 4), and the small pit chain between the two pitted grabens T1 and T2 on Fig. 7a. Grabens T1 and T2 on Fig. 7a have likely the same origin, but have evolved differently. The pit morphology at both ends of T2 indicates that probably it firstly widened by processes similar to those that formed T1, and then broadened by further geomorphological processes leading to the current “U”-shape cross-section. The histogram of the high albedo slope of T1 has been stretched in order to enhance the contrasts on the slope. The resulting image (Fig. 7b) indicates that the processes of graben widening include mass wasting, leading to mid-slope landslides responsible for the circular or ovoid scars. T2 on Fig. 7a might have evolved from a “T1 stage” subsequently to such mechanisms.

Morphological comparisons between linear troughs in the Noctis Labyrinthus and the Valles Marineris regions (Figs 4 and 8, respectively) suggests the same mechanisms of trough widening occurred: compare T1 and T2 on Figs 4 and 8 with T1 and T2 on Fig. 7a. T3 on Fig. 8 is a trough chain which is wider than T2 still, it might represent a

further stage of geomorphologic evolution involving further mass wasting.

2.3.2. *Other linear troughs.* In the following examples pit formation and subsequent widening processes are supposed to have played a possible role in the first stages of linear trough formation. But the systematic smooth characteristic of many linear trough slopes over distances higher than 100 km suggests that a mechanism independent of pit formation should also exist. For instance the radial pattern on Fig. 10 gradually changes from a graben geometry southward, with clearly observed boundary faults, to a "U"-shaped trough, first bordered with one fault, then, northward, without any trace of faulting. No indication suggests that pits were involved in the process that led to the "U"-shaped morphology.

On Fig. 2, the *c* trough may be unrelated with pit formation mechanism. However, like on Fig. 10, its formation is clearly related to graben formation, since a graben structure is observed at both ends.

The common *en échelon* geometry of grabens also echoes the *en échelon* geometry of some flat-floored linear troughs (larger arrows on Fig. 2).

2.4. Origin of graben and trough morphology

The variety and complexity of the radial patterns is necessarily due to various combinations of extensional stress, and material (magma, water, bedrock) removal. Four possible mechanisms able to predict the morphological variety of the radial patterns are given and discussed below.

1. Collapse of material in deep tension cracks. It is a means to form troughs of various characteristics (Tanaka and Golombek, 1989). Collapse mostly involves bedrock material, with a possible major role of water in assisting gravity movements.
2. Pressure drop in dyke and collapse.
3. Hydrovolcanic explosions, and subsequent magma, water, and bedrock removal. Bedrock ejection is the far more efficient removal mechanism. This hypothesis requires the existence of dykes underneath (Lorenz, 1986).
4. Heating, then rising and release of volatiles contained in groundwater or permafrost along linear trends. This hypothesis is also consistent with dyke emplacement. It is reinforced by observations related to outflow and sapping channels.

2.5. Collapse of material in tension cracks

This hypothesis was suggested by Le Dain (1982) in Mar-eotis and Tempe Fossae and by Tanaka and Golombek (1989) in the Valles Marineris region. According to Tanaka and Golombek (1989), all the Valles Marineris troughs, from individual pits to chasmata, could be explained by successive stages of trough widening corresponding to the growth of tension cracks at depth in which part of the lacking material would have collapsed. Schultz (1992a,b) questioned this approach, pointing out that

deep tension cracks developing into shallower grabens is not strongly supported by terrestrial observations, nor rock mechanics since the Coulomb failure criterion (Byerlee's law) is not met at such shallow depths (Byerlee, 1978). Carter and Tsenn's study (Carter and Tsenn, 1987) questions the application of this law to Martian depths greater than a few km. Tension cracks beneath the pitted grabens should systematically focus the location and development of collapse features on the graben boundary faults (Fig. 6 of Tanaka and Golombek (1989)). Clearly, the observations reported above (Section 2.2) are not consistent with such a relationship. Also mass wasting processes would dominate wall morphology, in contradiction with the widespread faceted spur outcrops (Lucchitta, 1977; Mège and Masson, 1994a,b; Peulvast *et al.*, 1996).

Tanaka and Golombek (1989) suggested that, contrary to the pits and troughs observed in the Valles Marineris region, those in the Alba Patera region should be related to dyke emplacement. However the difference between the two series of features may simply result from a difference in intensity of erosional processes (compare Fig. 8 with Figs 5, 6 and 7a). Peulvast *et al.* (1996) have pointed out geomorphological evidence of erosional susceptibility increase of the Valles Marineris slopes during trough evolution. Surface observations show that the higher intensity in the Valles Marineris region cannot be correlated to special climatic conditions in the past. A reason for more pronounced erosion in the Valles Marineris area is given by a model of the hydrologic cycle on Mars which predicts subsurface desiccation in the equatorial regions (e.g. Fanale *et al.*, 1992). Such an evolution would decrease the cohesion of the bedrock in the Valles Marineris region, leading, together with the pronounced tectonic activity in Valles Marineris which produced high wallslopes, to increase the erosional efficiency compared with higher latitude regions. As an additional reason for greater erosion, anomalous magmatic heating in Valles Marineris, (see Section 6) would have melted the permafrost, desiccated the bedrock, lowered its cohesion and strength, increasing the erosional efficiency as well.

Therefore, if cracks exist beneath the Valles Marineris grabens, we expect them to be more likely filled by dykes. Such an hypothesis would be supported by the following simple reasoning: Tharsis is a magmatic region, and, consequently, if the state of stress in extensional, crustal stretching around the region of magma storage should be utilized for dyke emplacement.

2.6. Subsurface pressure drop and collapse

As suggested by Schultz (1988) for the formation of the Valles Marineris pit crater chains, some pits may result from pressure drop in a magma conduit — which must be a dyke since the pits are aligned — and bedrock collapse, following the mechanism of Icelandic-type pit crater formation. This mechanism may be exemplified by the largest pit on Fig. 3. Pit crater formation on Earth is accompanied by ring faulting, which is observed on Figs 4–8 (faults 1).

The inner troughs observed within some of the grabens (bounded by faults 3 on Figs 4–8) may also represent such



Fig. 2. Types of radial patterns in the Tharsis region. *a*: simple graben; *b*: simple graben changing to a deeper, "U"-shaped trough northeastward; *c*: "U"-shaped trough with flat floor, wider than *b*; *d*: elliptic troughs aligned with the radial patterns; *e, f, g*: volcanic constructs aligned with radial patterns. Arrows: examples of *en échelon* geometry. Tempe region. NASA-JPL Viking Orbiter image 857 A 30, 200 m pixel⁻¹. Width of the area displayed: 230 km. North is toward the top

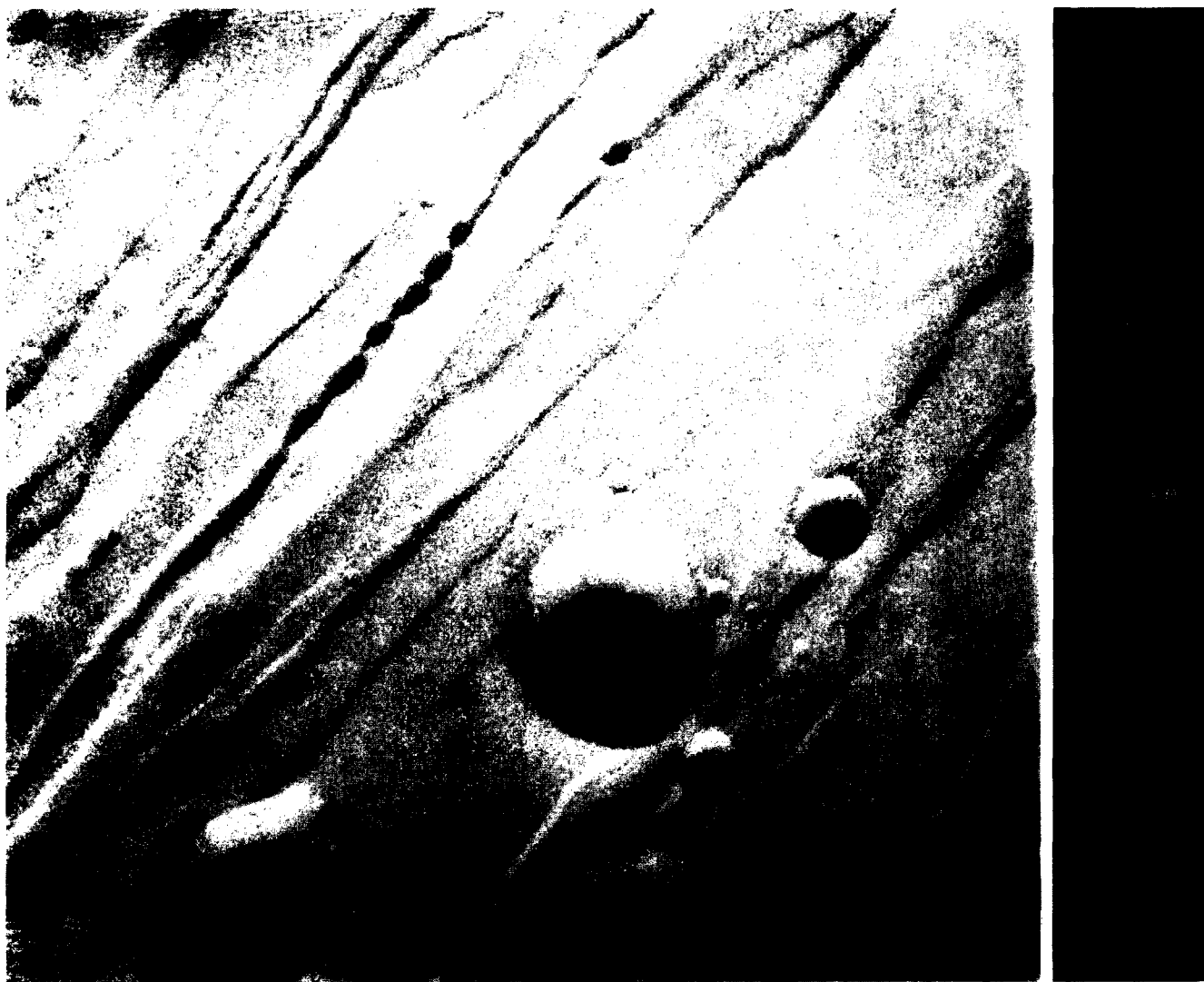


Fig. 3. Close-up on pits in the Alba Patera region. NASA-JPL Viking Orbiter image 341 A 13, 8.1 m pixel^{-1} . Distance across the area displayed: 16 km



Fig. 4. (Caption overleaf)

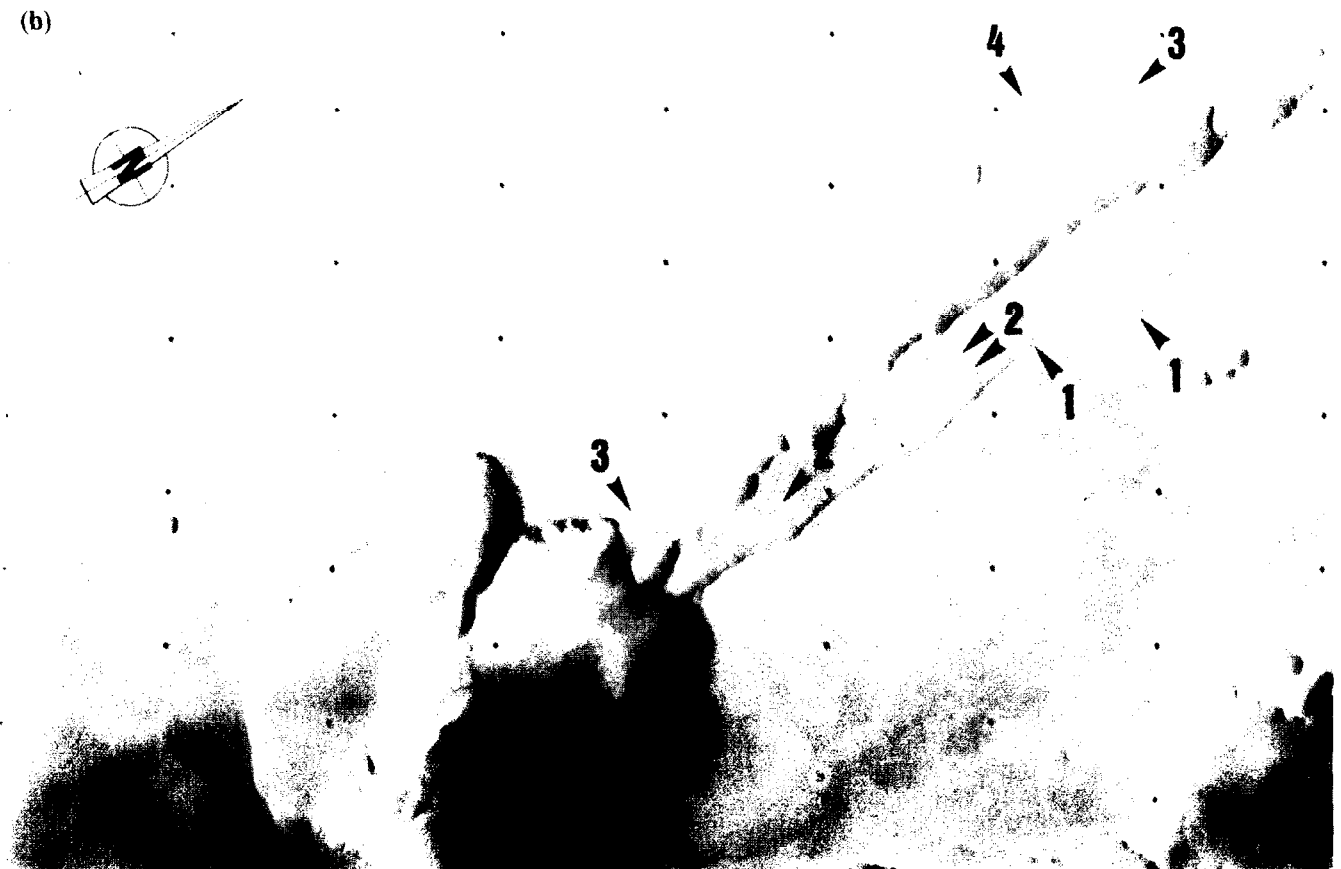


Fig. 4. (a) Graben and pits in the Noctis Labyrinthus/Syria Planum region. NASA–JPL Viking Orbiter images 643 A 84-86-88, 220 m pixel^{-1} . The area displayed on this image is 300 km wide. (b) Close-up on a pitted graben in Noctis Labyrinthus/Syria Planum (location on (a)). The pitted grabens display the following features: 1: sinuous border faults, sometimes splitting or nested; 2: secondary, smaller offset normal faults within the main graben; 3: curved normal faults bounding secondary troughs within the grabens, suggested to have formed in response to subsurface pressure drop; 4: graben border faults with high vertical throws resulting from both graben and secondary trough formation



Fig. 5. Graben and pits on the eastern flank of Alba Patera (Phlegethon Catena). Symbols: same as on Fig. 4b. NASA-JPL Viking Orbiter image 254 S 40, 66 m pixel⁻¹. Width of the area displayed: 90 km



Fig. 6. Grabens on the western flank of Alba Patera. Symbols: same as on Fig. 4b. Most of the pits seem to be conical, but the pits near the top of the image (M) have a shallow and smooth floor, and are strongly similar to maars on Earth. NASA-JPL Viking Orbiter images 252 S 17 to 22, 70 m pixel⁻¹. Width of the area displayed: 160 km



Fig. 7. (a) Pit chains within a graben (T1), and graben strongly widened to large ovoid and coalescing troughs by morphological processes (T2) on the southwestern flank of Alba Patera (Ceraunius Fossae). Symbols: same as on Fig. 4b. NASA-JPL Viking Orbiter images 253 S 50-52-54, 70 m pixel⁻¹. Width of the area displayed: 90 km. (b) Part of T1 western slope on (a), after histogram stretching of the high albedo pixels. Circular features are interpreted as mid-slope landslide scars. Length of the slope displayed: 80 km

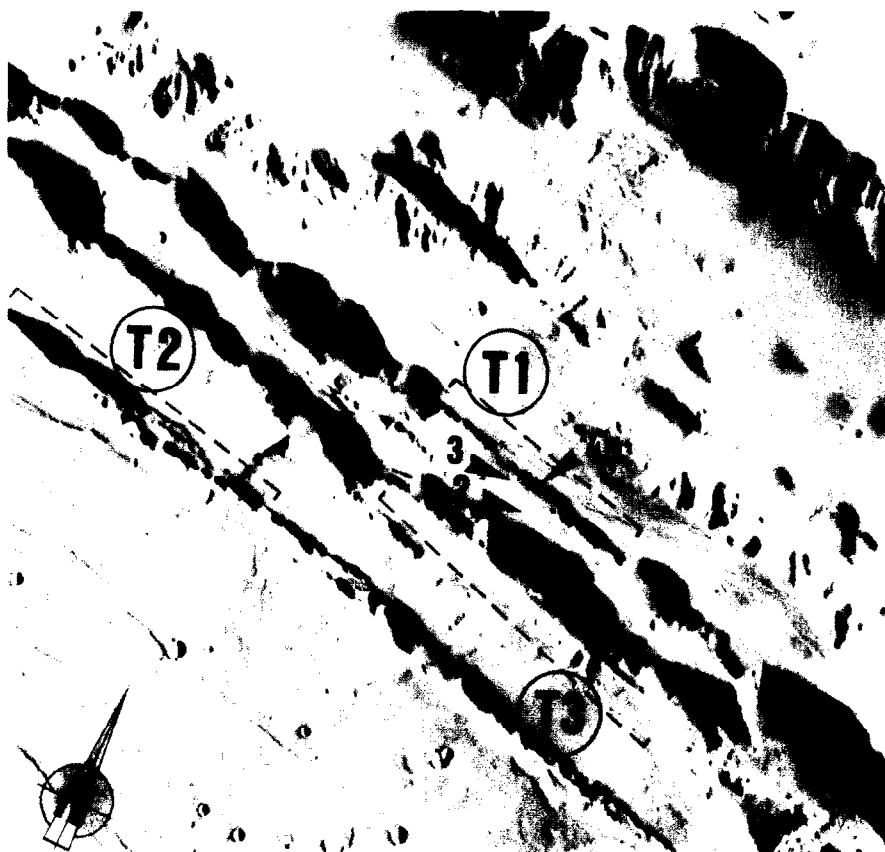


Fig. 8. Radial features (mostly *catenae*) on the Valles Marineris plateau, and one of the main grabens (northward), Coprates Chasma. The tectonic structures observed on the plateau can be analysed exactly the same way as in the Alba Patera region, and suggest a similar origin. Symbols: same as on Fig. 4b. The linear troughs on the plateau may be explained exactly as in the Alba Patera region as well: compare troughs T1 and T2 on this image with T1 and T2 on Fig. 7. Trough T3 formed by further mass wasting processes from troughs T2 and T3, it represents an evolution stage that was not followed in the Alba Patera region. Conversely, the formation of Coprates Chasma was chiefly completed by tectonic processes. NASA-JPL Viking Orbiter image 610 A 07, 180 m pixel⁻¹. Width of the area displayed: 250 km. North is toward the upper right corner

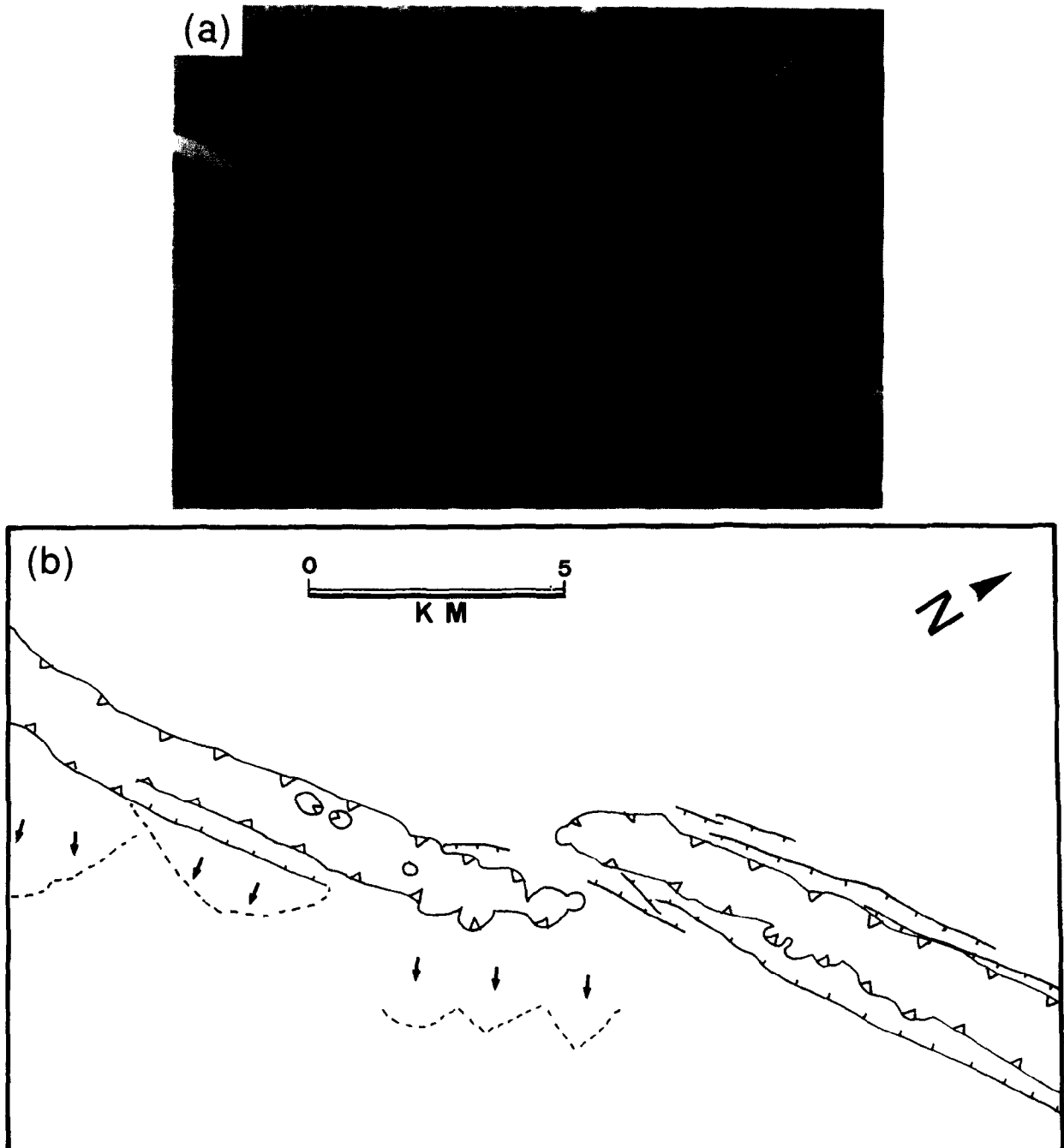


Fig. 9. (a) Set of radial patterns south of Uranus Patera. Viking Orbiter image 229 A 32, 44 m pixel⁻¹. (b) Interpretation of (a) emphasizing evidence of joint growth by mixed I and II mode (Pollard *et al.*, 1982) and possible magma extrusion around a joint tip (lava fronts displayed by dashed lines, and supposed main flow direction indicated by arrows)



Fig. 10. Radial features belonging to Mareotis Fossae. A small graben southward (G) gradually changes to a trough without any trace of tectonic structures (T). NASA-JPL Viking Orbiter image 254 S 47, 70 m pixel⁻¹. Width of the area displayed : 90 km

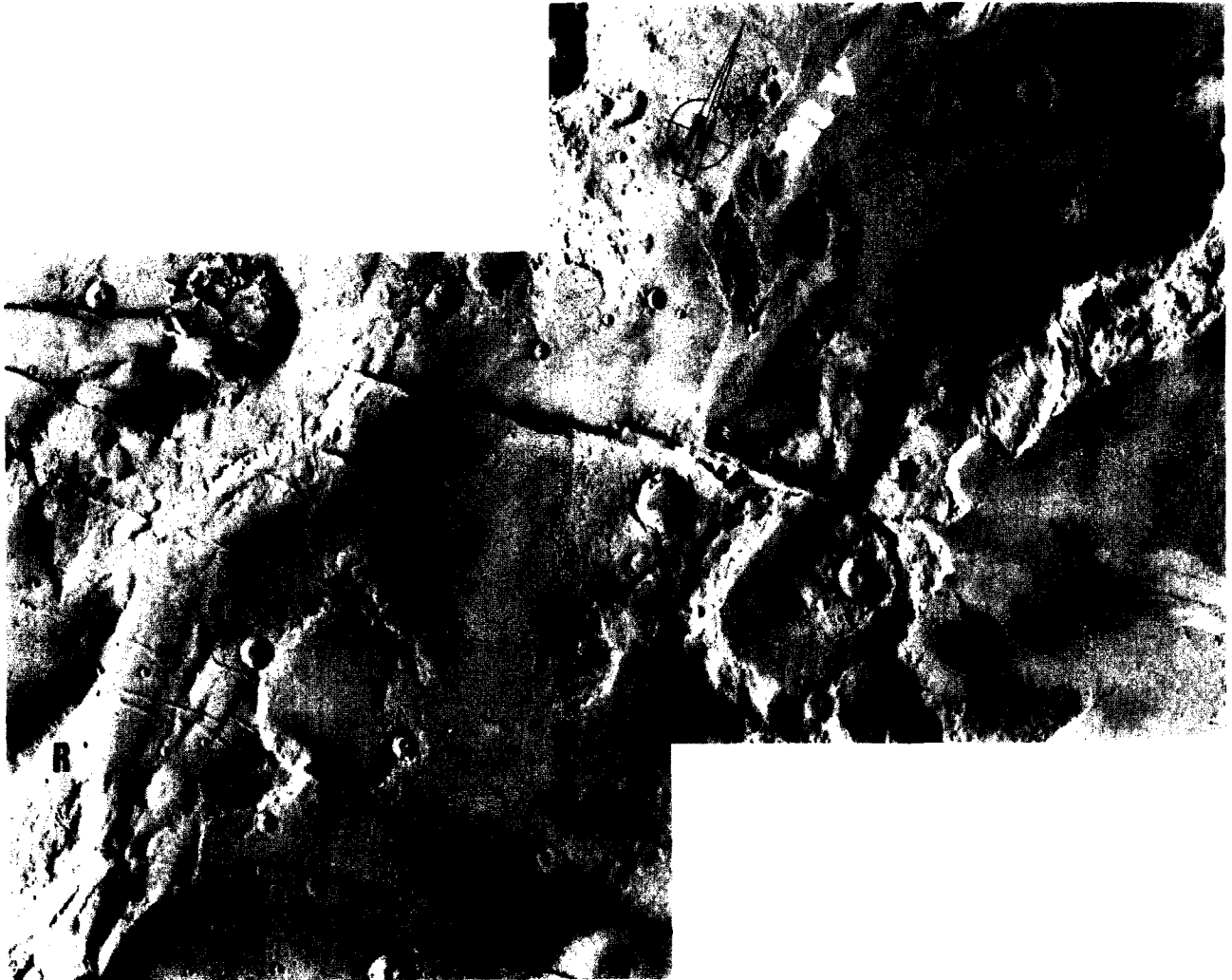
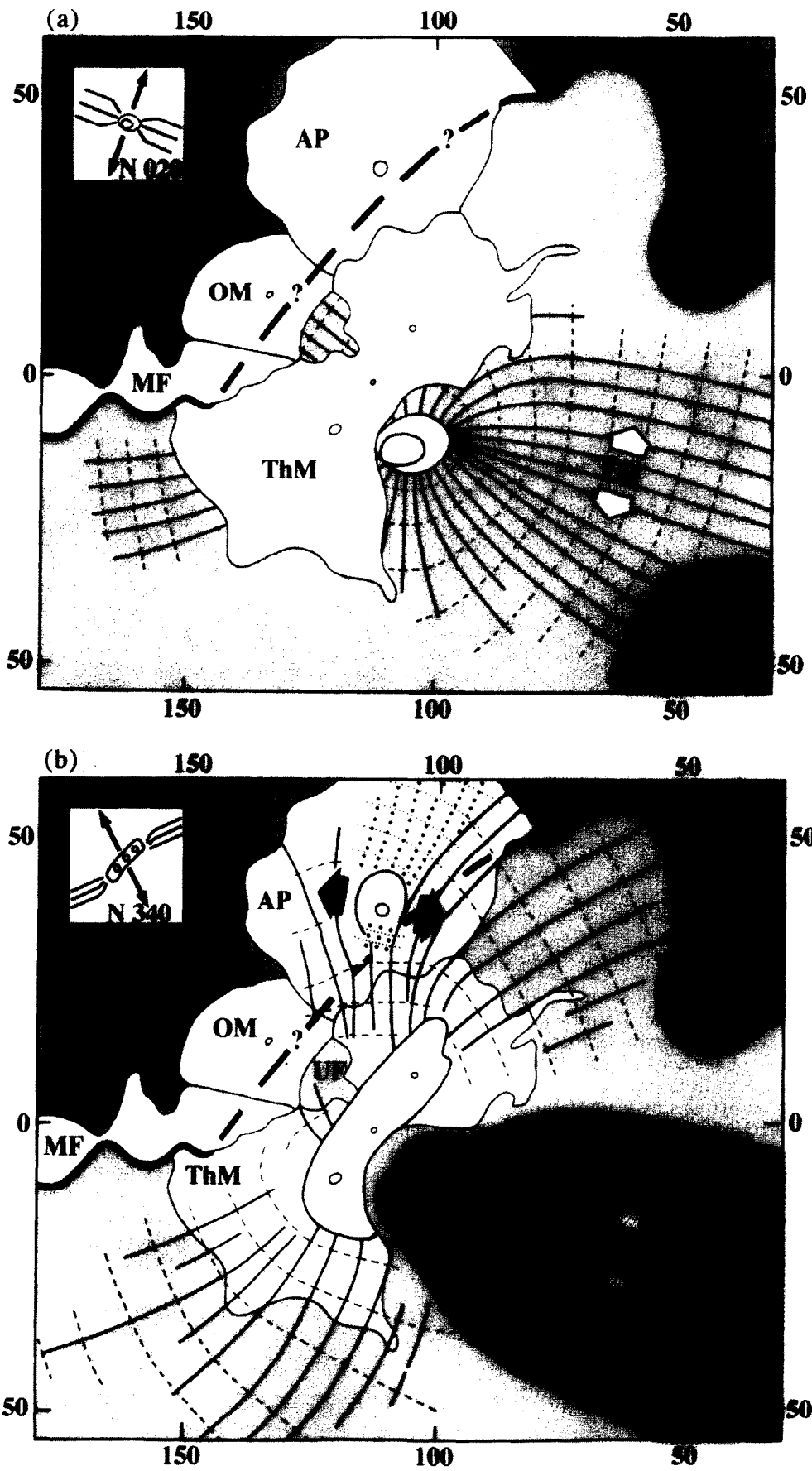


Fig. 11. Memnonia Fossae in the Mangala Valles (mv) area. R: ridge in the Noachian regolith (see Zimbelman, 1989); V: Hesperian, probably volcanic, materials (Scott and Tanaka, 1986). Two sets of grabens are observed. Grabens G1 are not Riedel joints because strike slip movements are never observed on the border faults of grabens G2. The border faults of grabens G1 are still observed both in regolith and volcanic materials. Grabens G2, 10° – 15° apart, were modified to linear troughs in the Hesperian terrains by mass wasting processes. If dykes lie underneath both graben sets, then the grabens G1 should have formed before water trapping in the hydrolithosphere, because no interactions between magmatic heat and permafrost occurred. Grabens G2 formed after water trapping in the hydrolithosphere. The absence of linear troughs in the ridged regolith may result from less efficient heating of the hydrolithosphere due to the higher distance between the top of the dykes and the bottom of the hydrolithosphere. White arrows indicate three grabens whose width variations depending on the Young's modulus of the host rock are especially clear. NASA–JPL Viking Orbiter images 637 A 81–82. Width of the area displayed: 300 km



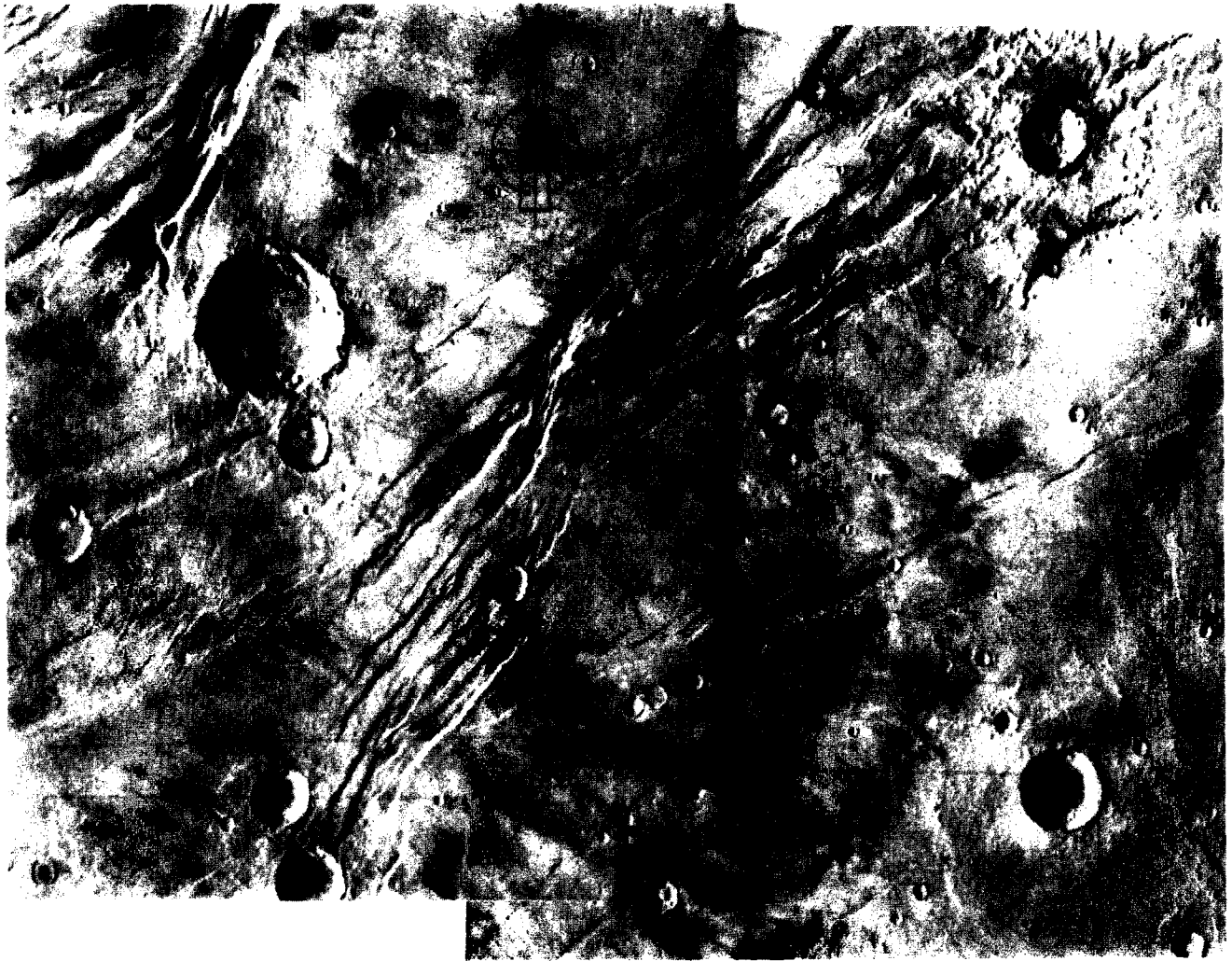


Fig. 18. (a) Minor magma centres in Tempe Terra and associated graben swarms maybe underlined by dykes. Interpretation on (b) and (c). NASA–JPL Viking Orbiter images 704 B 54 and 704 B 56, 172 m pixel^{-1} . Width of the area displayed: 300 km. North is toward the top. (b) Structural interpretation of (a). Plain lines: faults; plain lines with barbels: normal faults; circles with squares: impact craters; dotted ovals: topographic dome (paterra, extrusive dome?); double-lined ovals: trough (collapse caldeira?). (c) Sketch interpretation of (a) and (b). Same symbols as for (b); the features associated with local magma centres are displayed with heavy lines, and independent fault sets with thin lines. A and B: the two local magma centres; C1, C2: two graben sets from the Tharsis graben swarm; D: later faulting

Fig. 16. Extrapolation of Fig. 15 in terms of stress trajectories. (a) Hesperian; (b) upper Hesperian + Amazonian. Plain lines are dyke patterns inferred from graben trends and represent σ_1 or σ_2 trajectories. Dashed lines are σ_3 trajectory, deduced from the other horizontal principal stress trajectory. The dichotomy is drawn with the thickest line (inferred below recent volcanics). For each stage, the terrains younger than grabens are displayed. They are mostly volcanic flows (from: AP: Alba Patera; OM: Olympus Mons; ThM: Tharsis Montes), except the Medusae Fossae formation (MF). Argyre Planitia (APl) and Syria Planum (SP) acted as hard cores during stage (a) and (b) respectively because of the strength of the Argyre mascon and the strengthening of the Syria Planum region by intrusions of stage (a). Alba Patera and Valles Marineris (VM) were extensional regions, mostly during upper Hesperian (VM) and Amazonian (AP). Boxes show the regional σ_3 direction during the Syria (a) and Tharsis/Alba (b) magmato-tectonic periods

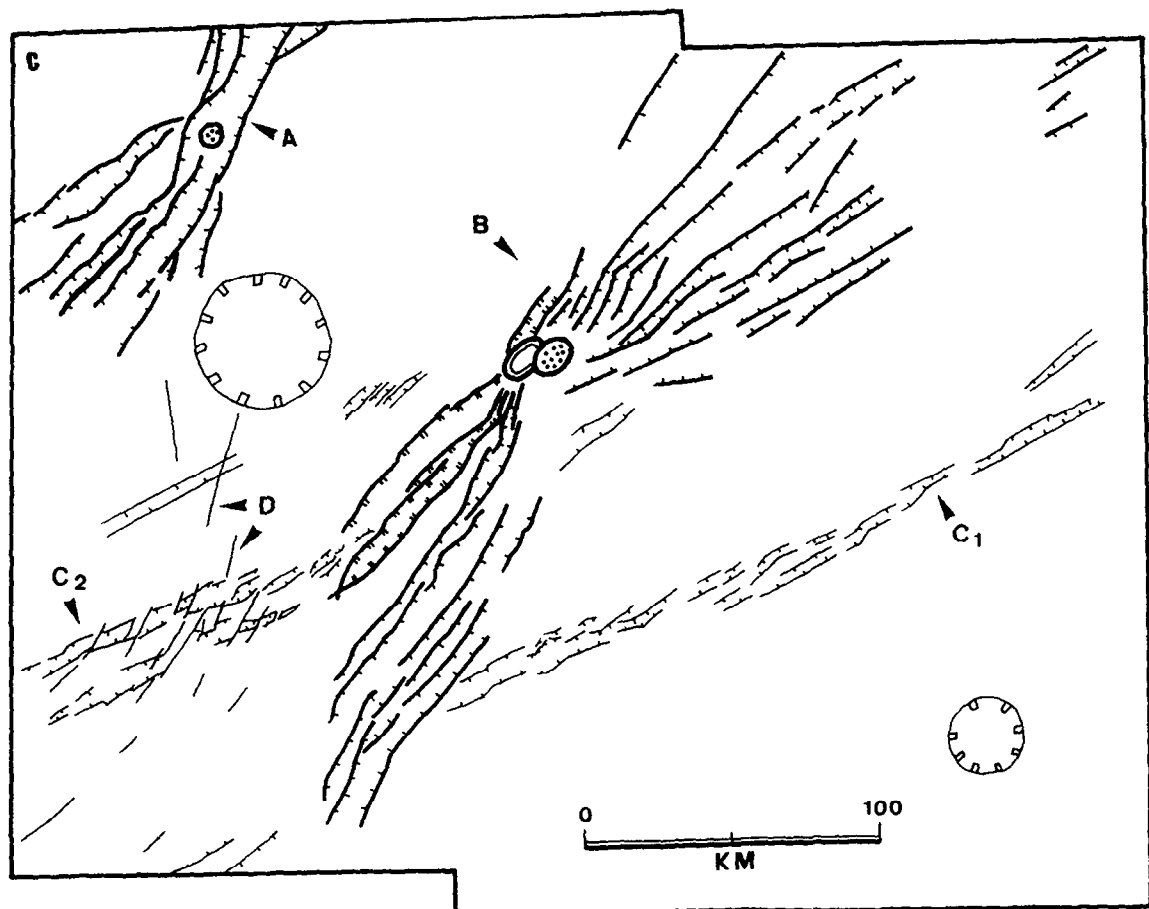
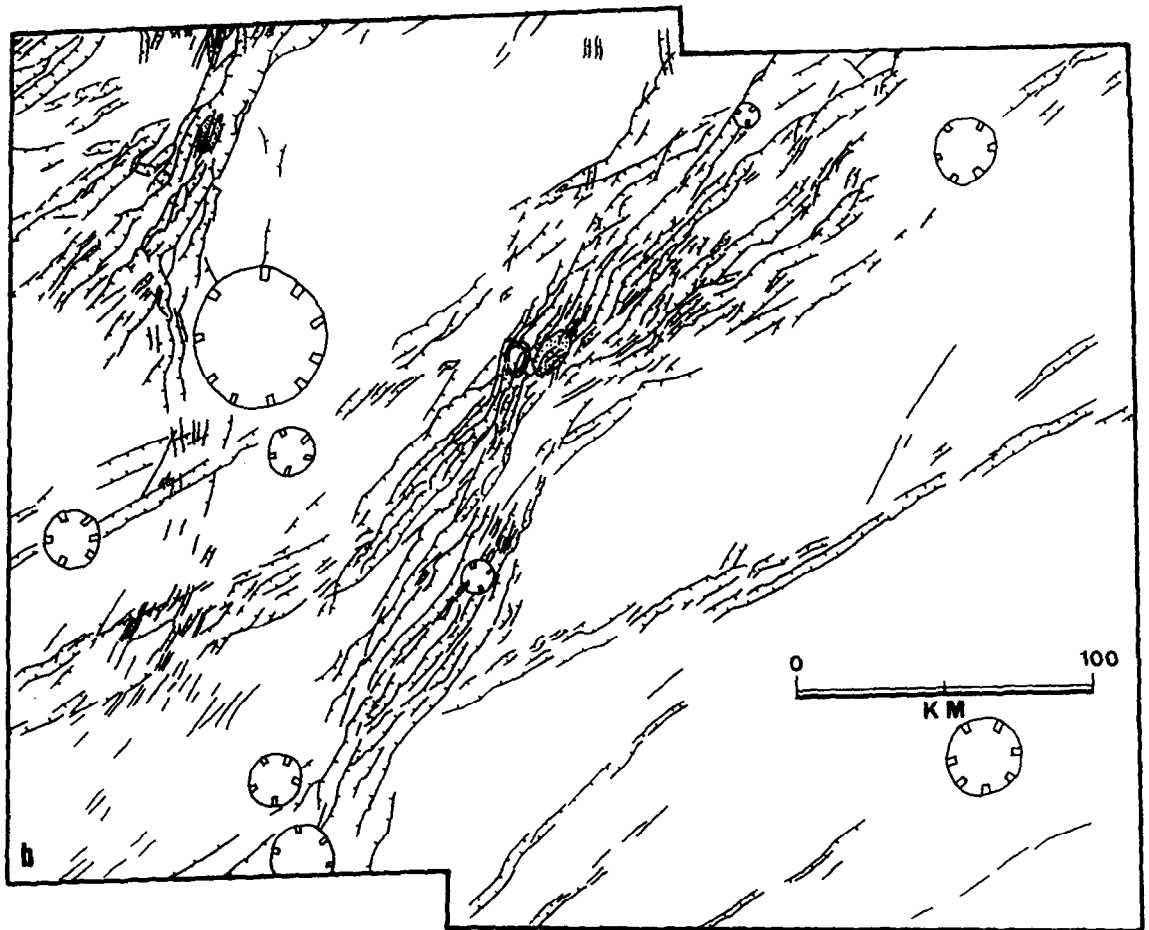


Fig. 18. (Continued)



Fig. 19. Other example of the influence of local magma centre (a) in graben formation. The arcuate grabens northward and southward of the magma centre might have been influenced by dyke swarm trends underneath. Note that pits in the upper right corner of the image follow the trend of a graben southward but are not located within a graben. Claritas Fossae, NASA-JPL Viking Orbiter image 56 A 52, 200 m pixel^{-1} . Distance across the area displayed: 150 km. See also Mariner 9 image DAS 05635983 for an oblique view of some grabens associated with a

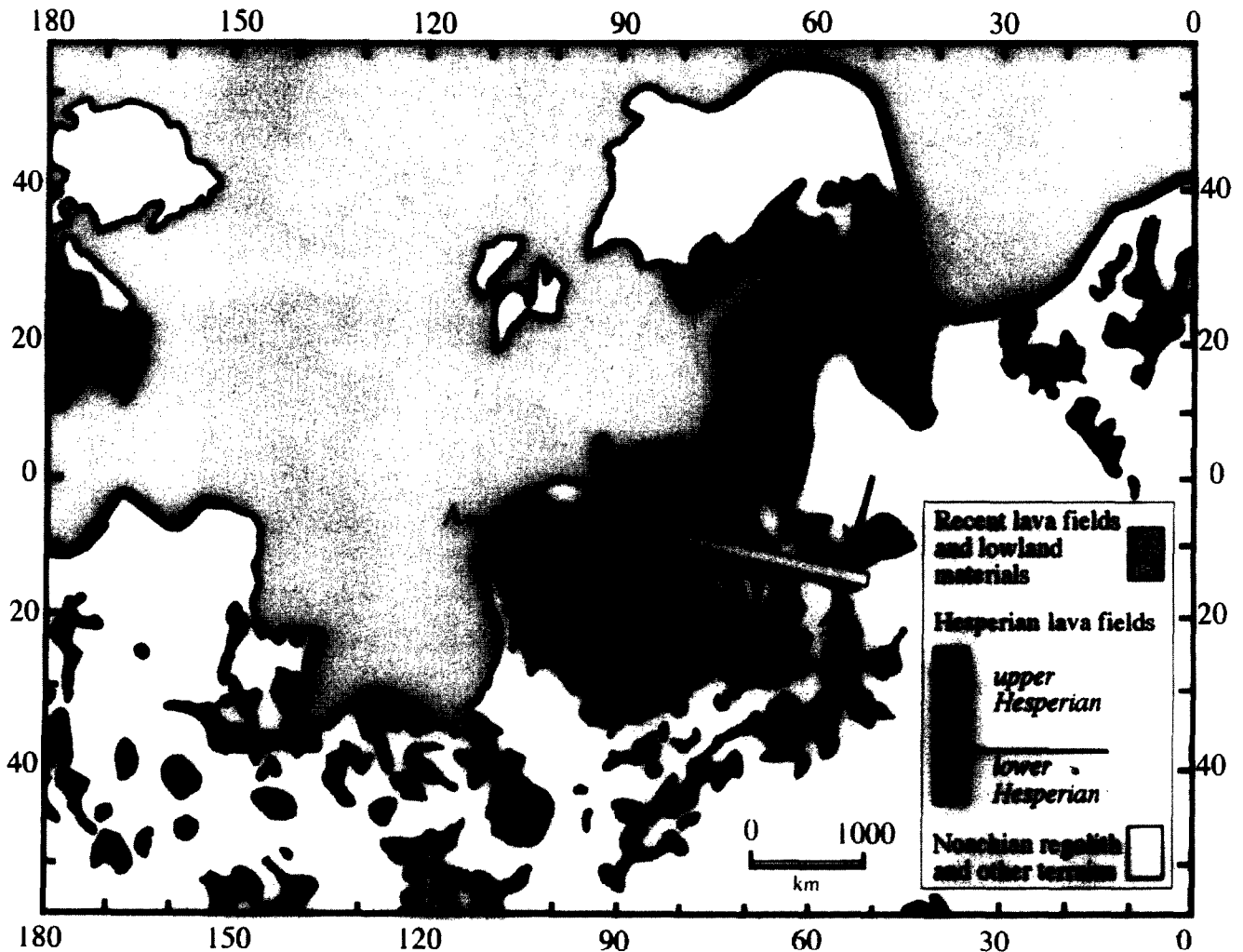


Fig. 20. Selected geologic mapping of the Tharsis hemisphere during Syria Planum magmatic activity. The recent lava fields correspond to the building of Tharsis, Alba Patera, and Olympus Mons, and also lowland formations. SP: location of the Syria Planum magma centre; VM sketches the trend of Valles Marineris. The arrows indicate the proposed boundary of the plume, based on the boundary between uplifted and non-uplifted parts of the Valles Marineris region. The thinnest lines separate the limits of terrains; the intermediate line separates the cratered highlands and Hesperian volcanic fields southward, and the more recent terrains northward; the thickest lines show the dichotomy boundary. AA': location of the cross-section on Fig. 22; BB': location of the cross-section on Fig. 23

collapse features. Some of them display striking similarities with normal fault scarps around the Mauna Loa caldera in Hawaii (Carr and Greeley, 1980, p. 27).

Figure 9 displays further evidence of a dyke underlying the pits. It is a close-up view of two *en échelon* morphotectonic patterns in the northeastern part of Tharsis, south of Uranus Patera. The trough evolution is midway between the present stages of T1 and T2. Two key observations are: (1) the evidence of overlapping patterns. Each *échelon* tip is deflected toward the other in the overlapping area, but this geometry is only underlined by pits, and not by tectonic patterns; (2) the lava flows extruded from at least one of the troughs (arrows). Deflected patterns are observed on Earth in various environments at all scales. At kilometric scale, like on Fig. 9, such patterns are observed in overlapping rift zones. Although an alternative view was published (Lonsdale, 1983), most interpretations are similar to interpretations made by Pollard *et al.* (1982) at a much smaller scale, involving propagating crack tips following a mixed I and II mode (McDonald *et al.*, 1984, 1986; Gudmundsson and Brynjolfsson, 1993). Owing to the observation of lava flows at joint tip, the grabens on Fig. 9 must be underlain by dykes.

2.7. Hydrovolcanic pits and other features related to magma and bedrock water interaction

Explosive hydrovolcanic craters (maars) form above dykes and involve water in the bedrock (e.g. Lorenz, 1986). They are consequently expected on Mars since Hesperian (Carr, 1979; Clifford, 1993; Costard, 1993). The existence of maars on Mars and comparisons with the Earth have been investigated in several works (McGetchin and Ullrich, 1973; Sharp, 1973; Mutch *et al.*, 1976; Greeley and King, 1977; Carr and Greeley, 1980). Fagents and Wilson (1995) expect them to be even more common on Mars than on the Earth. M on Fig. 6 is a possible example of maar, which should be filled in with sediments slid from the walls, and smoothed because of their deposition in a provisional lake. Some maars, however, have also been filled in with smooth lavas erupted from the feeder dyke, depending on explosion characteristics (Lorenz, 1986).

The craters produced this way present analogies with pit craters discussed above. However a difference is that maars are surrounded by ejecta blankets, and the morphology of pit craters is more conical. No ejecta blankets are found around the Martian pits on the Viking images, and this may be attributed to the resolution of the available images, which in most cases roughly corresponds to the expected thickness of ejecta. Also this may result from ashfall dispersion over distances greater than in Earth cases owing to the lower gravity on Mars (McGetchin and Ullrich, 1973; Wilson and Head, 1994; Fagents and Wilson, 1995). In addition, although wind erosion is weak on Mars, it may have significantly contributed to ejecta removal over the past hundred million years during the periodic dust storms, especially because maar ejecta are poorly indurated (Wohletz and Sheridan, 1983; Fagents and Wilson, 1995).

The expected Martian maars (e.g. M on Fig. 6) have a

size consistent with typical sizes of hydrovolcanic pits on Earth (Lorenz, 1986). Most of the Tharsis maars are a few kilometres in diameter — 5 km at most, and the largest ones Lorenz reported are about 3 km in diameter. This small difference, if significant, may be due to the lower Martian gravity and the poor cohesion of regolith, which favours easier ejecta removal than on the Earth (McGetchin and Ullrich, 1973).

Formation of explosive pits is expected when the water/magma mass ratio is close to 0.35 (Sheridan and Wohletz, 1981). Lower (<0.35) or higher (>0.5 and <5) ratios should give rise to cinder cones or tuff cones, respectively (Wohletz and Sheridan, 1983; Kokelaar, 1986). Other small edifices, such as spatter cones (akin to cinder cones) are indeed observed, especially in Tempe Terra (e.g. *g* on Fig. 2). Scott and Dohm (1990a) suppose that in Tempe Terra they formed a little time before the radial grabens. A wide range of other edifice morphologies of similar age are also observed in the same region (*e* and *f* on Fig. 2 see also Cattermole (1992), pp. 121–122, and Moore (1995)).

2.8. Groundwater release

2.8.1. *Thermokarstic depressions.* Interaction between subsurface water and dyke propagation does not necessarily result in dyke eruption. It may result in thermokarstic depressions. The volume of volatiles released involves both bedrock volatiles and part of the volatiles located at dyke tips (Lister, 1990; Lister and Kerr, 1991; Hoek, 1994, 1995). Squyres *et al.* (1987) carried out some calculations relating to the effect of sill emplacement in a permafrosted area with 25% ground ice, and showed that the layer thickness of ice melted or vaporized by magmatic heat is thicker than the sill, and can lead to significant depressions. The case for dyke intrusion was briefly discussed, but similar results are expected. Water or vapour release is favoured by increase of dyke thickness and increase of intrusion depth. Rubin (1993) and Bonafede and Olivieri (1995) have emphasised the role of suction in the fractured area above dyke tips in groundwater concentration (an effect not considered by Squyres *et al.* (1987)), which increases the efficiency of thermokarstic and hydrovolcanic processes. Linear troughs like on Figs 2, 10 and 11 may result from such thermokarstic processes. In particular, the aligned depressions *d* on Fig. 2 have morphological characteristics and dimensions presenting great similarities to thermokarstic depressions (alases) on Earth and elsewhere on Mars (Costard, 1990; Costard and Kargel, 1995).

2.8.2. *Outflow channels.* We report observations suggesting that dykes may have played a role in outflow channel formation, from upper Hesperian (Scott and Tanaka, 1986) and upper Amazonian (Mouginis-Mark, 1990).

Mangala Valles (MV) partly originate from a linear trough from Memnonia Fossae. Fluidized ejecta crater studies (Costard, 1990a, 1993) show that a permafrost developed in the Mangala Valles region 500 m below the surface. Tanaka and Chapman (1990) proposed that Mangala Valles formed from water release due to inter-

action of groundwater, tension fractures (following Tanaka and Golombek, 1989), and Tharsis magmatic heat. A problem is that the Mangala flows have several sources; some flows initiated 150 km northward of the above mentioned linear trough, in an apparently non-fractured area. It is unlikely that the Tharsis magmatic heat can be channelled up to this area so far away from the tension cracks. The mechanism proposed by Tanaka and Chapman (1990) becomes more realistic if the cracks are filled by magma. Mangala Valles flows would have been essentially triggered by hydrothermal flow in the dyke surroundings, as well as dramatic pore pressure increase above the dykes. This interpretation is consistent with the evidence for dykes and lower Hesperian sills given by Squyres *et al.* (1987) and Wilhelms and Baldwin (1989) in the lowlands close to Mangala Valles.

In details, the mechanism generating and sustaining the flows in Mangala Valles would have been the following. The occurrence of groundwater along a dyke pathway lowers the dyke propagation speed. The thermal conductivity and the thermal diffusivity of the host rock increase, and the temperature of the dyke margins decreases by some 75°C (Delaney, 1987). Thermal expansion of groundwater increases pore pressure, favouring hydrovolcanic activity, but only weakly affects dyke propagation because thermal expansion is poorly efficient for heat transport (Delaney, 1982). Hydrothermal flow sets up after the pore pressure has decreased, and transports heat more efficiently. Hydrothermal flow is likely for dykes a few tens of metres thick, i.e. for typical plausible radial dykes in the Tharsis region (Section 4, Table 1). The thickness of the dykes in the Tharsis region strongly suggests that they result from many pulses. Flow in a dyke resulting from multiple pulses can be sustained for weeks, years, and maybe thousands of years (Gudmundsson, 1984, 1995b). This duration is enough for discharge in the catastrophic scenarios of Mangala Valles and Kasei Vallis formation (Tanaka and Chapman, 1990; Robinson and Tanaka, 1990), and also in scenarios suggesting flow discharge for a longer time arising from comparison with Siberian outburst valleys (Costard, 1990a,b).

Frozen dykes may also have played a role in outflow channel formation. Water freezing in aquifers increases pore pressure. Sudden water release can occur when the pore pressure reaches the lithostatic pressure (Carr, 1979). The existence of frozen dyke barriers can help this mechanism to occur by laterally confining the aquifers, like the dyke barriers in Hawaii (Kochel and Piper, 1986).

2.8.3. Sapping channels. Groundwater heating by dykes and hydrothermal flow may also explain the formation of some sapping channels. Two small sapping channels seem to originate from a linear trough in the Memnonia region (Fig. 6 of Tanaka and Chapman (1990)), and, similar to Mangala Valles, may be a consequence of dyke emplacement beneath this trough.

Louros Valles, a series of sapping channels located south of Valles Marineris, have been shown to follow structural trends (Kochel and Capar, 1982). Local high reliefs follow the Louros Valles trends in the Valles Marineris chasmata trends. They have been interpreted as the summit of eroded dyke that were preserved owing to differential erosion (Lucchitta, 1981; Mège, 1994, p. 94;

Table 1. Depth range for the dyke tops below the Tharsis radial faults and elliptic faults around Syria Planum from relations on Fig. 13. When one value is reported it means that the graben widths were quite the same in the study area; when two values are reported they are the lower and upper bounds; "max" indicates that all the widths, from the picture resolution bound to the indicated value, were observed. Symbols as on Fig. 13

<i>h</i>	α	<i>L</i> (m)	$z_1 = L/2$ (m)	$z_2 = L/3$ (m)
Valles Marineris				
<i>Ius/Tithonium plateau (MTM — 05077)</i>				
<i>h</i> = 200 m	$\alpha = 60^\circ$	1230	615	410
	$\alpha = 80^\circ$	1070	535	360
<i>h</i> = 50 m	$\alpha = 60^\circ$	1060	530	350
	$\alpha = 80^\circ$	1020	510	340
<i>Tithonium/Echus plateau (MC 18 NW)</i>				
<i>h</i> = 200 m	$\alpha = 60^\circ$	1560–2900	780–1450	520–970
	$\alpha = 80^\circ$	1400–2740	700–1370	470–910
<i>h</i> = 50 m	$\alpha = 60^\circ$	1390–2720	695–1360	460–905
	$\alpha = 80^\circ$	1350–2680	675–1340	450–895
<i>South Valles Marineris plateau (MC 18 SE)</i>				
<i>h</i> = 200 m	$\alpha = 60^\circ$	900–3560	450–1780	300–1190
	$\alpha = 80^\circ$	740–3400	370–1700	250–1135
<i>h</i> = 50 m	$\alpha = 60^\circ$	720–3390	360–1700	240–1130
	$\alpha = 80^\circ$	680–3350	340–1675	230–1120
<i>East Valles Marineris plateau (MC 19 SW)</i>				
<i>h</i> = 200 m	$\alpha = 60^\circ$	3560	1780	1190
	$\alpha = 80^\circ$	3400	1700	1135
<i>h</i> = 50 m	$\alpha = 60^\circ$	3390	1695	1130
	$\alpha = 80^\circ$	3350	1675	1120
bounds		680–3560	340–1780	340–1190
Claritas Fossae – Noctis Labyrinthus				
<i>Claritas Fossae (MC 17 SE)</i>				
<i>h</i> = 200 m	$\alpha = 60^\circ$	2900	1450	970
	$\alpha = 80^\circ$	2740	1370	910
<i>h</i> = 50 m	$\alpha = 60^\circ$	2720	1360	905
	$\alpha = 80^\circ$	2680	1340	895
<i>Claritas Fossae (MC 25 SW)</i>				
<i>h</i> = 200 m	$\alpha = 60^\circ$	1560–2900	780–1450	520–970
	$\alpha = 80^\circ$	1400–2740	700–1370	470–910
<i>h</i> = 50 m	$\alpha = 60^\circ$	1390–2720	695–1360	460–905
	$\alpha = 80^\circ$	1350–2680	675–1340	450–895
<i>Noctis Labyrinthus (MC 17 NE)</i>				
<i>h</i> = 200 m	$\alpha = 60^\circ$	max. 2900	max. 1450	max. 970
	$\alpha = 80^\circ$	max. 2740	max. 1370	max. 910
<i>h</i> = 50 m	$\alpha = 60^\circ$	max. 2720	max. 1360	max. 905
	$\alpha = 80^\circ$	max. 2680	max. 1340	max. 895
bounds		0–3560	0–1780	0–970
Icaria Fossae				
<i>MC 25 NW</i>				
<i>h</i> = 200 m	$\alpha = 60^\circ$	900	450	300
	$\alpha = 80^\circ$	740	370	250
<i>h</i> = 50 m	$\alpha = 60^\circ$	720	360	240
	$\alpha = 80^\circ$	680	340	230
<i>MC 24 NE</i>				
<i>h</i> = 200 m	$\alpha = 60^\circ$	900–1560	450–780	300–520
	$\alpha = 80^\circ$	740–1400	370–700	250–470
<i>h</i> = 50 m	$\alpha = 60^\circ$	720–1390	360–695	240–460
	$\alpha = 80^\circ$	680–1350	340–675	230–450
<i>MC 24 SE</i>				
<i>h</i> = 200 m	$\alpha = 60^\circ$	1560–2230	780–1115	520–740
	$\alpha = 80^\circ$	1400–2070	700–1035	470–690
<i>h</i> = 50 m	$\alpha = 60^\circ$	1390–2060	695–1030	460–690
	$\alpha = 80^\circ$	1350–2020	675–1010	450–670
bounds		680–2230	340–1115	230–740

(Continued)

Table 1. (Continued)

h	α	L (m)	$z_1 = L/2$ (m)	$z_2 = L/3$ (m)
Sirenum Fossae – Memnonia Fossae				
<i>Sirenum/Memnonia (MC 16 SE – SW)</i>				
$h = 200$ m	$\alpha = 60^\circ$	max. 1560	max. 780	max. 520
	$\alpha = 80^\circ$	max. 1400	max. 700	max. 470
$h = 50$ m	$\alpha = 60^\circ$	max. 1390	max. 695	max. 460
	$\alpha = 80^\circ$	max. 1350	max. 675	max. 450
<i>Sirenum Fossae (MC 29 NE)</i>				
$h = 200$ m	$\alpha = 60^\circ$	900–2230	450–1115	300–740
	$\alpha = 80^\circ$	740–2070	370–1035	250–690
$h = 50$ m	$\alpha = 60^\circ$	720–2060	360–1030	240–690
	$\alpha = 80^\circ$	680–2020	340–1010	230–670
bounds		0–2230	0–1115	0–740
North Alba Patera (Vastitas Borealis)				
<i>(MC 3 NE – NW)</i>				
$h = 200$ m	$\alpha = 60^\circ$	max. 2900	max. 1450	max. 970
	$\alpha = 80^\circ$	max. 2740	max. 1370	max. 910
$h = 50$ m	$\alpha = 60^\circ$	max. 2720	max. 1360	max. 905
	$\alpha = 80^\circ$	max. 2680	max. 1340	max. 895
bounds		0–2900	0–1450	0–970
West and East Alba Patera				
<i>West (MTM 35117 – MTM 40117)</i>				
$h = 200$ m	$\alpha = 60^\circ$	900–5560	450–2780	300–1850
	$\alpha = 80^\circ$	740–5400	370–2700	250–1800
$h = 50$ m	$\alpha = 60^\circ$	720–5390	360–2695	240–1800
	$\alpha = 80^\circ$	680–5350	340–2675	230–1780
<i>East (MC 3 SW)</i>				
$h = 200$ m	$\alpha = 60^\circ$	max. 2900	max. 1450	max. 970
	$\alpha = 80^\circ$	max. 2740	max. 1370	max. 910
$h = 50$ m	$\alpha = 60^\circ$	max. 2720	max. 1360	max. 905
	$\alpha = 80^\circ$	max. 2680	max. 1340	max. 895
bounds		0–2900	0–1450	0–970
West and East Alba Patera				
<i>West (MTM 35117 – MTM 40117)</i>				
$h = 200$ m	$\alpha = 60^\circ$	900–5560	450–2780	300–1850
	$\alpha = 80^\circ$	740–5400	370–2700	250–1800
$h = 50$ m	$\alpha = 60^\circ$	720–5390	360–2695	240–1800
	$\alpha = 80^\circ$	680–5350	340–2675	230–1780
<i>East (MC 3 SW)</i>				
$h = 200$ m	$\alpha = 60^\circ$	max. 2900	max. 1450	max. 970
	$\alpha = 80^\circ$	max. 2740	max. 1370	max. 910
$h = 50$ m	$\alpha = 60^\circ$	max. 2720	max. 1360	max. 905
	$\alpha = 80^\circ$	max. 2680	max. 1340	max. 895
bounds		0–5560	0–2780	0–1850
Tempe Terra				
<i>(MC 3 SE – MC 4 SW – MC 10 NE)</i>				
$h = 200$ m	$\alpha = 60^\circ$	max. 2900	max. 1450	max. 970
	$\alpha = 80^\circ$	max. 2740	max. 1370	max. 910
$h = 50$ m	$\alpha = 60^\circ$	max. 2720	max. 1360	max. 905
	$\alpha = 80^\circ$	max. 2680	max. 1340	max. 895
bounds		0–2900	0–1450	0–970

compare with similar morphology on the Earth, e.g. Greeley, 1989, p. 59).

2.9. Summary of graben and pit formation

Figure 12 shows that when subsurface water exists it is possible to explain a variety of radial features as a function of dyke and watertable depths. Formation of Iceland-

like pit craters, which is not considered here, is a further mechanism which explains the formation of some pits and troughs without involving water. For dyke emplacement in the crust below watertable, driving pressure favours simple graben formation (Fig. 12A). At shallower depth, dykes are able to heat the groundwater and induce water and vapour release. Fracturing around dyke tips would help buoyant ascent of water and vapour to the surface (Fig. 12B). The escape of both bedrock and magma volatiles would induce surficial collapse and linear trough formation. At shallower depths, dykes can directly interact with water, producing hydrovolcanic eruptions if the pressure conditions are suitable (Fig. 12C). Otherwise linear troughs form similarly to the B case. Propagation closer to the surface would probably lead to dyke eruption.

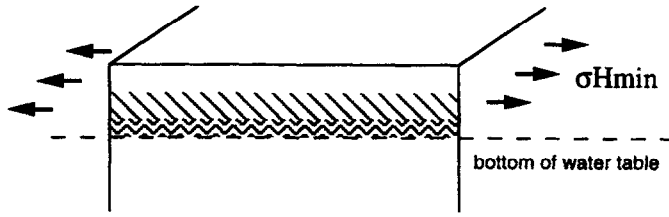
3. Graben formation



In this section the case that grabens lie above subsurface dykes is considered. Their length, up to 2500 km, is similar to the length of dykes observed in a number of giant mafic swarms on the Earth (e.g. Ernst *et al.*, 1996), and explaining such large horizontal propagation distances does not cause mechanical problems (e.g. Delaney, 1987). Consequently, arguing on the length of the Tharsis grabens against the dyke interpretation (Cyr and Melosh, 1993) is defensible with difficulty. Delaney (1987) showed that the main factors favouring propagation over large distances are magmatic crystallization heat (that may increase the wall temperature by 100°C and delay the solidification isotherm by three times) and dyke thickness e (increasing e increases the flow rate but has no influence on heat transfer toward the host rock, so that the propagation distance is a function of e^4). McDonald *et al.* (1988) calculated that if cooling did not occur, the 20 m wide Cleveland dyke in Scotland would have been able to travel over 4600 km with a constant 400°C wall temperature. Lister (1990) considered that the long propagation distances can be explained by primary dependence of dyke propagation on fluid mechanics laws (except near the dyke tip). All the terrestrial dyke swarms are mafic (Halls, 1987), and this plays a key role in explaining their lengths. Since Mars is smaller than the Earth, magma generation is easier (McKenzie and O'Nions, 1991), and is probably another factor favouring great propagation distances. Another reason, although not frequently observed on the Earth, is the possibility for melting of the nearby host rock when the rate of magma supply in a dyke is high, resulting in very long propagation time and distance before solidification (Bruce and Huppert, 1989). In fact, it appears that the length of the Tharsis grabens is not a barrier to the interpretation of dykes being underneath; it rather provides a formation mechanism which seems to cause far less trouble than other mechanisms, as also noted by Tanaka *et al.* (1991) and Mège and Masson (1996a).

3.1. Why non-feeder dykes?

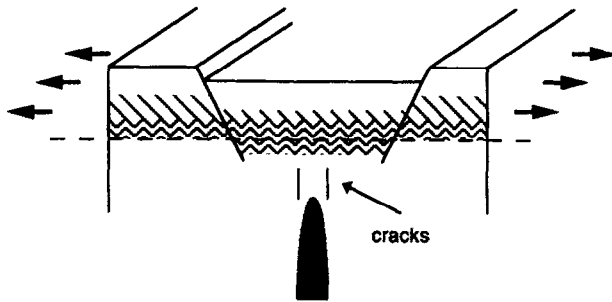
It may seem surprising that many Tharsis dykes did not reach the surface. Numerous grabens on Venus are also


INITIAL STATE



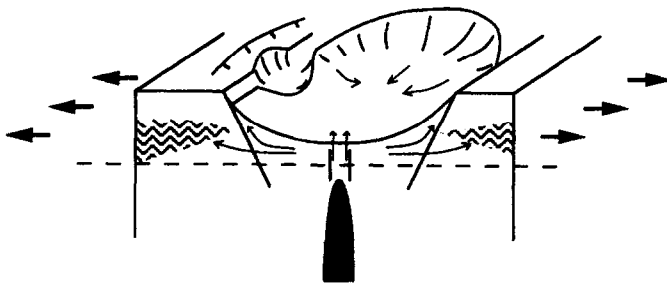
 permafrost
 liquid water
long term

A. DEEP DYKE



 dyke
location of faults influenced by the geometry of the process zone
instantaneous

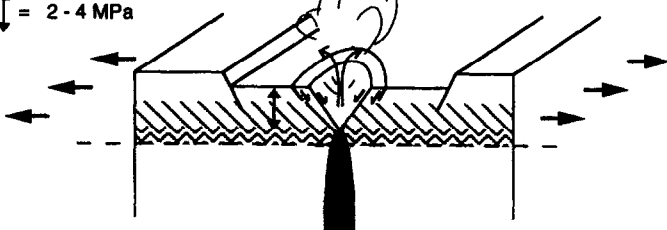
B. DYKE AT MIDDLE DEPTH



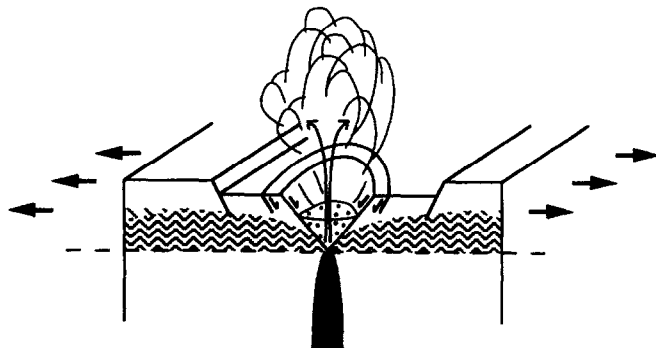
instantaneous to middle term
 • pressure pore increase and thermal pressurization flow
 • then hydrothermal flow
 → water escape

C. SHALLOW DYKE

↑ = 2-4 MPa



pressure pore increase → hydrovolcanism
 1. *instantaneous*



2. *short term*

suspected to have formed above dykes (McKenzie *et al.*, 1992; Parfitt and Head, 1993; Grosfils and Head, 1994; Ernst *et al.*, 1995b), and most of them are non-feeders. Geochemical analyses in Labrador (Cadman *et al.*, 1994), structural evidence in Iceland (Gudmundsson, 1983, 1984, 1995a), and geomorphological observations in Greenland (Peulvast, 1991) suggest that in these areas most of the dykes were non-feeders. First, dykes should be injected laterally from magma chambers. This is expected for crustal chambers when the density of the roof of the chamber is less than the density of the crust along the pathway of the dyke (Gudmundsson, 1987a). This situation should be common in large dyke swarms because of their mafic composition. Then, once dykes have begun to propagate laterally, they should continue doing so until magma flow stops. Several reasons for the propagation of non-eruptive dykes have been given, but only the two last ones from the list below seem to explain the formation of non-eruptive dyke swarms in virtually all the situations.

1. Watertable can help to freeze dykes at shallow levels (Gudmundsson, 1984). The efficiency of this mechanism is however limited since it does apparently not affect eruptions on the Earth's sea floor.
2. Dykes propagating upwards in a high Young's modulus layer tend to thin upwards (Gudmundsson, 1984), so that most of the magma may remain below this layer if it is continuous over large distances.
3. Rubin (1990) suggested that the probability of dyke eruption decreases when the regional context is strongly extensional, resulting in high driving pressure but low magma pressure.
4. Lister (1991) and Lister and Kerr (1991) showed that a level of neutral buoyancy in the crust might exist, above which the vertical propagation of dykes is impeded and stops. It would be located at the depth where the vertical gradient of magma pressure becomes greater than the gradient of horizontal stress in the host rock. Furthermore, Bonafede and Olivieri (1995) have shown that when the level of neutral buoyancy has been reached, most of the magma may remain below the upper tip if the dyke is shallow enough. However, if a level of neutral buoyancy exists in the crust, it does not explain field observation that dykes from a given swarm appear to stop propagating upwards at various crustal depths.
5. Lister (1995) has recently shown that solidification is an important mechanism for determining the height of ascent of melts in the lithosphere, suggesting that dyke tip solidification provides a cause for the arrest of vertical dyke propagation in the crust.

6. Early dyke emplacement in the crust generates compressional stress at shallow depth, so that they create a compressional stress barrier for dykes propagating later, which should then transform into sills at this crustal level (Gudmundsson, 1990a).

3.2. Origin of stress

That dyke emplacement may be responsible for graben formation is an old idea (Walker, 1965). Anderson (1951, pp. 152–153) had already noted the wedging effect of dykes. Field work indicates that tension cracks may occur around dyke tips (Delaney *et al.*, 1986). The “process zone” concept has been used to conveniently define the volume of rock around the dyke tip in which brittle failure occurs and graben formation may be predicted. It has to be noted, however, that other modelling concepts exist which cannot predict graben formation — see Pollard (1987) and Rubin (1993). In perfectly elastic material the process zone is spherical (Fig. 13), and its size depends on the driving pressure ΔP , which is the sum of P_m , the magma pressure, and σ_r , the remote stress:

$$\Delta P = P_m + \sigma_r \quad (1)$$

3.2.1. *Role of magma pressure.* Pollard *et al.* (1983) showed that the elastic stress field generated by dyke magma pressure can focus extensional strain on both sides above the dyke, and may therefore encourage graben initiation. The limitations of elastic modelling could not give information on graben formation (evolution, geometry) once the boundary faults have been initiated. Pollard *et al.* found field examples of slip on graben faults during dyke emplacement in Hawaii and in Iceland, however these faults already existed before dyke emplacement. Numerical modelling of fault slip induced by dyke emplacement was investigated by Rubin and Pollard (1988) and Rubin (1992) in incorporating a fault and a Coulomb-type friction law in elastic models. They showed that the tensile stress induced above the top of a dyke propagating between 4.4 and 0.4 km below the surface without remote stress is a few MPa; it is less than 1 MPa 2 km in front of the dyke. Such values are large enough to produce brittle failure or slip along pre-existing faults in jointed volcanic rocks, that Schultz (1993) estimates to have a tensile strength ranging from 0.2 to 2 MPa. Simi-

Fig. 12. Influence of dyke depth and presence of groundwater (including permafrost) on trough formation. The influence of pressure drop in dyke is not taken into account; pressure drop may be responsible for either additional normal faults and increasing the border fault throws (following mechanisms described in Section 1.2 and Figs 4–8). Initial state: extensional remote stress is applied and lasts throughout the trough formation mechanism. A: If the dyke intrudes deeply enough not to have any influence on groundwater and surficial tectonics, the process zone above the dyke helps focusing the remote stress on both sides of the dyke. B: If the dyke intrudes at shallower depth and heats the groundwater, volatiles escape, and contribute to trough formation above the dyke, or graben widening if the addition of remote stress and magma pressure reach the tensile strength of the bedrock. C: If the dyke reaches the watertable, pit formation (C1) results from hydrovolcanism under adequate pressure conditions. Ring faults are used as weakness planes during further explosion (C2)

of low magnitude stresses that may be released in a different way from that of high extensional stress instantaneously produced.

Seismic response to dyke intrusion in the south flank of Kilauea, Hawaii, on 2 January 1983 (Dvorak *et al.*, 1985) suggests that several pulses occurred within a few days, but most of the extension (tension cracks, small-scale normal faults) recorded at the surface along a line perpendicular to the dyke occurred within less than one day, at the end of the intruding event. Shortening contemporaneous to extension was recorded closer to the ocean, at a lower topographical level, in a landslide area. All the stress produced by dyke emplacement was thus not instantaneously released. Such a delay in the release of stress resulting from dyke emplacement has also been observed in Iceland (Sigurdsson, 1980).

In Hawaii, seismic activity associated to extension and landsliding of the south flank of Kilauea is more or less continuous, contrary to dyke emplacement. Consequently, it appears that dyke intrusion is a minor factor in surface extension, although it is a quite common phenomenon (Delaney and Wallace, 1995).

3.2.3. Origin of extensional stress in the Tharsis case. The geometry and location of faults 2, e.g. on Fig. 7a, are analogous to those of the structures obtained in Mastin and Pollard's experiments (Mastin and Pollard, 1988). Although other mechanisms of formation can be suggested, they might indicate migration of deformation toward the graben centre, like in Mastin and Pollard's experiments, indicating an important role of magma pressure in graben formation. However, most radial grabens in the Tharsis province do not display similarities to Mastin and Pollard's grabens. If magma pressure plays an important role of graben formation, then a mechanism for focusing most of deformation on two conjugate faults should be found. The simpler mechanism that may be suggested consists in releasing the stress generated by dyke emplacement after the end of the dyke emplacement, like in the Hawaiian case.

However, the basic problem if the magma pressure played a significant role in Tharsis graben formation is that the grabens induced by dyke emplacement on the Earth have depths ≤ 1 m, some hundred times less than the Tharsis grabens. This suggests that, in a general way, the remote stress should have played a major role in graben formation. Moreover, the formation of pit chains without grabens suggests that the magma pressure in a number of dykes somewhat similar to other dykes associated to graben formation was unable to cause significant surface deformation.

Schematically, σ_r may be analysed in the following way :

$$\sigma_r = \sigma_{TH} + \sigma_{REG} \quad (2)$$

where σ_{TH} is the part of the stress field generated by Tharsis, and σ_{REG} is Tharsis-independent.

We consider three possible Tharsis-generated sources of stress.

1. Inflation events in magma chambers produce extensional stress favouring radial extension, and subsequent deflation favours concentric extension (e.g. McKenzie *et al.*, 1992). Succession of inflation/

deflation events may thus explain the formation of both radial grabens and the concentric grabens around Syria Planum. In particular, dyke emplacement decreases the pressure in the magma chamber, and consequently should by itself induce remote extensional stresses (e.g. Bonafede and Olivieri, 1995). Since the magma chambers of the Tharsis province are probably larger than magma chambers on the Earth, this source of stress may have played a greater role in extension and may contribute to explain, to some extent, why some Tharsis grabens are deeper than the Earth's ones. However, numerous Tharsis grabens may be too far from the magma centres to have undergone a significant influence of these stresses.

2. Gravitational stresses generated by the Tharsis topography may have also contributed to produce extension at the surface (Chadwick and Dieterich, 1995). Similarly, they could not affect the longest grabens over their whole length.
3. Loading stresses may have contributed to produce the grabens (Banerdt *et al.*, 1982, 1992; Sleep and Phillips, 1985). Broad-scale loading stress on the Earth first follow rifting events (and thus early dyke swarm emplacement), and then the ending of all thermal and tectonic processes related to the rift activity (Grana and Richardson, 1996; Zoback and Richardson, 1996). Thus dyke swarm emplacement would likely be separated from crustal loading by an interval of at least a few tens of million years. Consequently, such stresses are not expected to have played a crucial role during dyke swarm intrusion within the framework of the plume tectonics model presented in Section 6, nor prior to dyke swarm emplacement, because they are generated by magma once frozen. Loading is an important source of stress on the Earth. If such stresses are involved in Tharsis graben formation, we expect them to have focused above the dykes because of the density and strength contrast between dyke and bedrock (e.g. Zoback, 1992). Nevertheless, the graben boundary faults are often deflected by pits and other kinds of troughs, but the latter appear to have never been affected by faults. The pits and troughs appear not to have been deformed by later tectonic processes. Thus the exact role of loading stress in graben formation cannot be clearly established. See Mège and Masson (1996a) for a discussion on sources of stress in the tectonic evolution of Tharsis, and Tanaka *et al.* (1991) and Banerdt *et al.* (1992) for alternative views.

Two other sources of stress can also be discussed :

1. Radial fracturing may have resulted from mega-impacts in the Tharsis region. Evidence of ancient impact basins in the Tharsis history have been discovered by Schultz and Glicken (1979) in the Syria Planum area, by Craddock *et al.* (1990) in the Daedalia Planum area, and by Frey and Roark (1995) in the Thaumasia Planum area. However, stratigraphic studies (e.g. Scott and Tanaka, 1986) clearly show that most of the grabens formed later than the possible impacts these authors have considered. Furthermore, grabens similar in dimensions to the simple grabens around Tharsis are not observed around large impact

basins on Mars nor on the Moon, so that formation of grabens following impact basin formation prior to dyke swarm emplacement is unlikely. Nevertheless, it is possible that radial fracturing produced by the mega-impacts guided later dyke propagation.

2. Geometrical analysis of dyke swarms given in Section 5 demonstrates the existence of a steady Tharsis-independent regional extensional stress source over the whole Tharsis hemisphere. We think that the magnitude of this source of stress, which is interpreted to be behind the formation of Valles Marineris, should have been high enough to have produced much of the extension observed in the Tharsis province. Graben location would be influenced by stress anisotropy or fracturing (without graben formation) on both sides of the dykes resulting from dyke propagation and emplacement (e.g. Pollard *et al.*, 1983), since the regional stress field was contemporaneous to dyke emplacement. If this regional field lasted for a long time after dyke swarm emplacement, the late stresses should have also focused on dykes because of the density and strength contrast between the frozen dykes and the bedrock, and also on earlier graben boundary faults.

4. Thickness, depth, and height of dykes

4.1. Theory

Some works mentioned above provide results that can be used to estimate the depth and thickness of dykes (Pollard *et al.*, 1983; Mastin and Pollard, 1988; Rubin and Pollard, 1988; Rubin, 1992), and were used by Head and Wilson (1994) to determine the depth and thickness of dykes on the Moon. These results can be used if P_m was strong enough to influence the location of the boundary faults. They are valid only if the grabens formed contemporaneously to the dykes, or if dyke emplacement was responsible for immediate formation of brittle structures that were reworked later.

It is convenient to summarize the results obtained by these works in classifying them as a function of the ratio ξ between the height and the depth to centre of the dyke (Fig. 13). An agreement has been found that the graben width is about 3 times the depth of the dyke top when ξ is close to 1, and its width decreases to 2 times when ξ decreases. There is conversely a noticeable discrepancy between the dyke thickness predicted by numerical and analogical models. When more than two structures form at the surface, the relations presented on Fig. 13 should be applied between the outermost surficial structures (Mastin and Pollard, 1988).

4.2. Depth and thickness of the Tharsis dykes

The relations on Fig. 13 were used to define the dyke depths and thicknesses in the Tharsis region. Nevertheless, it should be pointed out that these relations do not take into account the influence of the density contrast between

the magma and host rock (Halls, 1982) or the Young's modulus of the host rock (Gudmundsson, 1984) in graben width, although this factor clearly plays a role in the simple grabens of the Tharsis province. Indeed, observation on U.S.G.S. mosaics shows that the simple grabens are systematically wider in the regolith than in the Hesperian lava flows, e.g. in the Memnonia region (Fig. 11). This difference is consistent with the smaller value of the Young's modulus E in regolith than in lavas: $0.1 < E_{\text{sandstone}} < 0.6 \times 10^{11}$ MPa and $0.6 < E_{\text{basalt}} < 0.8 \times 10^{11}$ MPa (Turcotte and Schubert, 1982).

Relations on Fig. 13 are convenient since both dyke depths and thicknesses may be deduced from aerial observations. It is, however, impossible to choose the best value for ξ . In addition topographic data are not accurate enough to allow precise estimation of vertical and horizontal throws of the boundary faults (h and ε). The amount of erosion of the graben walls is also unknown, so that fault dips α cannot be defined either, neither the observed graben widths, nor the horizontal throws ε are representative of the real structure of the grabens. Based on observation, we made the rough approximation that slopes constitute 1/3 of the observed graben widths L_{obs} , and the floors constitute the remaining 2/3 of L_{obs} . Thus we considered that:

$$L \approx 2/3 L_{\text{obs}} + \varepsilon \quad (3)$$

where L is the real (structural) distance between the boundary faults and $\varepsilon = 2h/\tan \alpha$. In Iceland, vertical tension cracks horizontally grow up to a length of a few hundred metres, and then vertical throws develop. Eighty per cent of normal faults have 65–79° dips and the mean is 73° (Forslund and Gudmundsson, 1992). Consequently, in the calculations we assumed that graben faults dip 60° to 80°. In the Tithonium and Ius chasmata region of Valles Marineris the maximum value of h is less than 200 m (U.S.G.S., 1980), and observation of images suggests that the grabens in the other regions around Tharsis should not be deeper. We estimated that most of the fault throws range between 50 and 200 m. The 50 m value was chosen partly because few pictures have a better resolution than 50 m pixel⁻¹: without doubt smaller fault throws exist. Table 1 gives the ranges of dyke top depths for numerous quadrangles in the western hemisphere and Table 2 gives the range of plausible dyke thickness for the whole Tharsis region, as deduced from the relations on Fig. 13.

The results presented on Table 1 suggest that some dyke tops may be at depths of 2–3 km. Great depth discrep-

Table 2. Range of dyke thicknesses in the Tharsis region for the range of parameters discussed in the text. Symbols as on Fig. 13. Estimated realistic thicknesses are in bold italic

Dyke thickness		ε (m)	$e = 1.5 \varepsilon$ (m)	$e = 2.4 \varepsilon$ (m)	$e = 4.5 \varepsilon$ (m)
$h = 200$ m	$\alpha = 60^\circ$	230	345	555	1040
	$\alpha = 80^\circ$	70	105	170	320
$h = 100$ m	$\alpha = 60^\circ$	115	175	275	520
	$\alpha = 80^\circ$	35	53	85	160
$h = 50$ m	$\alpha = 60^\circ$	58	87	140	260
	$\alpha = 80^\circ$	18	27	43	81

ancies exist among the values displayed on Table 1, and if ξ is very close to 1 and dips close to vertical, a few hundred metres depth is in general sufficient to fit the graben characteristics. Table 2 shows that dyke thicknesses range from a few tens of metres to 1 km, but only three configurations predict thicknesses over 400 m. The best relation should be $e = 1.5 \varepsilon$ because it results from analogical modelling which explicitly accounts for brittle rock failure. The dyke thickness beneath the Tharsis grabens would thus be chiefly within the range 30–300 m, very close to the dyke thicknesses in the Mackenzie swarm (e.g. Fahrig, 1987).

4.3. Dyke height

The results obtained by Pollard *et al.* (1983) and Mastin and Pollard (1988) on dyke heights are subject to considerable error bars. However, according to their results, ξ tends toward 0.7 for deep dykes, and for shallow dykes ξ tends toward 1. Thus ξ for the deepest dykes on Table 1 should be quite close to 0.7. The deepest dykes (2–3 km) appear to have intruded the crust near Alba Patera. The diameter of hydrovolcanic pits directly gives the dyke depth during the first pulse (Lorenz, 1986), and similar values (~ 2 km) are given by the hydrovolcanic pits displayed in the northernmost part of the area on Fig. 6. Assuming $\xi = 0.7$ and $d = 2$ km, the dykes below the grabens of the western flank of Alba Patera should be about $2a = 15$ km high. If ξ were 0.8 or 0.9, $2a$ would be close to 24 or 54 km, respectively. For comparison, according to Wilson and Parfitt (1990), dyke thickness is mainly a function of ΔP and the dyke depth to centre d , and $\Delta P = 30$ MPa would be required to get a dyke more than a few tens of metres thick. Their calculations also show that the maximum possible dyke widths on Mars is 200 m, corresponding to a 30 MPa driving pressure and a depth to centre $d = 40$ km.

On Earth, dyke swarms can originate from shallow-level crustal magma chambers, e.g. in the Spanish Peaks case (Smith, 1987) and possibly for the Mackenzie swarm (Halls, 1987). Dyke swarms originating from chambers at the crust/mantle boundary are also common, e.g. the regional dyke swarms in Iceland (Gudmundsson, 1990b, 1995b), and the Scourie dyke swarm in Scotland (Halls, 1987). The thickness of Martian crust at the beginning of the Tharsis history is estimated to be 50 km in the crustal differentiation model by Schubert *et al.* (1992). Thus the dykes west of Alba Patera could have propagated over much of the crust.

5. Dyke swarms

5.1. Geometry and succession

Figure 14 shows regional dating of the Hesperian and Amazonian radial faults and elliptical faults around the Syria bulge. Dating is derived from the geologic map of Tharsis (Scott and Tanaka, 1986), studies by Tanaka and Davis (1988), Scott and Dohm (1990a), and personal

observations on 1:2 M and 1:500 K photomosaics from U.S.G.S. in the Tharsis region. Dating is also fully consistent with those more recently obtained by Dohm and Tanaka (1995). Since dyke emplacement is far quicker than the time span between terrain resurfacing, the grabens that could not be precisely dated from stratigraphic studies were attributed the age of grabens whose orientation and location suggest that they formed above the same dykes. To this end the grabens located close to Tharsis were especially helpful owing to the occurrence of recent lava flows. For instance some grabens in the cratered uplands of Memnonia were assumed to have the same age as some grabens of Daedalia Planum that formed on Amazonian Tharsis lava flows. This methodology is probably a chief difference between our mapping and those by Plescia and Saunders (1982), Tanaka and Davis (1988), and Scott and Dohm (1990a). It explains why we have not attempted to establish refined chronological relationships between graben sets.

We classified each continuous and discontinuous graben (as defined above) in four categories. The first graben category (Fig. 15a) includes structural features that could not be dated, and various Noachian graben sets. Among these structures is expected to be the first dyke swarm of the Tharsis history, centred on Solis Planum. It would correspond to the upper Noachian/lower Hesperian Thaumasia Fossae. Evidence comes from (1) the fan-like geometry of Thaumasia Fossae, typical of radiating dyke swarms (see several examples in Fahrig (1987)); (2) the high topography (11 km, one of the highest parts of the Tharsis area without the volcanoes) of the magma chamber that would have fed the dykes (A on Fig. 1). This interpretation is consistent with Frey's (1979a) interpretation of an early stage of Tharsis uplift.

Further indications would arise from pits and troughs, but dyke/water interactions are not expected so early in the Martian history. No material removal from grabens, nor collapse features, can be shown to have formed prior to upper Hesperian on the basis of the stratigraphic map by Scott and Tanaka (1986). This agrees with the works by Carr (1979) and Pollack (1979), who suggest that the grabens modified by geomorphological processes formed later than the others, after hydrolithosphere trapping in the porous regolith (Battistini, 1984), probably close to the Noachian/Hesperian boundary.

The three other graben categories are (1) Hesperian grabens formed prior to the Tharsis Montes volcanic fields (Fig. 15b), (2) upper Hesperian/Amazonian grabens clearly linked with the Tharsis Montes (Fig. 15c), (3) grabens in the Alba Patera area (Fig. 15d). The grabens east and north of Tharsis were rather easy to classify, but for the southern and western grabens we additionally took geomorphological criteria into account. We based our interpretations on the observation that some grabens have kept their structural morphology whereas some others, 10–15° apart, were intensely modified by geomorphological processes involving groundwater release (G1 and G2, respectively, Fig. 11). The angle between the two graben sets would not be significant in terms of stress if the grabens had formed in response to purely tectonic processes, however it clearly corresponds to a modification of principal stress trajectories in a dyke swarm context

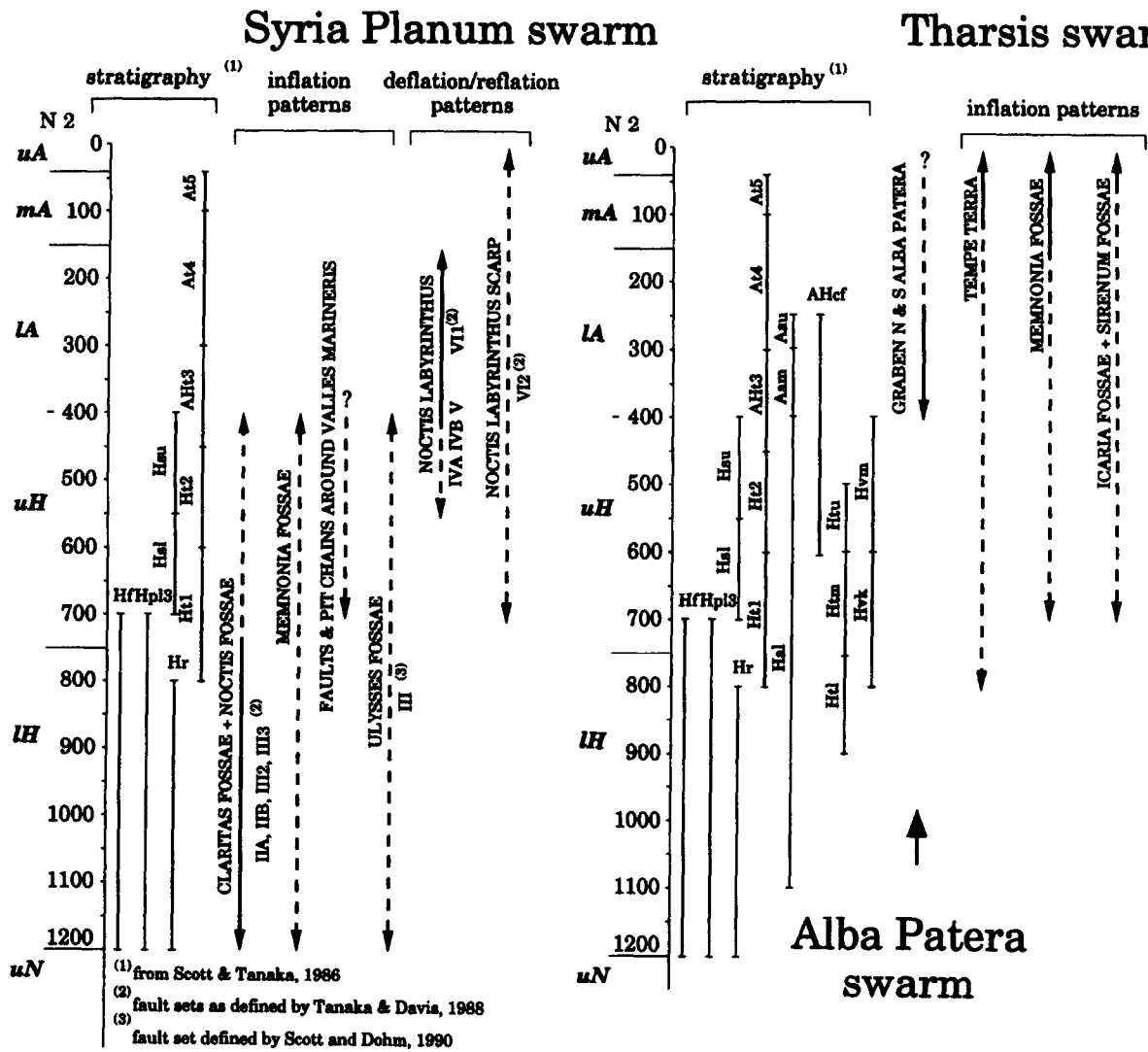


Fig. 14. Stratigraphic and geographic classification of Hesperian and Amazonian grabens in the Tharsis region.

(Halls, 1987). Therefore we classified some of the Memnonia Fossae on Fig. 15b and some others on Fig. 15c.

5.2. Direction of propagation

Figures 16a and b are extrapolations of graben trends on Figs 15b, c, and d the same way May (1971) did for dykes in the North Atlantic region before oceanization. Giant dyke swarms provide reliable broad-scale stress trajectories on Earth. The mean dyke trends propagate perpendicular to the least compressive stress (σ_3), as flaired by Geikie in 1893 and suggested by Stevens in 1911 (references in Pollard (1987)). Geologists have found that this is correct even in fractured regions (Halls, 1987; Gudmundsson, 1995a). The direction of propagation is not much influenced by weakly extensional stress states nor by stress states encouraging strike-slip faulting (Halls, 1987).

Delaney *et al.* (1986) studied the conditions required for a propagating dyke to reactivate previous joints. Most of their results are difficult to apply without field work. Nevertheless, two clues to dyke propagation along previous discontinuities can be used in remote sensing studies

such as the present one. First, splay faults should be observed, similar to those observed by Segall and Pollard (1983), should denote an attempt to reorganize the dyke trend perpendicularly to σ_3 (Delaney *et al.*, 1986). Secondly, individual dykes in dyke swarms that do not follow the same trend as most of the others may be suspected to have been influenced by previous fractures (although this could also arise in the case of small-scale variations of remote stress trajectories). From observation of Fig. 15, these two reasons confirm that dyke emplacement was perpendicular to σ_3 .

5.3. Stress field analysis

5.3.1. The Syria Planum-related stress field. The swarm trends present analogies with stress patterns due to superimposition of an isotropic field induced by events in a magma chamber and a non-null regional field (Odé, 1957; Muller and Pollard, 1977; McKenzie *et al.*, 1992). During magma inflation episodes, in the absence of a regional field, dykes injecting perpendicular to σ_3 are radial. This is not observed on Mars: the western part of Valles Mari-

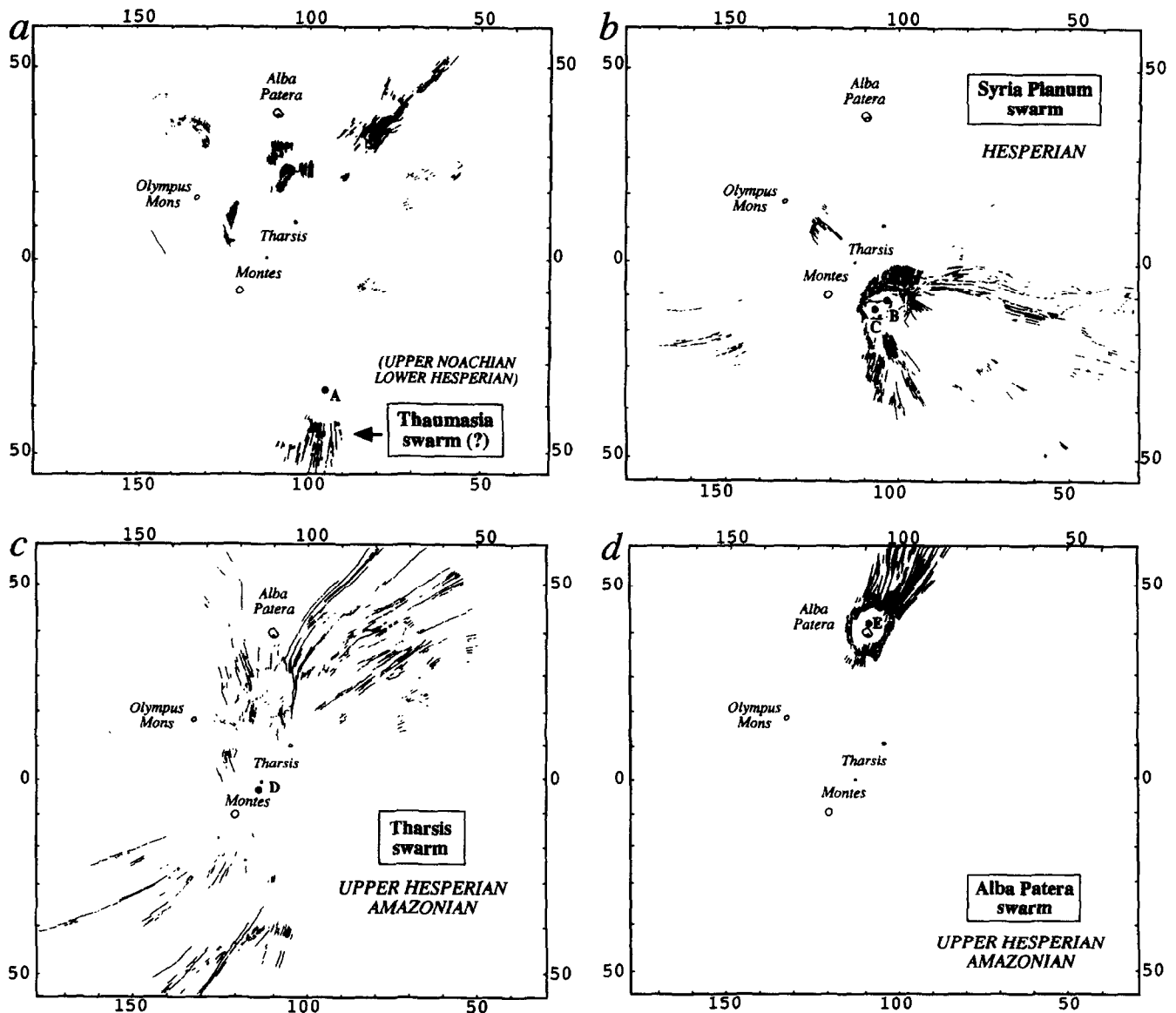


Fig. 15. Graben sets used to define Tharsis dyke swarms. The location of the Ascreaeus, Pavonis, Arsia, Alba, and Olympus calderas is indicated. The approximate location of the centre of the magma chambers responsible for dyke swarm emplacement is shown (A–E). (a) Various grabens (Noachian features, including the possible Thaumasia dyke swarm centred on Solis Planum, and other sets inconsistent with the graben sets displayed on (b), (c), and (d)); (b) grabens related to the Syria Planum centre (dashed line underlines Argyre basin); (c) grabens related to the Tharsis centre; (d) grabens related to the Alba Patera centre

neris strikes E–W whereas the eastern part of Valles Marineris strikes N105°E oriented. This observation can be explained considering the stress field generated by a chamber beneath Syria Planum during an inflation period. Close to Syria Planum, the local stress field dominates. Eastwards, another stress field dominates, and geometric relationships show that in this field the σ_3 trajectory trends about N020°E. Thus, one could speculate that the Tharsis rise in lower Hesperian consisted chiefly of the Syria Planum rise, located within a regional (wider) stress field. Elliptical grabens around Syria Planum are consistent with injection of new magma in the Syria chamber after magma withdrawal (McKenzie *et al.*, 1992). The difficulties for dating most grabens in the Syria region from crosscutting relations (Masson, 1980; Tanaka and Davis, 1988) may fundamentally arise from this mechanism:

since many episodes of magmatic inflation/deflation cycles occur in usual chambers (all the more in a large one such as in Syria Planum), many tectonic episodes may exist. A single graben may have formed in several stages. At least two major deflation episodes occurred corresponding to two elliptical graben annuli with different axis lengths (graben sets IVa and IVb1 of Tanaka and Davis (1988)). The great scarp of Claritas Fossae (fault set VIA of Tanaka and Davis) might have formed by roof collapse after a late withdrawal stage of the Syria chamber, from a striking analogy with the great Mauna Loa scarp (Carr and Greeley, 1980). Graben dating obtained by Tanaka and Davis suggest that the whole swarm mostly formed during lower and upper Hesperian. Consistent results have been obtained by Dohm and Tanaka (1994).

5.3.2. The Tharsis-related stress field. The Tharsis and

Alba swarms are interpreted on Fig. 16b since both evolved at the same time (upper Hesperian/Amazonian). The major difference between the Tharsis swarm here and the one modelled (and ruled out) by Carr (1974) (Fig. 3) is that Carr considered the three volcanoes as three interacting circular centres. Here, dyke swarm mapping reveals a single chamber located somewhere beneath the three Tharsis Montes. Consequently, one deep and three shallower magma reservoirs are required below the Tharsis central area. The wide chamber might lie at, e.g. the crust/mantle boundary, and would have been responsible for the emplacement of the Tharsis dyke swarm, whereas the formation of the three giant volcanoes would result from three individual chambers located, e.g. at the ductile/brittle crust boundary (Bonin, 1982), or at shallower depths, as a result of merging sills above dykes reaching a compressional stress barrier in the crust (Gudmundsson, 1990a). Zuber and Mouginis-Mark (1992) suggested that a magma chamber could exist within the Olympus Mons edifice.

The Tharsis swarm appears to be influenced by a regional stress field which slightly differs from the earlier one: σ_3 is N340°E. Systematic mapping reveals that about all the *échelon* patterns of radial grabens show right-lateral steps (Fig. 15c) and most are included in this swarm. This is interpreted as evidence of broad-scale tendency of reorientation of the propagating dykes from the domain where the Tharsis-related stress is dominant to a domain where the regional stress is dominant (propagation following a mixed I and III mode).

The deflection of the Tharsis stress patterns around Alba Patera (Fig. 16b) suggests that the dykes in this area were injected during a deflation event in the Alba Patera centre (McKenzie *et al.*, 1992).

5.3.3. The Alba Patera-related stress field. No graben in the vicinity of Alba Patera shows evidence of dyke emplacement (except the catenae that are interpreted as part of the Tharsis swarms). Close to Alba Patera, the grabens are also significantly wider than typical grabens associated with dyke emplacement in other areas of Mars. Their formation requires a purely tectonic extension mechanism. However, a few hundred kilometres northwards, in the Vastitas Borealis lowlands, the Alba Patera grabens display morpho-structural characteristics ("U"-shaped depressions, spatter cone chains; *en échelon* segments) suggesting dyke propagation. The transition in graben characteristics occurs after about 3 km topographic lowering from the caldera (U.S.G.S., 1991).

For comparison, in Icelandic fissure swarms like that of Krafla, the role of horizontal plate movements compared with bending stresses above magma reservoirs in the formation of extensional structures is unknown, but surface extension (through normal faults and open tension fractures) is due to some combination of both processes (Fig. 17) (Gudmundsson, 1987b; Opheim and Gudmundsson, 1989; Forslund and Gudmundsson, 1991). At deeper crustal level above magma chambers, extension would be mainly achieved through dyke intrusion.

Similar reasoning might apply to Alba Patera. Deep dykes from an Alba Patera swarm would have propagated horizontally up to Vastitas Borealis, where topographic lowering would have induced a shallower propagation

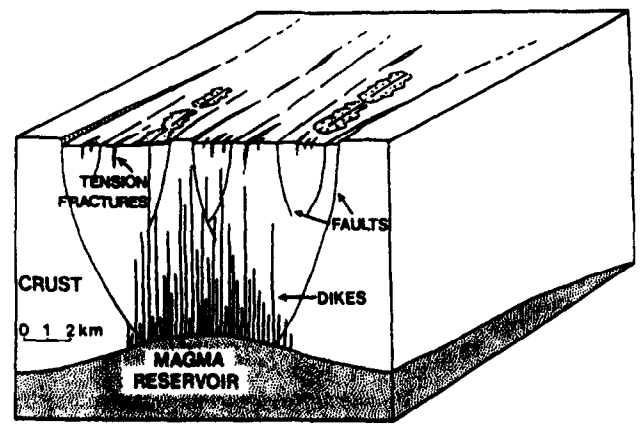


Fig. 17. Schematic cross-section of an Icelandic fissure swarm, due to horizontal plate movements and magmatic stresses (Forslund and Gudmundsson, 1991)

depth, leading to dyke/water interactions. The *en échelon* geometry of the grabens may reflect the geometry of dyke underneath. These dykes and grabens correspond to the Alba Patera swarm indicated by the dotted lines on Fig. 16b. Like in Iceland, dyke injection from the Alba Patera chamber would have been favoured by magma reservoir bending. The dykes could have also participated to deep extension above the reservoir.

Neither reservoir bending nor the regional stress field can explain the existence of the grabens far from the reservoir, like in Vastitas Borealis. The latter trend N-S to NNE-SSW, consistent with regional stress orientation, but alone it would have produced transtensional movements, in contradiction with the observation that the faulted lava flows are unshaped. Furthermore, in the absence of an additional stress source, the Alba Patera dyke swarm would tend to converge toward the horizontal stress trajectory perpendicular to the regional σ_3 (i.e. N070E), in contradiction with observations.

The existence of this additionally required stress field has been pointed out for a long time (Wise, 1976). It was recently considered again by Cyr and Melosh (1993) and Turtle and Melosh (1994). These authors supposed that this stress field could be linked with the Tharsis centre, and emphasized that it could have been disrupted by a stress field generated by the Alba Patera flexural load. The superimposition of both fields would have resulted in the deflection of grabens around the volcano. Existence of an Alba Patera-centred dyke swarm indicates that Alba Patera was located above a hot plume, an interpretation supported by the results of a gravity study carried out by Janle and Erkul (1991). In this interpretation, the ring grabens around Alba Patera can be alternatively produced by reservoir deflation stress. Reservoir deflation and later volcanic loading may have both contributed to ring graben formation.

5.4. Other dyke swarms in the Tharsis hemisphere

Locally some small magma centres should have also been responsible for radiating dyke swarm emplacement and subsequent graben formation. Two possible small swarms (more than 100 km long however) located in Tempe Terra

are shown on Fig. 18. No pits nor linear troughs are observed, however the graben sets shown with thick lines on Fig. 18c are local and centred on ovoid topographic lows and heights (A and B) interpreted to be volcanic troughs and constructs. Analysis of the trends of the local graben sets indicates that dyke emplacement occurred during a period of extensional remote stress field. The inferred stress trajectories are oblique to the stress trajectories inferred from the Tharsis graben swarm (grabens displayed with thin lines). This difference can be explained by the difference in graben age. The Tharsis swarm is dated upper Hesperian/Amazonian, whereas the two local graben sets have been dated middle to upper Noachian by Scott and Dohm (1990a). They would have formed during a period of early major extension of the palaeo-Tharsis province, which is not considered in the present paper (see Crumpler and Aubele, 1978; Scott and Tanaka, 1981). This early major tectonic activity produced the "Tharsis rift line" (Crumpler and Aubele, 1978) which denotes a least compressional stress trajectory roughly trended NW/SE, consistent with the bulk trend of the two local graben sets around the centres A and B on Fig. 18c.

Figure 19 shows another example of tectonic features possibly related to local dyke swarm emplacement, in Claritas Fossae. The timing of tectonic structure development in this area is extremely complex (Masson, 1980, 1986; Tanaka and Davis, 1988) and, like in the case of the Syria Planum swarm, the dyke swarm interpretation may help to overcome the problem caused by contradictory crosscutting relationships between structural features. Although which grabens formed above dykes on Fig. 19 and which did not cannot be accurately defined because the area is pervasively faulted, the fan grabens north and south of centre A (roughly the late Hesperian III 1 fault set of Tanaka and Davis, 1988) might have been influenced by dyke swarm trends. Other local magma centres should be expected in the area of Fig. 19 and in other places of Claritas Fossae from observed local disturbances and superimposition of small-scale and broad-scale strain fields. Small-scale dyke swarm emplacement also seems to have occurred in Acheron Fossae (Mège, 1994, p. 184).

6. Geodynamical implications

6.1. Plume tectonics: the Syria Planum example

6.1.1. *Basic considerations and summary of the model.* Giant radiating dyke swarms on Earth are commonly interpreted as direct consequences of hot plumes, above which further rifting may take place (e.g. Fahrig, 1987; recently Radhakrishna *et al.*, 1994; Zoback *et al.*, 1994; Ernst *et al.*, 1995a). The dyke swarms in the Tharsis province are consequently expected to have been also due to a hot mantle plume. On Earth the crust above plumes is thermally weakened and uplifted, and, provided that the regional context is suitable, may focus triple junctions. Intrusions occur within the three rift arms, two of them becoming a running rift, and the third one failing. The occurrence of crustal extension, and the geometry of

deformation, depend on the stress induced by plate motions. Without plate tectonics, the existence of three arms is expected to occur. The Syria Planum and Tharsis dyke and graben swarms have only two arms, 180° apart.

Below is developed a "plume tectonics" model (from a definition by Hill *et al.* (1992) reproduced in the Introduction). It is powerful in that it is based on some observations, both geomorphological and structural; it provides reliable stress patterns and clear indications for a lithospheric support, which consequences are shown below to predict the formation of all the tectonic structures formed during the Tharsis history that were not used to constrain the model (i.e. the wrinkle ridges of the western hemisphere, Valles Marineris, and the South Tharsis Ridge Belt) from simple considerations on terrestrial plume evolution (Mège and Masson, 1995).

Like all the swarm centres displayed on Fig. 1, the Syria Planum centre lies on a topographic high. The elevation of Syria Planum must be partly due to a permanent uplift mechanism because the lavas mantling its surface are 2–3 Ga old (Neukum and Wise, 1976; Hartmann *et al.*, 1981). However, in order to be in agreement with terrestrial evidence, dynamic uplift, produced by the thermal anomaly of a hot blob (White and McKenzie, 1989) rising from the core/mantle boundary (Morgan, 1971), should have to have preceded the lava floods by a few million years at least (Hill, 1991; Hill *et al.*, 1992). Models predict blob flattening below the lower boundary of the mechanical lithosphere, spreading of the hot material and formation of a hot mushroom head, and then eruption of voluminous basaltic-type lava flows named large continental igneous provinces on Earth (White and McKenzie, 1989, 1995; Griffiths and Campbell, 1991; Coffin and Eldholm, 1994). Stratigraphical studies (Scott and Tanaka, 1986) suggest that the lower Hesperian lava fields (mostly those affected by the wrinkle ridges) could be Martian analogues (Fig. 20). The crust must have been intruded with thick plutonic rocks lighter than the host rock, in order to induce buoyant crustal uplift and counterbalance the subsidence forces induced by the high density lavas at the surface (McKenzie, 1984; Finnerty *et al.*, 1988; Phillips *et al.*, 1990). An analogy may thus exist between (1) the Syria Planum intrusion, the lower Hesperian lava floods, and the Syria dyke swarm on Mars, and, e.g. (2) the Muskox intrusion, the Coppermine River flood basalts, and the Mackenzie dyke swarm on Earth (LeCheminant and Heaman, 1989; Ernst and Baragar, 1992). A point of interest arising from the comparison between lava floods and non-feeder dyke swarms on the Earth and on Mars is that the Tharsis lava floods might originate from the same source as the dykes, but could have a different composition (Cadman *et al.*, 1994).

Plumes are responsible for weakening of the crust and upper mantle (Hill *et al.*, 1992), which has important effects on crustal growth (McKenzie, 1984; Warner, 1990). The Martian highlands in the vicinity of Syria Planum are fully compensated (Smith *et al.*, 1993), and appear to have an average elevation 1 km higher than on the eastern hemisphere (U.S.G.S., 1991), implying a thicker crust. However, the topographic error bars are as high as this altitude difference. Schultz and Tanaka (1994) have already emphasized the 5–9 km elevation of the

Syria/Solis/Sinai plana area and the inferences for crustal thickness. This increased thickness could be direct consequence of mantle partial melting and accretion to the crust. Crustal uplift above plumes should generate radial compressional stress at the surface at the boundary between the uplifted and non-uplifted regions (e.g. Price and Cosgrove, 1990). The South Tharsis Ridge Belt appears to be correlated with such stress. Possible traces of compressional patterns at the boundary between the weakened crust and the normal crust can definitely not be observed around the outcropping dyke swarms on Earth, because of erosion.

In the following part of the text we consider that the number of plumes equals the number of dyke swarms. This does not mean that we are considering as many hot spots. A number of hot spots have been shown to have had a recurrent activity responsible for the emplacement of more than one dyke swarm on Earth: the 2.42–1.99 Ga Scourie dyke swarm in Scotland (Heaman and Tarney, 1989); the 1.27 Ga Mackenzie and 0.72 Ga Franklin dyke swarms, the 2.1 Ga Marathon, 2.08 Ga Fort Frances, and 1.14 Ga Abitibi dyke swarms, and possibly the 1.24 Ga Sudbury and 590 Ma Grenville dyke swarms in Canada (H. C. Halls, pers. commun., 1995). Although the reason for this to occur is speculative, three hypotheses can be proposed: (1) thermal instabilities at the core/mantle boundary; (2) plume separation at a viscosity discontinuity in the mantle (Bercovici and Mahoney, 1994), and (3) partial melting along the axis of a superheated Tharsis mega-plume; exothermic phase changes in the mantle would result in acceleration of the mantle flow, and production of distinct melting zones in the mantle (Breuer *et al.*, 1996). Consequently, perhaps the Thaumasia, Syria Planum, and Tharsis dyke swarms could have successively formed in response to the same plume. One reason for the occurrence of distinct volcanic centres could be lithosphere moving above the hot spot (Plescia and Saunders, 1982). Asthenospheric circulation may also cause plume deflection (e.g. Corrieu-Sipahimalani, 1995). In addition, the Alba Patera plume might represent a secondary effect of the major Tharsis plume (Janle and Erkul, 1991). Further modelling and observations on Earth should help understand these relations.

6.1.2. Prediction of wrinkle ridge formation in the western hemisphere. A number of compressional structures exist on both Martian hemispheres (Chicarro, 1983; Chicarro *et al.*, 1985; Watters and Maxwell, 1983, 1986; Plescia and Golombek, 1986; Watters, 1991, 1993). A ridge classification was established by Watters (1993). Those that are useful to chronologically and geographically constrain the Tharsis history are wrinkle ridges, which formed in smooth volcanic fields. They are typically a few hundred metres high, 10 km wide, and more than 100 km long. Most have arbitrary trends, however, in the Tharsis hemisphere they are roughly concentric about the dome. The largest wrinkle ridge concentration is on the eastern Tharsis flank (Fig. 1). Wrinkle ridges mainly occur in lower Hesperian lava materials, and probably formed rapidly after lava emplacement (Watters and Maxwell, 1983), as a result of buckling (Watters, 1991; Schultz and Watters, 1995; Watters and Schultz, 1995), resulting in either thin skin deformation (Suppe and Narr, 1989; Watters, 1991,

1993) or thick skin deformation (Plescia and Golombek, 1986; Zuber, 1995).

Their rough Tharsis-concentric geometry on the eastern Tharsis flank has been interpreted as an indication of the influence of Tharsis-related stress during their formation (Watters and Maxwell, 1983), but a secondary stress source is required to account for systematic deviation of some of them from a perfectly concentric geometry (Watters and Maxwell, 1986; Watters, 1993). Statistical analysis of wrinkle ridge trends (Watters, 1993) shows that the slightly non-Tharsis-concentric patterns can be explained by the presence of a secondary centre around which some ridges would have radially formed. The location of this centre does not correspond to any striking morphologic feature (major magma centre, impact basin, etc.). Consequently, we interpret Watters' results by the existence of a coherent Tharsis-independent stress source, responsible for a systematic deflection of wrinkle ridge trends which is reflected in the results of their statistical analysis. The formation of wrinkle ridges in the Tharsis hemisphere, which is contemporaneous to the Syria Planum dyke swarm formation, is consistent with the stress trajectories inferred from the swarm (Fig. 21). Therefore, the imperfect concentric geometry of wrinkle ridges around Tharsis would be a direct consequence of the existence of the regional stress field emphasized by the analysis of dyke swarm geometry.

Wrinkle ridge formation requires σ_3 to be vertical, which is inconsistent with dyke emplacement. One reason for this apparent inconsistency is the influence of lithostatic pressure at the depth of initiation of the structures. Dykes can form at deep crustal levels with σ_3 horizontal; at shallower depths, lithostatic pressure decrease lowers the magnitude of vertical stress, which may switch to σ_3 whereas σ_1 becomes horizontal, allowing wrinkle ridge initiation.

The above mechanism can explain simultaneous dyke and ridge formation. The scenario must however be refined, because (1) wrinkle ridges occur on lava flows only, not in the regolith (Watters, 1993), although regolith strength should be significantly smaller than that of the lava flows, and (2) ridge formation appears to be mostly contemporaneous to Syria Planum-centred radial faulting (Watters and Maxwell, 1983), which requires stress trajectories inconsistent with wrinkle ridge formation. Graben swarm formation lasted for a long period, thus wrinkle ridge formation must correspond to a short tectonic event either just before graben formation, or interspersed among the period of graben formation. In both cases the regional extensional stress source already existed when wrinkle ridges formed since it has been shown to have influenced their distribution.

Similar wrinkle ridges are also observed on the Moon, and have been interpreted to result from compressional stress induced by isostatic subsidence of the crust loaded by volcanic overburden (e.g. Schultz, 1972; Melosh, 1978). This mechanism is plausible on the Moon because the wrinkle ridges mostly occur in mare whose crust was thinned by giant impacts before lava flooding. Watters (1993) noted that some wrinkle ridges in the opposite hemisphere may also originate from this mechanism. Below we argue that the wrinkle ridges in the Tharsis

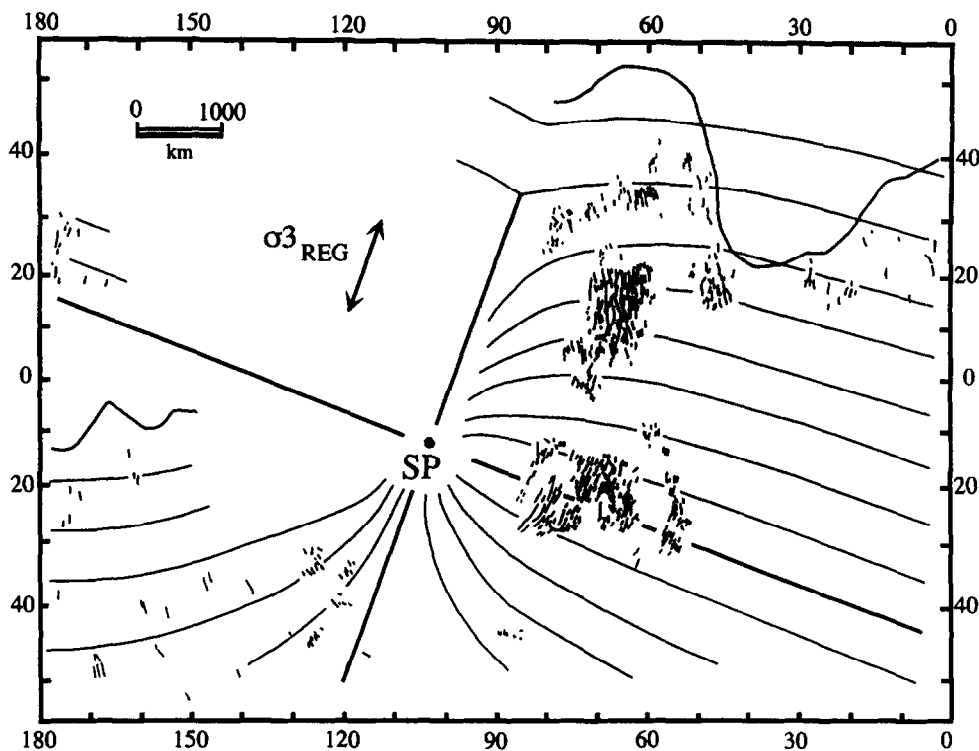


Fig. 21. Extrapolation of the stress field associated with the Syria Planum centre (Fig. 16a), and location of the wrinkle ridges (taken from Watters (1993)). Plain lines follow the horizontal principal stress perpendicular to σ_3 . The trend of σ_3 in the regional stress field is indicated by the arrow. The calderas of the three Tharsis volcanoes, Alba Patera, Olympus Mons, and the dichotomy boundary, are located

hemisphere may have the same origin, owing to the existence of the Syria plume.

The weakening effect of the Syria Planum plume should have increased the viscosity contrast between brittle and ductile crust, and thickened the ductile part at the expense of the thickness of the brittle part. (Alternatively, the crust might have been totally brittle before plume rising to the lithosphere, and the plume was entirely responsible for weakening part of the brittle crust. Unfortunately, thermal models are too poorly constrained to decide on the correct hypothesis — see Schubert *et al.* (1992).) Similar to the Moon, the lava load could have induced subsidence of the brittle crust in the ductile crust (Fig. 22, see also Fig. 6 in Mège and Masson (1996a)). Wrinkle ridge formation would be contemporaneous to, or would have formed very rapidly after lava emplacement, similar to wrinkle ridges observed in the Columbia River Basalt Group on the Earth (Reidel *et al.*, 1989). Rapid subsidence would have provided provisional compressional stresses at the surface, dominating over the other stress sources. After complete lava cooling and reaching of isostatic equilibrium, the total stress field in the ridged plains would have become extensional again, as before lava flooding, owing to the persistent extensional regional field.

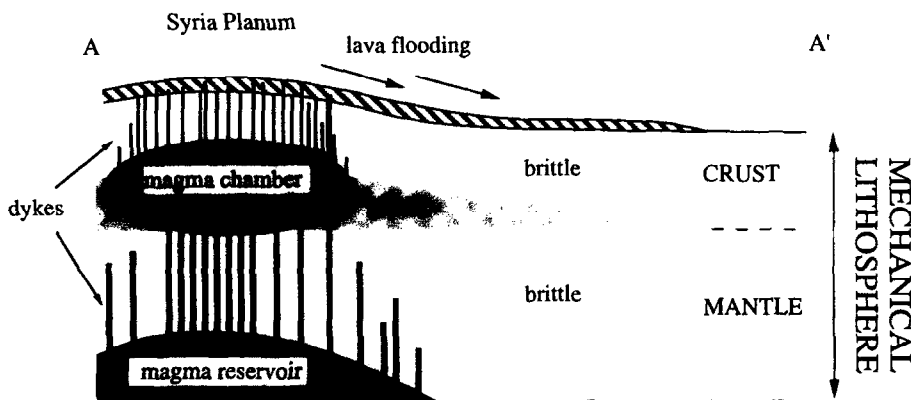
This mechanism for wrinkle ridge origin should be in agreement with topographic data. In some cases, wrinkle ridges occur in patches of lava flows, frequently corresponding to highly degraded upland craters, which are too small for the available topographic information to be very helpful (U.S.G.S., 1991). However, most wrinkle ridges of the Tharsis hemisphere are located in the larger

regions of Sinai Planum, Lunae Planum, and in the southern part of Tempe Terra. The most significant topographic evidence of subsidence is found in central Syria Planum, which is depressed 1–3 km compared with the surroundings. Gravity data indicates that the ridge plains are isostatically compensated, which is also in agreement with the isostatic subsidence interpretation (Frey *et al.*, 1995).

There are very scarce indications of wrinkle ridges that could be associated with later dyke swarms (especially the Tharsis one), in agreement with the plume tectonics model which predicts crustal thickening through magma accretion during the Syria Planum event. The crust should become sufficiently thick to support the lava load without significant further subsidence. Planetary cooling may also contribute to increase the crustal thickness (Schubert *et al.*, 1992).

6.1.3. *Prediction of Valles Marineris formation.* Structural aspects of the Valles Marineris evolution have been developed in several works (Blasius *et al.*, 1977; Masson, 1977, 1980; Frey, 1979b; Tanaka and Golombek, 1989; Schultz, 1991; Lucchitta *et al.*, 1992; Chadwick and Lucchitta, 1993; Anderson and Grimm, 1994; Mège and Masson, 1994a,b, 1996b; Peulvast *et al.*, 1996; Schultz, 1995). At least the major part of Valles Marineris formed after the formation of the ridged plains of the Tharsis province (Scott and Tanaka, 1986). On the basis of a work by Allemand *et al.* (1989), Mège and Masson (1996b) have emphasized the requirement for a weak crustal level and strong crust/mantle decoupling for explaining the formation of several parallel, roughly symmetric grabens

a Flood lava emplacement



b Wrinkle ridge formation

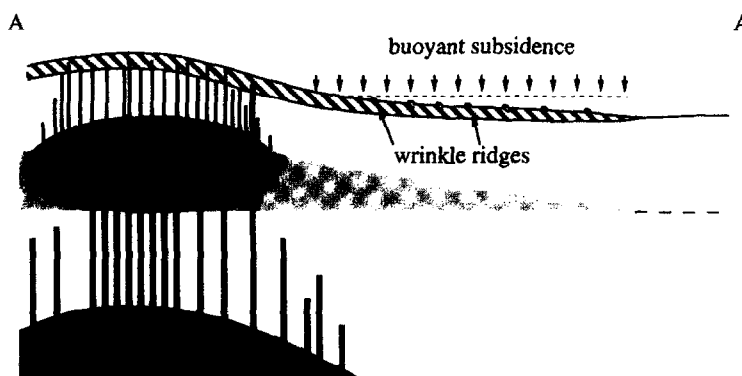


Fig. 22. Cross-section of Syria Planum and wrinkle ridge terrain south of Valles Marineris. (a) Syria Planum building and lava flooding above the plume head during lower Hesperian. The upper crust above the plume is decoupled from the mantle by a weak layer. In this interpretation, lava flows originate from above the area of melt generation and spread downhill, like expected above several hot spots on Earth (White and McKenzie, 1995). (b) Upper crustal subsidence after lava cooling and wrinkle ridges formation. Vertical axis not to scale. Location of profile on Fig. 20

instead of a single graben, like in, e.g. the east African and Baikal rift systems.

Valles Marineris is located on a secondary topographic bulge (U.S.G.S., 1991). Uplifting cannot be precisely dated, but appears to be linked with Valles Marineris extension. Uplifting did apparently not induce faulting and subsequent Valles Marineris extension. This follows because Valles Marineris did not form on the summit of the uplifted area, as noted by Schultz and Senske (1994), and because the amount of uplift cannot by far account for the vertical throws in the grabens (Chadwick and Lucchitta, 1993; Schultz and Senske, 1994). It may be argued that the current bulge does not reflect the initial thermal uplift at the onset of the Syria Planum plume activity, which might have been strong enough to trigger

the Valles Marineris formation by dynamic rifting (Chadwick and Lucchitta, 1993; Mège, 1994). However, rifting above a plume on Earth does not result from this early uplift (Hill, 1991; Hill *et al.*, 1992). Crustal weakening by a plume and thermal uplift merely allow “rifting to either proceed more rapidly or result in transfer of the axis of spreading to as near as is possible to the plume centre” (Hill *et al.*, 1992). We suggest that, like on Earth, both faulting and uplift in the Valles Marineris region resulted from extension induced by the regional stress field, and because of crustal weakening the location of the plume would have influenced the location of the graben system. The location and geometry of the Syria Planum dyke swarm would have guided those of the rift, by comparison to the Earth (Fahrig, 1987). Rifting should have been

Adiabatic decompression of mantle, partial melting, and uplift induced by Valles Marineris stretching

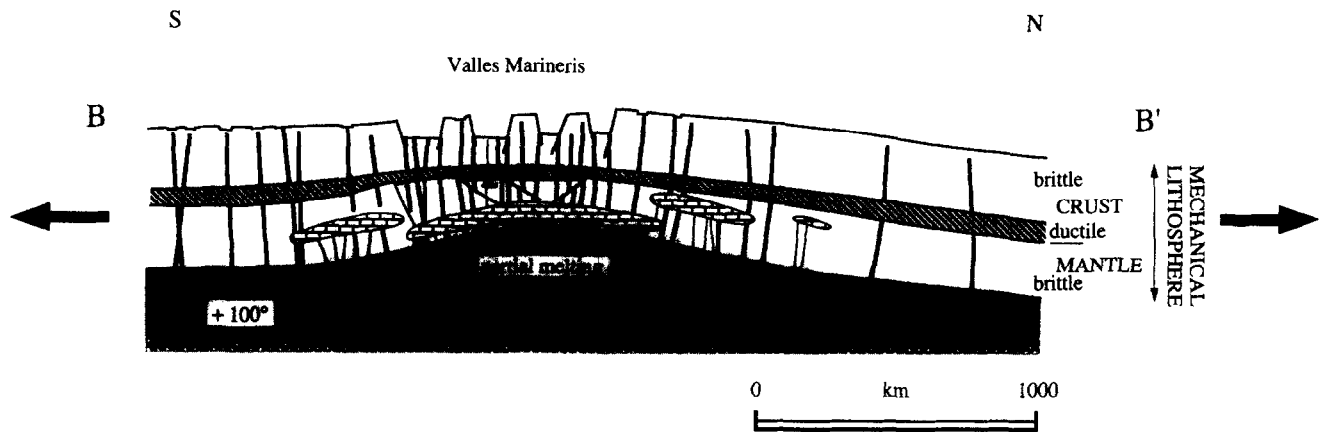


Fig. 23. Cross-section of the Valles Marineris region during extension, adiabatic mantle decompression, and partial melting, producing crustal thickening and topographic uplift. The thermal anomaly may not have exceeded 100°C above the normal potential temperature of the mantle. However a 200 or 300°C anomaly cannot be ruled out owing to uncertainty in lithosphere thickness. The early dykes dating back to the onset of the plume are shown with thick lines; most are non-feeders. The dykes feeding crustal intrusions induced by mantle decompression (bricked symbols) are indicated with thin lines. The location of intrusives in the crust, including dykes and other intrusives, is arbitrary. Vertical axis not to scale. Location of profile on Fig. 20

assisted by uplift-related stress (Houseman and England, 1986; Farnetani and Richards, 1994; Griffiths and Campbell, 1991).

Extension should have induced adiabatic decompression of the mantle, partial melting, and then local topographic uplift (McKenzie and Bickle, 1988; White and McKenzie, 1989) in the Valles Marineris area (Fig. 23). The location of the uplift summit would depend on the Valles Marineris location, but also on other parameters related to thermal plume characteristics. Uplift should vary as a function of the distance to the plume centre because less decompression occurs in distal parts of the plume, in accordance with observations (U.S.G.S., 1991). In details, variations of topography around Valles Marineris cannot be clearly correlated with variations of extension in the grabens. This case appears to be similar to the case of the Baikal rift on the Earth, where the location of magmatic activity is not simply correlated to the geometry of extension (Logatchev, 1993).

Voluminous volcanic materials have been suspected to lie within the Valles Marineris grabens under the form of stratified deposits, which date back to an early stage of Valles Marineris evolution (Nedell *et al.*, 1987). Other volcanic materials were emplaced more recently (Lucchitta, 1990). However, the Hesperian age of most of the Valles Marineris tectonic activity (Peulvast *et al.*, 1996) indicate that the topographic bulge observed is the result of a permanent process. We suggest therefore that most of the magma should lie within the crust or should be underplated (see McKenzie, 1984; Phillips *et al.*, 1990), as in common cases of rifting above hot spot (Hill *et al.*, 1992; McDonald and Upton, 1993).

The results by White and McKenzie (1989) show that the stretching factor β should be equal to 3 on Earth to

induce 1 km topographic uplift in stretched regions above plumes, if the thermal anomaly is 200°C . Mège and Masson (1996b) and Schultz (1995) showed that the maximum value of β in Valles Marineris does likely not exceed 1.1. For comparison, β is equal to 1.3 and 1.5 in the continental Baikal and East African rift system (references in Cloetingh *et al.* (1995)). Although a higher thermal anomaly should result in topographic uplift for such a small extension, it is not required because the acceleration of gravity (3.71 m s^{-2}) is one-third of that on the Earth. The amount of melt produced by the same quantity of adiabatic decompression should be significantly higher (McKenzie and O'Nions, 1991). The topographic uplift of the Valles Marineris area could have resulted from a low amount of stretching, limited adiabatic decompression, but production of a huge quantity of magma (Fig. 24). The quantity of molten material, the amount of partial melting, the intensity of the thermal anomaly generated by the plume, and the depth of the rheological boundaries in the lithosphere, are discussed below, depending on the current mode of Valles Marineris support. Despite uncertainty due to large error bars for small wavelengths corresponding to the Valles Marineris size, the most recent gravity model suggests that the Valles Marineris uplift is in partial isostatic equilibrium now (Smith *et al.*, 1993; Frey *et al.*, 1995). Therefore the true values of the parameters discussed should be in a transitional state between a fully dynamic and a fully compensated support.

Dynamic support. Up to at least 5 km uplift was produced in the Valles Marineris area (U.S.G.S., 1991), corresponding to a minimum of a 5 km thick melted layer (i.e. the uplift is not compensated at all). A 1250°C potential mantle temperature (the temperature the mantle would

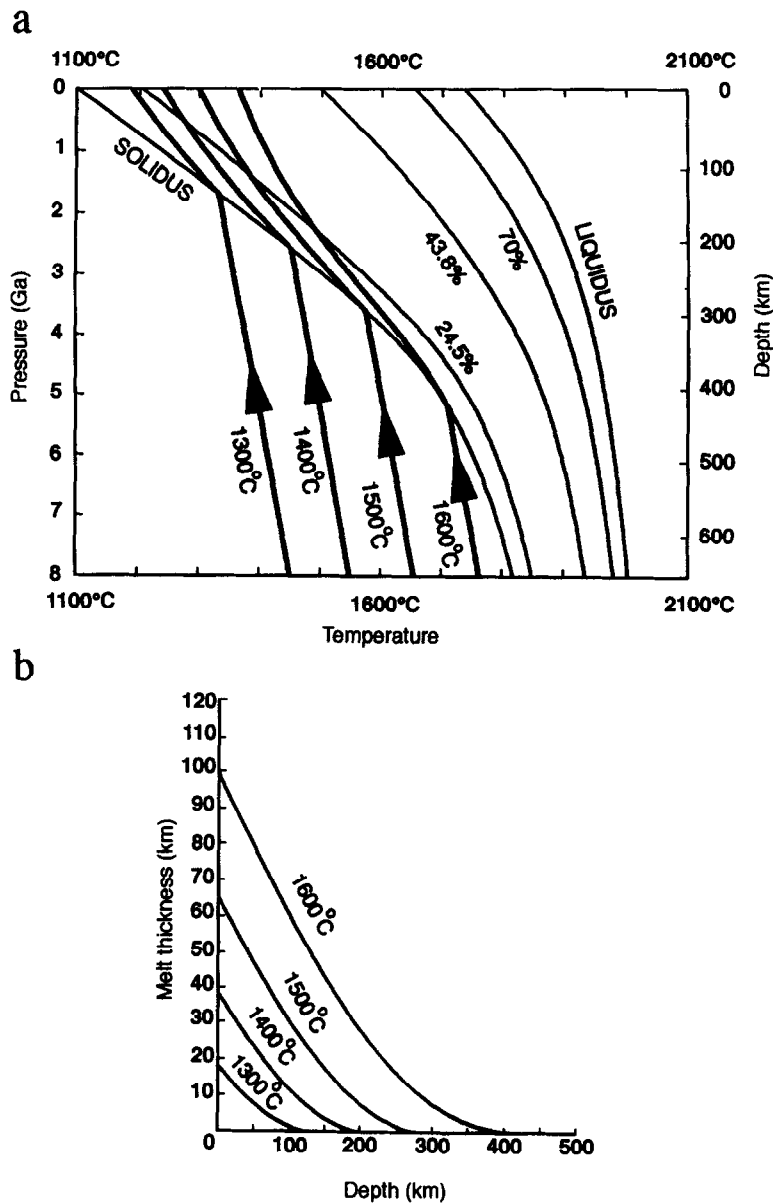


Fig. 24. (a) Effect of adiabatic decompression of the Martian mantle at four potential temperatures. (b) Melt thickness generated below the depth given on the horizontal axis. Entropy of melting: $400 \text{ J kg}^{-1} \text{ }^\circ\text{C}^{-1}$; solid density: 3300 kg m^{-3} ; melt density: 2800 kg m^{-3} ; acceleration of gravity: 3.71 m s^{-2} (figure from McKenzie and O’Nions (1991) adapted to Mars)

have at surface) is able to produce this layer, provided the melting depth is 20–30 km. Melting depth values must be higher than the crust/mantle boundary; 20–30 km would then be inconsistent with the 50 km crustal thickness obtained by Schubert *et al.* (1992) during the period of Valles Marineris formation, 3.5 Ga ago (Hartmann *et al.*, 1981). If the potential temperature of the normal mantle is similar to that on Earth, i.e. $\sim 1300^\circ\text{C}$, the 5 km thick layer could have been produced between 140 and 70 km depths. Adding a 100°C thermal anomaly generated by the plume would allow the mantle to melt between 210 and 140 km depths. By comparison, theoretical models often consider 150 km as a likely current Martian elastic lithospheric thickness. At 140 km depth the melt fraction would not exceed 10%.

Fully compensated support. Considering that Valles Marineris is fully Airy-compensated, and taking mantle

and crust densities to be 3300 and 2700 kg m^{-3} , respectively, the Airy compensation root would be 45 km thick. The whole thickness of accreted material would thus be 50 km. This maximum thickness could have been produced below a 100 or 150 km thick lithosphere, requiring a 1550 or 1600°C anomalous mantle, i.e. 250 or 300°C hotter than the current normal Earth mantle, respectively. The latter thermal anomaly would allow the melting of 270 km of mantle, between 420 and 150 km depths, corresponding to 25% of partial melting.

On Earth, plumes are generally 1000–2000 km in diameter. The ratio between the head diameter and the diameter of the central, hottest, region for the plumes taken as examples by White and McKenzie (1989) is within the range $R = 5$ –13. According to the current topography and morphology, the size of the Syria Planum plume central zone would be 500–1000 km at most (Fig. 20), i.e. the size

of the whole 110 Ma old Bermuda plume, but less than half the size of the Iceland plume. If the Valles Marineris eastern end is taken as the outer boundary of the weakened crust above the plume head, R ranges within 6 and 12, a value consistent with terrestrial values. The diameter of the weakened zone would be close to 6000 km, three times the size of large terrestrial plumes. The surface of the zone mantled by the lower Hesperian flood lavas on Lunae Planum (Fig. 20) exceeds the diameter of the plume, and can be explained by the topographic slope decrease toward Chryse Planitia.

Terrestrial modelling suggests that the duration of magmatic activity due to adiabatic decompression of mantle is also of the order of a few million years (White and McKenzie, 1989). Moreover, since decompression melting should be easier on Mars than on Earth, it may be an even faster process, and the Valles Marineris formation may have been completed within a very short time span.

6.1.4. *Prediction of the formation of the South Tharsis Ridge Belt.* Schultz and Tanaka (1994) studied a set of Noachian and/or early Hesperian broad compressional ridges, the South Tharsis Ridge Belt. The ridges are several hundred metres to 2 km high, a few hundred km long. Their distribution roughly defines a half-circle located south of Tharsis, centred on Syria Planum. The belt extends from the Memnonia region westward to the south of Valles Marineris eastward.

The radius of the half-circle is close to the radius of the plume head determined from the outer boundary of the Valles Marineris bulge. Twenty-nine ridges have been found, but only four ridges are clearly not consistent with the hemi-circular geometry (Schultz and Tanaka, 1994). The upper Noachian/lower Hesperian age of the South Tharsis Ridge Belt fits the age of the uplift predating the flood lavas above the plume. The uplift above the Syria plume should have induced compressional stresses at the boundary between the uplifted/non-uplifted areas in the upper part of the lithosphere (Price and Cosgrove, 1990, p. 190) which could have resulted in the South Tharsis Ridge Belt formation. Lithosphere weakening by the plume thermal anomaly should have enhanced wrinkle ridge formation in the part of the crust undergoing compression. There is thus a good conceptual agreement between the stresses predicted by the plume interpretation and the geometry of the South Tharsis Ridge Belt. The four ridges that do not fit with the South Tharsis Ridge Belt half-circle, together with the absence of ridges north of Valles Marineris, may be attributed to crustal heterogeneities and variations of crustal properties due to, e.g. buried impact craters or basins (Schultz and Glicken, 1979; Craddock *et al.*, 1990; Frey, 1995). The deposit of more recent materials (upper Hesperian, Scott and Tanaka, 1986) north of the dichotomy boundary may also have contributed to this apparent distribution asymmetry. It is also possible that formation of the dichotomy early in the Martian history worked as an arresting mechanism for the ridges to form. The correct reason is, obviously, unknown.

The Noachian compressional ridges observed in the Memnonia region by Zimbelman (1989) might correspond to traces of early Tharsis bending as well. However, they do not display any evidence of curvature around Tharsis.

Other clues of tectonic structures which might have resulted from early Tharsis crustal bending are given in the companion paper (Mège and Masson, 1996a).

6.2. *Timing of plume activity and dyke swarm emplacement*

Tharsis is sometimes considered to have been active as a single spot over a long period of time. Consequently, a thermal anomaly should have been necessary for as long as the magmatic activity lasted in the region, but, in contrast, it should have negligible or no effects in the other regions of Mars. Nevertheless, there is not any clear evidence that Tharsis evolved like a single spot, and over the whole time span of its history. The only available data on which the interpretation of the duration of the Tharsis activity are based are stratigraphic interpretations (Scott and Tanaka, 1986). These interpretations make it possible to give an age interval separating the formation of the outcropping terrains from today from the amount and size of impact craters: they have little implications on the duration of magmatic and tectonic events.

Plumes last over several tens of million years at least on Earth. The Iceland hot spot may be active for 130 Ma (Lawver and Müller, 1994). They should last for a long time on Mars as well. On Earth, formation of one dyke may take from hours to thousands of years (Gudmundsson, 1995b). Most of the giant dyke swarms emplaced in a few million years at most: for instance those linked with the Mackenzie (LeCheminant and Heaman, 1989), Scourie, Matachewan (Heaman and Tarney, 1989; Halls, 1991), Franklin (Heaman *et al.*, 1992), Long range (Kamo and Gower, 1994), Grenville (Kamo *et al.*, 1995), Harp, and Kikkertavak (Cadman *et al.*, 1993) igneous events. Although the total period of time covered by the Tharsis evolution may have been very long, 3 Ga or so, the comparison with the timing of dyke swarm emplacement on Earth suggests that much of the tectonic activity of Tharsis might have been concentrated within a few crisis events that did not take more than a couple of million years. Existence of several magmatic episodes separated by long periods of quiescence is also supported by stratigraphic studies (Neukum and Hiller, 1981; Hiller *et al.*, 1982).

Dyke swarm emplacement is usually not triggered by mantle decompression. However, because Mars is smaller than the Earth, mantle decompression and further partial melting around the plume may have been produced earlier in the hot spot history than on Earth. A magma layer around the plume head may have existed beneath the bent area. If for instance the depth of the mechanical boundary layer was 150 km, the normal mantle temperature 1300°C, and the thermal anomaly at the Syria Planum plume head 200°C, the melt layer could be 60 km thick and the amount of partial melting 20% at the mechanical boundary layer level (Fig. 24). The magma in the melt layer would have migrated toward the top of the bent area, i.e. toward the main magma chamber, from which the dykes were issued at the onset of plume activity. As long as the magma chamber could be fed, overpressure would have led to

dyke intrusion. Thus, contrary to the Earth dyke swarms, the Tharsis swarms might have intruded the crust around the same centre as long as the plume was active and allowed magma to ascend to the magma chamber.

6.3. Arresting mechanisms for dyke propagation: consequences for the models of lowland formation

Stiffness contrasts in the host rock affect dyke propagation, and can play a role as arresting mechanism (e.g. Pollard, 1987). For instance, the Argyre mascon might have stopped propagation of dykes injected from the Syria Planum centre (Fig. 16a). The Valles Marineris area may have been strengthened during extension by underplating and intra-crustal accretion, and may have impeded the propagation of dykes injected from the Tharsis centre (Fig. 16b). Similarly, the Olympus Mons magmatic materials may have impeded propagation of the Tharsis dyke swarm westward. The influence of the dichotomy boundary as a stiffness discontinuity is more difficult to evaluate. The recent huge Olympus Mons volcanic deposits prevent observation of a possible effect of the dichotomy boundary on the propagation of the Tharsis dyke swarm. Eastward, in the Tempe region, the dykes appear to have stopped propagating significantly before reaching the dichotomy boundary, so that its influence cannot be defined there.

The influence of the dichotomy boundary on the Alba Patera swarm cannot be assessed owing to the uncertainty on its location compared with the location of the volcano. Nevertheless, the Tharsis dykes propagating east and west of Alba Patera clearly cut across the dichotomy boundary but appear not to have been affected by its occurrence. Consequently, the analysis of dyke propagation pathways suggests that the stiffness contrast between the lowland and highland crusts may have been weak. Similar conclusions are implied by possible evidence of sill propagation across the dichotomy boundary (Squyres *et al.*, 1987; Wilhelms and Baldwin, 1989). (Sill emplacement requires a state of stress different than that for dyke emplacement, however switching between dyke and sill emplacement during a single geodynamic event appears to be common on Earth and can result from various mechanisms, as shown by Fyfe (1992) and Gudmundsson (1990a).) If this interpretation is correct, models of lowland crust formation from basaltic resurfacing over a thinned highland-type crust (e.g. Breuer *et al.*, 1993) would be more favoured than models involving an oceanic-type crust (Sleep, 1994).

7. Discussion

The "plume tectonics model" discussed above is based upon (1) the inelastic response of the crust to overpressure and underpressure within intrusive bodies, and (2) a non-negligible regional stress field. It is furthermore supported by common mechanisms on Earth, and is consistent with the suggestion that dyke swarm emplacement associated to graben formation should be a major process in the

tectonic evolution of silicated planets (e.g. McKenzie *et al.*, 1992; Head and Wilson, 1994; Ernst *et al.*, 1995a,b, 1996). Previous structural mapping in the Tharsis region is also in agreement with our results — the differences with the mapping by Frey (1979a), Plescia and Saunders (1982), and Scott and Dohm (1990b) result from our mapping hypotheses presented in Section 5.

Dynamic uplift was considered as unable to produce the Tharsis radial structures in previous tectonic models (Banerdt *et al.*, 1982, 1992), but these models only considered elastic processes and elastic stress. Giant radiating dyke swarms on Earth would never be interpreted as resulting from hot spots (e.g. LeCheminant and Heaman, 1989; Ernst *et al.*, 1995a, 1996) if the terrestrial crust were modelled as an elastic plate, because such modelling does not (by definition) consider stresses resulting from the existence of liquid magma.

The most recent model of Tharsis tectonic evolution has been suggested by Tanaka *et al.* (1991), and is based on the "detached crustal cap" model (Banerdt and Golombek, 1990). It considers that the peripheral parts of Tharsis are flexurally supported by a wholly brittle lithosphere, whereas the crust in the central part is sufficiently thicker to be partly ductile. The brittle crust would thus behave as a "detached cap" undergoing support stresses akin to isostatic stresses. Many tectonic features can be explained by this composite "quasi-isostasy" and flexural support (Tanaka *et al.*, 1991). Nevertheless, several structural concerns remain. Below is a discussion pointing out similarities, differences, difficulties and positive points of both Tanaka *et al.*'s model and the present one.

The first point is that the South Tharsis Ridge Belt was discovered too recently to be included in the detached crustal cap model, and its consistency with the latter has still to be checked.

In Tanaka *et al.*'s model, the radial patterns were produced by the stresses associated with the detached crustal cap system. The wrinkle ridges were attributed to global contraction induced by planetary cooling and a compressional state of stress near the periphery of the rise. Overburden removal could have increased the deviatoric stress because it decreases horizontal stress to 1/3 of the vertical stress. Tanaka *et al.*'s model presents analogies with ours: both models predict compressional features at the periphery of the rise (wrinkle ridges for Tanaka *et al.*; South Tharsis Ridge Belt for the plume tectonics model), and emphasize the role of a weak layer for radiating pattern formation. Furthermore, following Schultz (1988), dyke injection was also suggested by Tanaka *et al.* as a possible mechanism for the formation of the Tharsis grabens.

However, some inconsistencies between Tanaka *et al.*'s model and structural observations exist. Some were pointed out by Watters (1993): (1) Some wrinkle ridges are buried by more recent lava flows (Watters and Maxwell, 1986), and their location is likely inconsistent with the stresses predicted by the detached crustal cap. (3) Overburden removal would produce disorganized patterns because it tends to equalize the horizontal stress magnitudes (provided the material is isotropic and homogeneous). Moreover, according to Tanaka *et al.* the wrinkle ridges should have formed all around Tharsis,

but Watters (1993) showed that the wrinkle ridges occur in volcanic terrains only (other kinds of contractional ridges are not the so-called "wrinkle ridge" morphology). He concluded from the inconsistency between the wrinkle ridges and Tanaka *et al.*'s model that further models for the origin of the stresses must explain a series of features (p. 17057); those relevant for the Tharsis province are accounted for by the plume tectonics model.

Radial graben depths are mostly constant when they were not further deepened by geomorphological processes. Tanaka *et al.* presented several models for radial graben formation, all of them involve a shallow planar discontinuity where grabens initiate above dykes. Such discontinuities might be linked with permafrost, with the regolith/lava flows boundary, or with bedrock/regolith interface. However, the permafrost depth varies considerably throughout the Tharsis region (Costard, 1993), lava flows do not blanket the whole Tharsis province, and the depth of the bedrock/regolith interface depends on lava flow occurrence. Generally, dyke upper tips cannot be correlated with the existence of a planar discontinuity level on Earth (Pollard *et al.*, 1983; Mastin and Pollard, 1988; Rubin and Pollard, 1988; Rubin, 1992; Lister, 1991; Lister and Kerr, 1991; Schultz, 1992a,b; Agnon and Lyakhovsky, 1995; Bonafede and Olivieri, 1995). According to Table 1, the dyke upper tips in the Tharsis region should be at crustal depths of several hundred metres to a few kilometres, i.e. below the Hesperian lava floods that mantle much of the Tharsis hemisphere (Plescia and Saunders, 1980; De Hon, 1982), probably within a part of the crust supposedly affected by the intense early meteoritic bombardment. These terrains are well outcropping on the Valles Marineris walls, where they can be shown to have a poor cohesion (Peulvast *et al.*, 1996). Similar to some dykes in the Scoresby Sund of Greenland which appear to have stopped propagating vertically within a weak sedimentary layer, although this layer is stratigraphically located just beneath a strong basaltic layer (Peulvast, 1991 and pers. commun., 1994).

The model by Tanaka *et al.* does not account for the Valles Marineris formation, contrary to the plume model which considers its formation as a natural consequence of simultaneous occurrence of a regional stress field and a plume — a phenomenon well documented on Earth. In the present model the chasma geometry follows the previous dyke "skeleton" (see also Schultz, 1988), like for terrestrial rifts. The rift trend was influenced by the balance between magma overpressure and regional stress magnitudes. For this reason the chasma trend is E–W close to Syria Planum, and N075°W farther (Figs 1 and 15b). No quantitative model of the detached crustal cap is available yet, however the stress trajectories resulting from isostatic support were calculated by previous models (e.g. Banerdt *et al.*, 1982), and do not predict the E–W trend. Consequently isostatic stresses would have been responsible for strike-slip movements on these faults, which are not observed. Similarly, few tectonic structures in Claritas and Thaumasia fossae can be explained by the elastic models of loading.

Several kinds of reasons can be put forward to explain why the stresses calculated from elastic models do not fit the structural observations: (1) lithostatic pressure (Gol-

ombek, 1985) and pore pressure are not taken into account, consequently the models are valid only if the structures formed at the surface; (2) no failure criterion is taken into account (McGovern and Solomon, 1993; Schultz and Zuber, 1994).

The Elysium province, the second major (but smaller) volcano-tectonic region of Mars, can provide further information on this discrepancy between the predicted stresses and strain. Its age corresponds with the first stages of the evolution of the Tharsis volcanoes, so that it should currently undergo a loading support. Calculations by Hall *et al.* (1986) showed that the deviatoric stress produced by the load of the Elysium region is theoretically enough to induce brittle failure at the surface. Hall *et al.* investigated various combinations of elastic plate support and the resulting stress magnitudes, and all the combinations are theoretically suitable to produce major structural patterns at the surface. However, tectonic deformations in the Elysium province exist, but are very sparse. We conclude that most of the loading stresses must have been released through other processes during load growth. From stratigraphic dating of the lava flows, Tharsis is probably currently supported by a loading mechanism. Of course, grabens previously formed above dykes may have contributed to loading stress release; however, clearly, the Elysium case underlines that they may not have played a fundamental role. For instance, loading stresses, which result from body forces, could have primarily produced closing of pore discontinuities (due to compressional stress) or gravity sliding along these discontinuities (due to extensional stress) would have produced regolith packing.

Our approach considers what should have occurred before magma freezing and significant lithosphere loading. Consequently, our results are in complete agreement with classical loading supports (e.g. Banerdt *et al.*, 1982) as well the detached crustal cap support as presented by Banerdt and Golombek (1990), which are moreover supported by gravity and topography data. The plume tectonics model aims to describe the early stages of Tharsis evolution, during which most of the structures formed, and the loading models describe later stages of evolution. The Elysium case suggests that loading stress may not have played a significant role in the formation of the observed tectonic structures; this expectation is also in agreement with the observation that any pit in the Tharsis hemisphere seems to have been affected by further tectonic activity. Nevertheless, structural geomorphology analysis suggests that tectonic deformations in Valles Marineris were produced until recently (Mège, 1991; Peulvast *et al.*, 1996), and the most recent deformations might have been induced by the focus of both Tharsis and Valles Marineris bulge-related loading stresses in this area (Mège and Masson, 1996b). This appears to be in agreement with the observation that large-scale loading is an important source of stress on Earth (Fleitout and Froidevaux, 1982; Fleitout, 1991; Zoback, 1992), especially beneath continental rifts (Assumpção, 1992). Nevertheless, the plume tectonics model should answer the following difficulties.

1. The size of the dyke swarms involved would not be unrealistic on Earth, but Mars has half the Earth's

diameter and it could be argued that the plumes required are too large compared with the planet size to be realistic. Breuer *et al.* (1996) have shown that taking the exothermic phase transitions in the mantle into account allows formation of megaplumes in the Martian mantle. Such megaplumes are expected to produce several distinct episodes of magmatic activity, in agreement with our interpretations. However, the existence of megaplumes may not be necessary in the plume tectonics model. Analysis of stress trajectories (Figs 16 and 20) shows that much of the dyke lengths is actually due to the favourable regional stress field, not to the plume size.

2. The regional stress field has a major role in the model, however its origin has not been discussed. Both thermal and non-thermal stress sources may be considered. A number of authors have proposed that following accretion, planetary expansion occurred in response to internal heating of the planet. Then the planet slowly cooled down and horizontally hydrostatic retraction forces affected the crust (e.g. Toksöz and Hsui, 1978; also see Schultz, 1985). The timing of events is very unconstrained because there is currently no means to reliably correlate the timescale of thermal models on absolute scale. But the beginning of the magmato-tectonic activity of Tharsis, as deduced from stratigraphic studies (Scott and Tanaka, 1986), is consistent with the time span of planetary expansion proposed by Toksöz and Hsui (1978). Stevenson and Bittker (1990) have suggested that "heating crises" would be normal events in the history of planets without plate tectonics. Watters (1993) suggested that such a crisis could explain the magmatic peak corresponding to widespread resurfacing during lower Hesperian and subsequent wrinkle ridge formation. A recent model by Schubert *et al.* (1992) assumes that the Martian thermal history is dominated by cooling subsequent to very early core formation and rapid crustal formation. The wrinkle ridges are considered as arguments in favour of early planetary cooling, however numerous extensional features formed contemporaneously and prior to the wrinkle ridges (Scott and Tanaka, 1986). Some authors have furthermore considered that wrinkle ridge formation occurred after a global resurfacing event (e.g. Watters, 1993), which probably requires early extensional stress rather than compressional stress. Consequently these models do not provide adequate background to the plume tectonics model. Models predicting thermal expansion would not be inconsistent, but they require additional horizontal deviatoric stress.

Theoretical stress models of global processes that do not include the thermal effects of planetary expansion (tidal despinning, Melosh (1977); tidal distortion, Melosh (1980a); planet reorientation, Melosh (1980b)), do not provide suitable stress trajectories alone to explain the regional stress field shown in the present study. Perhaps a combination of such stress models with thermal models will provide enlightenment on its origin. The source of the regional stress is thus presently unknown. However, this should not significantly affect the validity of the plume tectonics model since

it is grounded on morphologic observations, whose interpretations are based on processes clearly established on Earth.

3. Another concern is the number of plumes required in the Tharsis hemisphere. The first dyke swarm, centred on Solis Planum, might correspond to an early stage of plume rising, heralding the onset of the major Syria Planum plume and dyke swarm, in accordance with cases of two dyke swarm emplacements above a supposedly single plume on Earth (Heaman and Tarney, 1989). It can be speculated, furthermore, that the megaplume model by Breuer *et al.* (1996) could predict the formation of a third dyke swarm later (i.e. the Tharsis dyke swarm).
4. The formation of Olympus Mons and Alba Patera is not clear. Olympus Mons was not mentioned previously in the present paper, because it does not belong to the Tharsis structural unit (it was built on the other side of the dichotomy boundary). Stratigraphic relationships suggest that its activity is mainly contemporaneous to the Tharsis and Alba Patera swarm activity. Thus three hot jets are required at the same time in a quite small perimeter, whereas only Elysium, a small volcanic unit compared with Tharsis, is a possible candidate for a contemporaneous hot spot in the remaining part of the planet. Alba Patera was already suggested to be a secondary plume linked with the major Tharsis plume (Janle and Erkul, 1991). Although what this physically implies is not well understood, this could give some ideas for future research aiming to explain the highly atypical shape of the volcano compared with the other magma centres suggested to have formed above a plume (by comparison, the Tharsis volcanoes present many morphological similarities to the shield volcanoes in, e.g. the Galapagos islands (Chadwick and Howard, 1991)). Some similarity between Alba Patera and some kind of coronae on Venus, interpreted by most authors as formed in relation to a hot plume, has already been pointed out (Cyr and Melosh, 1993; Watters and Janes, 1995). The simultaneous activity (Scott and Tanaka, 1986) of the major Tharsis and possible Olympus Mons plumes may address an even more serious question relating to plume stability. Alba Patera might have been an effect of Tharsis formation, for instance as resulting from a secondary convection induced by the Tharsis plume, but Olympus Mons can probably not be assumed to be a secondary effect of Tharsis formation (or reciprocally). In order to explain the whole heat released through the nearby Tharsis, Olympus Mons, and Alba Patera, the possibility of a common origin should be investigated, maybe by studies of unstable processes at the core/mantle boundary (Morgan, 1971; see illustrations of possible instabilities during plume development in Watson and McKenzie, 1991) or at some depth within the mantle (e.g. Anderson, 1994).
5. The earliest (Noachian) stages of tectonic activity in the Tharsis region must be more accurately studied. The early Solis Planum fracturing centre appears to be unrelated to the possibly contemporaneous NW/SE extension event which played a key role in the Tempe Terra region and should be responsible for the align-

ment of many volcanoes in the Tharsis province, including the Tharsis Montes.

Acknowledgements. Thanks to Agust Gudmundsson for many discussions and for significant improvement of the manuscript, to Dan McKenzie for discussions and enthusiastic support throughout the achievement of this work; to Jean-Pierre Peulvast and Pierre Vergely for discussions; to Richard Ernst, Jim Head, and Konrad Hiller for critical reviews of the manuscript at various stages of elaboration; to Maurizio Bonafede, Agust Gudmundsson, Randy Richardson, and Rich Schultz for preprints. This paper represents a research effort supported by Programme National de Planétologie from Institut National des Sciences de l'Univers (CNRS, France). D.M. is also grateful to Société de Secours des Amis des Sciences and Fondation Singer-Polignac for financing part of this work. The data used in this study were made available by the Regional Planetary Image Facility at Université Paris-Sud (Orsay, France) under the auspices of NASA Planetary Geology and Geophysics Program.

References

- Agnon, A. and Lyakhovsky, V.,** Damage distribution and localization during dyke intrusion, in *Physics and Chemistry of Dykes* (edited by G. Baer and A. Heimann), pp. 65–78. Proc. Third Int. Dyke Conf., Jerusalem, Sept. 4–7, 1995. Balkema, Rotterdam, 1995.
- Allemand, P., Brun, J. P., Davy, P. and Van Den Driessche, J.,** Symétrie et asymétrie des rifts et mécanismes d'amincissement de la lithosphère. *Bull. Soc. Géol. Fr.* **8**(3), 445–451, 1989.
- Anderson, D. L.,** Komatiites and picrites: evidence that the 'plume' source is depleted. *Earth Planet. Sci. Lett.* **128**, 303–311, 1994.
- Anderson, E. M.,** *The Dynamics of Faulting and Dyke Formation with Applications to Britain*, 2nd Edn, 206 pp. Oliver & Boyd, Edinburgh, 1951.
- Anderson, F. S. and Grimm, R. E.,** Lithospheric controls on the formation of Valles Marineris, *Lunar Planet. Sci. Conf.*, Vol. XXV, pp. 29–30. Lunar and Planetary Institute, Houston, 1994.
- Assumpção, M.,** The regional intraplate stress field in South America. *J. Geophys. Res.* **97**(B8), 11,889–11,903, 1992.
- Banerdt, W. B. and Golombek, M. P.,** The evolution of Tharsis: implications of gravity, topography, and tectonics, in *Scientific Results of the NASA-sponsored Study Project on Mars: Evolution of Volcanism, Tectonics and Volatiles* (edited by S. C. Solomon, V. L. Sharpton and J. R. Zimbelman), LPI Technical Rept 90-06, pp. 63–64. Lunar and Planetary Institute, Houston, 1990.
- Banerdt, W. B., Phillips, R. J., Sleep, N. H. and Saunders, R. S.,** Thick shell tectonics on one-plate planets: application to Mars, *Proc. 3rd International Colloquium on Mars. J. Geophys. Res.* **87**(B12), 9723–9733, 1982.
- Banerdt, W. B., Golombek, M. P. and Tanaka, K. L.,** Stress and tectonics on Mars, in *Mars* (edited by Kiefer *et al.*), pp. 249–297. University of Arizona Press, Tucson, 1992.
- Battistini, R.,** L'utilisation des cratères météoritiques à ejecta fluidisés comme moyen d'étude spatiale et chronologique de l'eau profonde (hydroliothosphère) de Mars. *Rev. Geomorph. Dyn.* **XXXIII**(1), 25–41, 1984.
- Blasius, K. R., Cutts, J. A., Guest, J. E. and Masursky, H.,** Geology of the Valles Marineris: first analysis of imaging from the Viking I Orbiter Primary Mission. *J. Geophys. Res.* **82**(28), 4067–4091, 1977.
- Bercovici, D. and Mahoney, J.,** Double flood basalts and plume head separation at the 660-kilometer discontinuity. *Science* **266**, 1367–1369, 1994.
- Bonafede, M. and Olivieri, M.,** Displacement and gravity anomaly produced by a shallow vertical dyke in a cohesionless medium. *Geophys. J. Int.* **123**(3), 639–652, 1995.
- Breuer, D., Spohn, T. and Wüllner, U.,** Mantle differentiation and the crustal dichotomy of Mars. *Planet. Space Sci.* **41**(4), 269–283, 1993.
- Breuer, D., Zhou, H. and Yuen, D. A.,** Phase transitions in the Martian mantle: implications for the planet's volcanic history. *J. Geophys. Res.* **101**(E3), 7531–7542, 1996.
- Bruce, P. M. and Huppert, H. E.,** Thermal control of basaltic fissure eruptions. *Nature* **342**, 665–667, 1989.
- Byerlee, J. D.,** Friction of rocks. *Pure Appl. Geophys.* **116**, 415, 615–626, 1978.
- Cadman, A. C., Heaman, L., Tarney, J., Wardle, R. and Krogh, T. E.,** U–Pb geochronology and geochemical variation within two Proterozoic mafic dyke swarms, Labrador. *Can. J. Earth Sci.* **30**, 1490–1504, 1993.
- Cadman, A. C., Tarney, J., Baragar, W. R. A. and Wardle, R. J.,** Relationship between Proterozoic dykes and associated volcanic sequences: evidence from the Harp Swarm and Seal Lake Group, Labrador, Canada. *Precamb. Res.* **68**, 357–374, 1994.
- Carr, M. H.,** Tectonism and volcanism of the Tharsis region of Mars. *J. Geophys. Res.* **79**(26), 3943–3949, 1974.
- Carr, M. H.,** Formation of Martian flood features by release of water from confined aquifers. *J. Geophys. Res.* **84**(B6), 2995–3007, 1979.
- Carr, M. H. and Greeley, R.,** Volcanic features of Hawaii — a basis for comparison with Mars. NASA SP-403, 211, 1980.
- Carter, N. L. and Tsenn, M. C.,** Flow properties of continental lithosphere. *Tectonophysics* **136**, 27–63, 1987.
- Cattermole, P.,** *Mars, the Story of the Red Planet*, 224 pp. Chapman & Hall, London, 1992.
- Chadwick, D. J. and Lucchitta, B. K.,** Fault geometries and extension in the Valles Marineris, Mars, *Lunar Planet. Sci. Conf.*, Vol. XXIV, pp. 263–264. Lunar and Planetary Institute, Houston, 1993.
- Chadwick, W. W. and Dieterich, J. H.,** Mechanical modeling of circumferential and radial dike intrusion on Galapagos volcanoes. *J. Volcanol. Geotherm. Res.* **66**, 37–52, 1995.
- Chadwick, W. W. and Howard, K. A.,** The pattern of circumferential and radial eruptive fissures on the volcanoes of Fernandina and Isabela islands, Galapagos. *Bull. Volcanol.* **53**, 259–275, 1991.
- Chicarro, A. F.,** Structures compressives sur Mars, Ph.D. Dissertation, 156 pp. Université Paris-Sud, Orsay, 1983.
- Chicarro, A. F., Schultz, P. H. and Masson, P.,** Global and regional ridge patterns on Mars. *Icarus* **63**, 153–174, 1985.
- Clifford, S. M.,** A model for the hydrologic and climatic behavior of water on Mars. *J. Geophys. Res.* **98**(E6), 10,973–11,016, 1993.
- Cloetingh, S., van Wees, J. D., van der Beek, P. A. and Spadini, G.,** Role of pre-rift geology in kinematics of extensional basin formation: constraints from thermomechanical models of Mediterranean and intracratonic basins. *Marine Petroleum Geol.* **12**(8), 793–807, 1995.
- Coffin, M. F. and Eldholm, O.,** Large igneous provinces: crustal structure, dimensions, and external consequences. *Rev. Geophys.* **32**(1), 1–36, 1994.
- Corrieu-Sipahimalani, V.,** Modèles dynamiques du manteau terrestre: observations et contraintes, Ph.D. Dissertation, 220 pp. Ecole Normale Supérieure, Paris, 1995.
- Costard, F.,** Distribution et caractéristiques du pergélisol sur Mars: son influence sur certains traits de la géomorphologie, Ph.D. Dissertation, 327 pp. Université Paris-Sorbonne, 1990a.
- Costard, F.,** Vallées de débâcle et processus cryokarstiques sur

- Mars et en Sibérie (in French with English abstract and captions). *Géogr. Phys. Quaternaire* **44**(1), 97–104, 1990b.
- Costard, F.**, Le pergélisol martien (in French with English abstract). *Int. J. Refrig.* **16**(2), 91–100, 1993.
- Costard, F. M. and Kargel, J. S.**, Outwash plains and thermokarst on Mars. *Icarus* **114**, 93–112, 1995.
- Craddock, R. A., Greeley, R. and Christensen, P. R.**, Evidence for an ancient impact basin in Daedalia Planum, Mars. *J. Geophys. Res.* **95**(B7), 10,729–10,741, 1990.
- Crumpler, L. S. and Aubele, J. C.**, Structural evolution of Arsia Mons, Pavonis Mons, and Ascraeus Mons: Tharsis region of Mars. *Icarus* **34**, 496–511, 1978.
- Cyr, K. E. and Melosh, H. J.**, Tectonic patterns and regional stresses near Venusian coronae. *Icarus* **102**, 175–184, 1993.
- Davis, P. A. and Golombek, M. P.**, Discontinuities in the shallow Martian crust at Lunae, Syria, and Sinai Plana, *Proc. 4th International Conference on Mars. J. Geophys. Res.* **95**(B9), 14,231–14,248, 1990.
- Davis, P. A., Tanaka, K. L. and Golombek, M. P.**, Topography of closed depressions, scarps, and grabens in the north Tharsis region of Mars: implications for shallow crustal discontinuities and graben formation. *Icarus* **114**, 403–422, 1995.
- De Hon, R. A.**, Martian volcanic materials: preliminary thickness estimates in the eastern Tharsis region, *Proc. 3rd International Colloquium on Mars. J. Geophys. Res.* **87**(B12), 9821–9828, 1982.
- Delaney, P. T.**, Rapid intrusion of magma into wet rock: groundwater flow due to pore pressure increases. *J. Geophys. Res.* **87**(B9), 7739–7756, 1982.
- Delaney, P. T.**, Heat transfer during emplacement and cooling of mafic dykes, in *Mafic Dyke Swarms* (edited by H. C. Halls and W. F. Fahrig), Sp. Pap. 34, pp. 31–46. Proc. Int. Dyke Conf., Toronto, June 4–7, 1985. Geol. Assoc. Canada, 1987.
- Delaney, P. T. and Wallace, M. H.**, Dyke intrusion and the rift system of Kilauea volcano, in *Program and Abstracts* (edited by A. Agnon and G. Baer), p. 26. 3rd International Dyke Conference, Jerusalem, Israël, 4–8 septembre, 1995.
- Delaney, P. T., Pollard, D. D., Ziony, J. I. and McKee, E. H.**, Field relations between dikes and joints: emplacement processes and paleostress analysis. *J. Geophys. Res.* **91**(B5), 4920–4938, 1986.
- Dohm, J. M. and Tanaka, K. L.**, Geologic history of the Thaumasia region of Mars, *Lunar Planet. Sci. Conf.*, Vol. XXV, pp. 331–332. Lunar and Planetary Institute, Houston, 1994.
- Dohm, J. M. and Tanaka, K. L.**, Geologic summary of the Thaumasia region of Mars based on detailed stratigraphy and rater statistics, *Lunar Planet. Sci. Conf.*, Vol. XXVI, pp. 337–338. Lunar and Planetary Institute, Houston, 1995.
- Dvorak, J., Okamura, A. T., English, T. T., Koyanagi, R. Y., Nakata, J. S., Sako, M. K., Tanigawa, W. T. and Yamashita, K. M.**, Mechanical response of the south flank of Kilauea volcano, Hawaii, to intrusive events along the rift zones. *Tectonophysics* **124**, 241–269, 1985.
- Ernst, R. E. and Baragar, W. R. A.**, Evidence from magnetic fabric for the flow pattern in the Mackenzie giant radiating dyke swarm. *Nature* **356**, 511–513, 1992.
- Ernst, R. E., Buchan, K. L. and Palmer, H. C.**, Giant dyke swarms: characteristics, distribution and geotectonic applications, in *Physics and Chemistry of Dykes* (edited by G. Baer and A. Heimann), pp. 3–21. Proc. Third Int. Dyke Conf., Jerusalem, Sept. 4–7, 1995. Balkema, Rotterdam, 1995a.
- Ernst, R. E., Head, J. W., Parfitt, E., Grosfils, E. and Wilson, L.**, Giant radiating dyke swarms on Earth and Venus. *Earth-Sci. Rev.* **39**, 1–58, 1995b.
- Ernst, R. E., Buchan, K. L., West, T. D. and Palmer, H. C.**, Diabase (dolerite) dyke swarms of the world: first edition. *Geol. Surv. Can. Open File* **3241**, 104, 1996.
- Fagents, S. A. and Wilson, L.**, Basaltic volcanic activity on Mars: numerical modelling of lava fountain eruptions. *Lunar Planet. Sci. Conf.*, Vol. XXVI, pp. 383–384. Lunar and Planetary Institute, Houston, 1995.
- Fahrig, W. F.**, The tectonic settings of continental mafic dyke swarms: failed arm and early passive margin, in *Mafic Dyke Swarms* (edited by H. C. Halls and W. F. Fahrig), Sp. Pap. 34, pp. 331–348. Proc. Int. Dyke Conf., Toronto, June 4–7, 1985. Geol. Assoc. Canada, 1987.
- Fanale, F. P., Postawko, S. E., Pollack, J. B., Carr, M. H. and Pepin, R. O.**, Mars: epochal climate change and volatile history, in *Mars* (edited by W. S. Kiefer *et al.*), pp. 1135–1179. University of Arizona Press, Tucson, 1992.
- Farnetani, C. G. and Richards, M. A.**, Numerical investigations of the mantle plume initiation model for flood basalt events. *J. Geophys. Res.* **99**(B7), 13,813–13,833, 1994.
- Finnerty, A. A., Phillips, R. J. and Banerdt, W. B.**, Igneous processes and closed system evolution of the Tharsis region of Mars. *J. Geophys. Res.* **93**(B9), 10,225–10,235, 1988.
- Fleitout, L.**, The sources of lithospheric tectonic stress, in *Tectonic Stress in the Lithosphere* (edited by R. B. Whitmarsh, M. H. P. Bott, J. D. Fairhead and N. J. Kusznir). *Phil. Trans. R. Soc. Lond.* **337**, 73–81, 1991.
- Fleitout, L. and Froidevaux, C.**, Tectonics and topography for a lithosphere containing density heterogeneities. *Tectonics* **1**(1), 21–56, 1982.
- Forslund, T. and Gudmundsson, A.**, Crustal spreading due to dikes and faults in southwest Iceland. *J. Struct. Geol.* **13**(4), 443–457, 1991.
- Forslund, T. and Gudmundsson, A.**, Structure of Tertiary and Pleistocene normal faults in Iceland. *Tectonics* **11**(1), 57–68, 1992.
- Frey, H. V.**, Thaumasia: a fossilized early forming Tharsis uplift. *J. Geophys. Res.* **84**(B3), 1009–1023, 1979a.
- Frey, H. V.**, Martian canyons and African rifts: structural comparisons and implications. *Icarus* **37**, 142–155, 1979b.
- Frey, H. V. and Roark, J. H.**, A multi-ring impact basin in Thaumasia, *Lunar Planet. Sci. Conf.*, Vol. XXVI, pp. 425–426. Lunar and Planetary Institute, Houston, 1995.
- Frey, H. V., Bills, B. G. and Nerem, R. S.**, The isostatic state of Martian topography — revisited, *Lunar Planet. Sci. Conf.*, Vol. XXVI, pp. 427–428. Lunar and Planetary Institute, Houston, 1995.
- Fyfe, W. S.**, Magma underplating of continental crust. *J. Volcanol. Geotherm. Res.* **50**, 33–40, 1992.
- Golombek, M. P.**, Fault type predictions from stress distributions on planetary surfaces: importance of fault initiation at depth. *J. Geophys. Res.* **90**(B4), 3065–3074, 1985.
- Grana, J. P. and Richardson, R. M.**, Tectonic stress within the New Madrid seismic zone. *J. Geophys. Res.* 1996 (in press).
- Greeley, R.**, *Planetary Landscapes*, 275 pp. Allen and Unwin, Boston, 1989.
- Greeley, R. and King, J. S.** (eds), Volcanism of the Eastern Snake River plain, Idaho: a comparative planetary geology guidebook, 307 pp. NASA Contract. Rept. CR-154621, 1977.
- Griffiths, R. W. and Campbell, I. H.**, Interaction of mantle plume heads with the Earth's surface and onset of small-scale convection. *J. Geophys. Res.* **96**(B11), 18,295–18,310, 1991.
- Grosfils, E. and Head, J. W.**, The global distribution of giant radiating dike swarms on Venus: implications for the global stress state. *Geophys. Res. Lett.* **21**(8), 701–704, 1994.
- Gudmundsson, A.**, Form and dimensions of dykes in eastern Iceland. *Tectonophysics* **95**, 295–307, 1983.
- Gudmundsson, A.**, Tectonic aspects of dykes in northwestern Iceland. *Jökull* **34**, 81–96, 1984.
- Gudmundsson, A.**, Lateral magma flow, caldera collapse, and a mechanism of large eruptions in Iceland. *J. Volcanol. Geotherm. Res.* **34**, 65–78, 1987a.
- Gudmundsson, A.**, Geometry, formation and development of tectonic fractures on the Reykjanes Peninsula, Southwest Iceland. *Tectonophysics* **139**, 295–308, 1987b.
- Gudmundsson, A.**, Emplacement of dikes, sills and crustal

- magma chambers at divergent plate boundaries. *Tectonophysics* **176**, 257–275, 1990a.
- Gudmundsson, A.**, Dyke emplacement at divergent plate boundaries: in *Mafic Dykes and Emplacement Mechanisms* (edited by A. J. Parker, P. C. Rickwood and D. H. Tucker), pp. 47–62. Proc. 2nd Int. Dyke Conf., Adelaide, Sept. 12–16, 1990. Balkema, Rotterdam, 1990b.
- Gudmundsson, A.**, Infrastructure and mechanics of volcanic systems in Iceland. *J. Volcanol. Geotherm. Res.* **64**, 1–22, 1995a.
- Gudmundsson, A.**, The geometry and growth of dykes, in *Physics and Chemistry of Dykes* (edited by G. Baer and A. Heimann), pp. 23–34. Proc. Third Int. Dyke Conf., Jerusalem, Sept. 4–8, 1995. Balkema, Rotterdam, 1995b.
- Gudmundsson, A. and Brynjólfsson, S.**, Overlapping rift-zone segments and the evolution of the south Iceland seismic zone. *Geophys. Res. Lett.* **20**(18), 1903–1906, 1993.
- Hall, J. L., Solomon, S. C. and Head, J. W.**, Elysium region, Mars: test of lithospheric loading models for the formation of tectonic features. *J. Geophys. Res.* **91**(B11), 11,377–11,392, 1986.
- Halls, H. C.**, The importance and potential of mafic dyke swarms in studies of geodynamic processes. *Geoscience Canada* **9**(3), 145–154, 1982.
- Halls, H. C.**, Dyke swarms and continental rifting: some concluding remarks, in *Mafic Dyke Swarms* (edited by H. C. Halls and W. F. Fahrig), Sp. Pap. 34, pp. 483–492. Proc. Int. Dyke Conf., Toronto, June 4–7, 1985. Geol. Assoc. Canada, 1987.
- Halls, H. C.**, The Matachewan dyke swarm, Canada: an early Proterozoic magnetic field reversal. *Earth Planet. Sci. Lett.* **105**, 279–292, 1991.
- Hartmann, W. K., Strom, R. G., Weidenschilling, S. J., Blasius, K. R., Woronov, A., Dence, M. R., Grieve, R. A. F., Diaz, J., Chapman, C. R., Shoemaker, E. M. and Jones, K. L.**, Chronology of planetary volcanism by comparative studies of planetary cratering, in *Basaltic Volcanism on the Terrestrial Planets* (edited by Members of the Basaltic Volcanism Study Project), pp. 1049–1127. Pergamon Press, 1981.
- Head III, J. W. and Wilson, L.**, Lunar graben formation due to near-surface deformation accompanying dike emplacement. *Planet. Space Sci.* **41**(10), 719–727, 1994.
- Heaman, L. M. and Tarney, J.**, U–Pb baddeleyite ages for the Scourie dyke swarm, Scotland: evidence for two distinct intrusion events. *Nature* **340**, 705–708, 1989.
- Heaman, L. M., LeCheminant, A. N. and Rainbird, R. H.**, Nature and timing of Franklin igneous events, Canada: implications for a late Proterozoic mantle plume and the break-up of Laurentia. *Earth Planet. Sci. Lett.* **109**, 117–131, 1992.
- Hill, R. I.**, Starting plumes and continental break-up. *Earth Planet. Sci. Lett.* **104**, 398–416, 1991.
- Hill, R. I., Campbell, I. H., Davies, G. F. and Griffiths, R. W.**, Mantle plumes and continental tectonics. *Science* **256**, 186–193, 1992.
- Hiller, K. H., Janle, P., Neukum, G. P. O., Guest, J. E. and Lopes, R. M. C.**, Mars: stratigraphy and gravimetry of Olympus Mons and its aureole, *Proc. 3rd International Colloquium on Mars. J. Geophys. Res.* **87**(B12), 9905–9915, 1982.
- Hoek, H.**, Mafic dykes of the Vestfold Hills, East Antarctica. An analysis of the emplacement mechanism of tholeiitic dyke swarms and of the role of dyke emplacement during crustal extension, Ph.D. Dissertation, 133 pp. University of Utrecht, 1994.
- Hoek, H.**, Dyke propagation and arrest in Proterozoic tholeiitic dyke swarms, Vestfold Hills, East Antarctica, in *Physics and Chemistry of Dykes* (edited by G. Baer and A. Heimann), pp. 79–93. Proc. Third Int. Dyke Conf., Jerusalem, Sept. 4–7, 1995. Balkema, Rotterdam, 1995.
- Houseman, G. and England, P.**, A dynamical model of lithosphere extension and sedimentary basin formation. *J. Geophys. Res.* **91**(B1), 719–729, 1986.
- Janle, P. and Erkul, E.**, Gravity studies of the Tharsis area on Mars. *Earth Moon Planets* **53**, 217–232, 1991.
- Kamo, S. L. and Gower, C. F.**, U–Pb baddeleyite dating clarifies age of characteristic paleomagnetic remanence of Long Range dykes, southeastern Labrador. *Atlantic Geol.* **30**, 259–262, 1994.
- Kamo, S. L., Krogh, T. E. and Kumarapeli, P. S.**, Age of the Grenville dyke swarm, Ontario – Quebec: implications for the timing of Iapetan rifting. *Can. J. Earth Sci.* **32**, 273–280, 1995.
- Kochel, R. C. and Capar, A. P.**, Structural control of sapping valley networks along Valles Marineris, Mars, in *Repts Planet. Geol. Program, NASA Technical Memorandum 85127*, 295–297, 1982.
- Kochel, C. R. and Piper, J.**, Morphology of large valleys on Hawaii: evidence for ground water sapping and comparisons with Martian valleys, *Proc. 17th Lunar and Planetary Conference. J. Geophys. Res.* **91**(Suppl.), E171–E192, 1986.
- Kokelaar, P.**, Magma–water interactions in subaqueous and emergent basaltic volcanism. *Bull. Volcanol.* **48**, 275–289, 1986.
- Lawver, L. A. and Müller, R. D.**, Iceland hot spot track. *Geology* **22**, 311–314, 1994.
- LeCheminant, A. N. and Heaman, L. M.**, Mackenzie igneous events, Canada: middle Proterozoic hotspot magmatism associated with ocean opening. *Earth Planet. Sci. Lett.* **96**, 38–48, 1989.
- Le Dain, A.-Y.**, Application de la télédétection à deux exemples de tectonique cassante à grande échelle: le mouvement relatif Inde-Indochine, l'extension sur la planète Mars, Ph.D. Dissertation, 99 pp. Université des Sciences et Techniques du Languedoc, Montpellier, 1982.
- Lister, J. R.**, Buoyancy-driven fluid fracture: the effects of material toughness and of low-viscosity precursors. *J. Fluid Mech.* **210**, 263–280, 1990.
- Lister, J. R.**, Steady solutions for feeder dykes in a density-stratified lithosphere. *Earth Planet. Sci. Lett.* **107**, 233–242, 1991.
- Lister, J. R.**, Fluid-mechanical models of the interaction between solidification and flow in dykes, in *Physics and Chemistry of Dykes* (edited by G. Baer and A. Heimann), pp. 115–124. Proc. Third Int. Dyke Conf., Jerusalem, Sept. 4–7, 1995. Balkema, Rotterdam, 1995.
- Lister, J. R. and Kerr, R. C.**, Fluid-mechanical models of crack propagation and their application to magma transport in dykes. *J. Geophys. Res.* **96**(B6), 10049–10077, 1991.
- Logatchev, N. A.**, History and geodynamics of the Lake Baikal rift in the context of the Eastern Siberia rift system: a review. *Bull. Centres Rech. Explor.-Prod. Elf Aquitaine* **17**(2), 353–370, 1993.
- Lonsdale, P.**, Overlapping rift zones at the 5.5°S offset of the East Pacific Rise. *J. Geophys. Res.* **88**(B11), 9393–9406, 1983.
- Lorenz, V.**, On the growth of maars and diatremes and its relevance to the formation of tuff rings. *Bull. Volcanol.* **48**, 265–274, 1986.
- Lucchitta, B. K.**, Morphology of chasma walls, Mars. *J. Res. U.S. Geol. Surv.* **6**(5), 651–662, 1977.
- Lucchitta, B. K.**, Valles Marineris — Faults, volcanic rocks, channels, basin beds. NASA Technical Memorandum 84211, pp. 419–421, 1981.
- Lucchitta, B. K.**, Young volcanic deposits in the Valles Marineris, Mars? *Icarus* **86**, 476–509, 1990.
- Lucchitta, B. K., McEwen, A. S., Clow, G. D., Geissler, P. E., Singer, R. B., Schultz, R. A. and Squyres, S. W.**, The canyon system on Mars, in *Mars* (edited by W. S. Kiefer et al.), pp. 453–492. University of Arizona Press, Tucson, 1992.
- McDonald, K. C., Sempere, J.-C. and Fox, P. J.**, East-Pacific Rise from Siqueiros to Orozco fracture zones: along-strike continuity of axial neovolcanic zone and structure and evol-

- ution of overlapping spreading centers. *J. Geophys. Res.* **89**(B7), 6049–6069, 1984.
- McDonald, K. C., Sempere, J.-C. and Fox, P. J.**, The debate concerning overlapping spreading centers and mid-ocean ridge processes (reply). *J. Geophys. Res.* **91**(B10), 10,501–10,511, 1986.
- McDonald, R. and Upton, B. G. J.**, The Proterozoic Gardar rift zone, south Greenland: comparisons with the East African Rift System, in *Magmatic Processes and Plate Tectonics* (edited by H. M. Prichard, T. Alabaster, N. B. Harris and C. R. Neary), Geol. Soc. Sp. Publ. 76, pp. 427–442, 1993.
- McDonald, R., Wilson, L., Thorpe, R. S. and Martin, A.**, Emplacement of the Cleveland Dyke: evidence from geochemistry, mineralogy and physical modelling. *J. Petrol.* **29**, 559–583, 1988.
- McGetchin, T. R. and Ullrich, G. W.**, Xenoliths and diatremes with inferences for the Moon, Mars, and Venus. *J. Geophys. Res.* **78**(11), 1833–1853, 1973.
- McGovern, P. J. and Solomon, S. C.**, State of stress, faulting, and eruption characteristics of large volcanoes on Mars. *J. Geophys. Res.* **98**(E12), 23553–23579, 1993.
- McKenzie, D.**, A possible mechanism for epirogenic uplift. *Nature* **307**, 616–618, 1984.
- McKenzie, D. and Bickle, M. J.**, The volume and composition of melt generated by extension of the lithosphere. *J. Petrol.* **29**(3), 625–679, 1988.
- McKenzie, D. and O'Nions, R. K.**, Partial melt distributions from inversion of rare earth element concentrations. *J. Petrol.* **32**, 1021–1091, 1991.
- McKenzie, D., McKenzie, J. M. and Saunders, R. S.**, Dike emplacement on Venus and on Earth. *J. Geophys. Res.* **97**(E10), 15,977–15,990, 1992.
- Masson, P.**, Structure pattern analysis of the Noctis Labyrinthus – Valles Marineris region of Mars. *Icarus* **30**, 49–62, 1977.
- Masson, P.**, Contribution to the structural interpretation of the Valles Marineris – Noctis Labyrinthus – Claritas Fossae regions of Mars. *Moon Planets* **22**, 211–219, 1980.
- Masson, P.**, Contribution à l'Etude Géologique Comparée des Planètes Internes du Système Solaire, Doctorat d'Etat 3111, 347 pp. Université Paris-Sud, Orsay, 1986.
- Mastin, L. G. and Pollard, D. D.**, Surface deformation and shallow dike intrusion processes at Inyo craters, Long Valley, California. *J. Geophys. Res.* **93**(B11), 13,221–13,235, 1988.
- May, P. R.**, Pattern of Triassic–Jurassic diabase dikes around the North Atlantic in the context of predrift position of the continents. *Geol. Soc. Am. Bull.* **82**, 1285–1292, 1971.
- Mège, D.**, Etude morphostructurale de la partie ouest de Valles Marineris (Mars), part II: Interprétation géomorphologique et tectonique, DEA Memoir, Université Paris-Sud, Orsay, p. 70, 1991.
- Mège, D.**, Aspects structuraux du complexe magmato-tectonique de Tharsis sur Mars, Ph.D. Dissertation No. 3394, Université Paris-Sud, Orsay, p. 384, 1994.
- Mège, D. and Masson, P.**, Past and current geometry of Valles Marineris, EGS XIX General Assembly, Grenoble, 25–29 avril 1994. *Annales Geophysicae* **12**(Suppl. III), C653, 1994a.
- Mège, D. and Masson, P.**, Dans quelles mesures peut-on comparer Valles Marineris et les rifts terrestres continentaux? (extended French abstract with English abstract), in *Proc. Colloque National de Planétologie CNRS/INSU* (edited by B. R. Bernhard, M. D. Festou and F. Foucaud), S17-3, 1994b.
- Mège, D. and Masson, P.**, Dyke swarms in the Tharsis province of Mars, in *Program and Abstracts* (edited by A. Agnon and G. Baer). 3rd International Dyke Conference, Jerusalem, Israël, 4–8 septembre 1995.
- Mège, D. and Masson, P.**, Stress models for Tharsis formation, Mars. *Planet. Space Sci.* **44**, 1471–1497, 1996a.
- Mège, D. and Masson, P.**, Amounts of crustal stretching in Valles Marineris, Mars. *Planet. Space Sci.* **44**, 749–782, 1996b.
- Melosh, H. J.**, Global tectonics of a despun planet. *Icarus* **31**, 221–243, 1977.
- Melosh, H. J.**, The tectonics of mascon loading, *Proc. Lunar Planet. Sci. 9th. Geochim. Cosmochim. Acta* **10**(Suppl.), 3513–3525, 1978.
- Melosh, H. J.**, Tectonic patterns on a tidally distorted planet. *Icarus* **43**, 334–337, 1980a.
- Melosh, H. J.**, Tectonic patterns on a reoriented planet: Mars. *Icarus* **44**, 741–745, 1980b.
- Melosh, H. J. and Williams Jr, C. A.**, Mechanics of graben formation in crustal rocks: a finite element analysis. *J. Geophys. Res.* **94**(B10), 13961–13973, 1989.
- Moore, H. J.**, Geology of the Tempe-Mareotis region, Mars, *Lunar Planet. Sci. Conf.*, Vol. XXVI, pp. 993–994. Lunar and Planetary Institute, Houston, 1995.
- Morgan, W. J.**, Convection plumes in the lower mantle. *Nature* **230**, 42–43, 1971.
- Mouginis-Mark, P. J.**, Recent water release in the Tharsis region of Mars. *Icarus* **84**, 362–373, 1990.
- Muller, O. H. and Pollard, D. D.**, The state of stress near Spanish Peaks, Colorado, determined from a dike pattern. *Pure Appl. Geophys.* **115**, 69–86, 1977.
- Mutch, T. A., Arvidson, R. E., Head, J. W., Jones, K. L. and Saunders, R. S.**, *The Geology of Mars*, p. 400. Princeton University Press, 1976.
- Nedell, S. S., Squyres, S. W. and Andersen, D. W.**, Origin and evolution of the layered deposits in the Valles Marineris, Mars. *Icarus* **70**, 409–441, 1987.
- Neukum, G. and Hiller, K.**, Martian ages. *J. Geophys. Res.* **86**(B4), 3097–3121, 1981.
- Neukum, G. and Wise, D. U.**, Mars: a standard crater curve and possible new time scale. *Science* **194**, 1381–1387, 1976.
- Odé, H.**, Mechanical analysis of the dyke pattern of the Spanish Peaks area, Colorado. *Geol. Soc. Am. Bull.* **68**, 567–576, 1957.
- Opheim, J. A. and Gudmundsson, A.**, Formation and geometry of fractures, and related volcanism, of the Krafla fissure swarm, Northeast Iceland. *Geol. Soc. Am. Bull.* **101**, 1608–1622, 1989.
- Parfitt, E. A. and Head, J. W.**, Buffered and unbuffered dike emplacement on Earth and Venus: implications for magma reservoir size, depth, and rate of magma replenishment. *Earth Moon Planets* **61**, 249–281, 1993.
- Peulvast, J.-P.**, Structural geomorphology and morphotectonic evolution of an uplifted rifted margin: the Scoresby Sund area, East Greenland. *Z. Geomorph.* **82**, 17–34, 1991.
- Peulvast, J.-P., Mège, D., Chiciak, J., Costard, F. and Masson, P.**, Very high wallslopes in Valles Marineris (Mars): morphology, evolution, relationships with tectonics and volatiles. *Geomorphology* 1996 (in press).
- Phillips, R. J., Sleep, N. H. and Banerdt, W. B.**, Permanent uplift in magmatic systems with application to the Tharsis region of Mars. *J. Geophys. Res.* **95**(B4), 5089–5100, 1990.
- Plescia, J. B. and Golombek, M. P.**, Origin of planetary wrinkle ridges based on the study of terrestrial analogs. *Geol. Soc. Am. Bull.* **97**, 1289–1299, 1986.
- Plescia, J. B. and Saunders, R. S.**, Estimation of the thickness of the Tharsis lava flows and implications for the nature of the topography of the Tharsis plateau, *Proc. 11th Lunar Planet. Sci. Geochim. Cosmochim. Acta* **12**, 2423–2436, 1980.
- Plescia, J. B. and Saunders, R. S.**, Tectonic history of the Tharsis region, Mars, *Proc. 3rd International Colloquium on Mars. J. Geophys. Res.* **87**(B12), 9775–9791, 1982.
- Pollack, J. B.**, Climatic change on the terrestrial planets. *Icarus* **37**, 479–553, 1979.
- Pollard, D. D.**, Elementary fracture mechanics applied to the structural interpretation of dykes, in *Mafic Dyke Swarms* (edited by H. C. Halls and W. F. Fahrig), Sp. Pap. 34, pp. 5–24. Proc. Int. Dyke Conf., Toronto, June 4–7, 1985. Geol. Assoc. Canada, 1987.

- Pollard, D. D., Segall, P. and Delaney, P. T.**, Formation and interpretation of dilatant echelon crack. *Geol. Soc. Am. Bull.* **93**, 1291–1303, 1982.
- Pollard, D. D., Delaney, P. T., Duffield, W. A., Endo, E. T. and Okamura, A. T.**, Surface deformation in volcanic rift zones. *Tectonophysics* **94**, 541–584, 1983.
- Price, N. J. and Cosgrove, J. W.**, *Analysis of Geological Structures*, p. 502. Cambridge University Press, Cambridge, 1990.
- Radhakrishna, T., Dallmeyer, R. D. and Joseph, M.**, Palaeomagnetism and $^{36}\text{Ar}/^{40}\text{Ar}$ vs. $^{39}\text{Ar}/^{40}\text{Ar}$ isotope correlation ages of dyke swarms in central Kerala, India: tectonic implications. *Earth Planet. Sci. Lett.* **121**, 213–226, 1994.
- Reidel, S. P., Fecht, K. R., Hagoood, M. C. and Tolan, T. L.**, The geologic evolution of the Central Columbia Plateau, in *Volcanism and Tectonism in the Columbia River Flood-Basalt Province* (edited by S. P. Reidel and P. R. Hooper), Sp. Pap. 239, pp. 247–264. Geol. Soc. Am., 1989.
- Robinson, M. S. and Tanaka, K. L.**, Magnitude of catastrophic flood event at Kasei Valles, Mars. *Geology* **18**, 902–905, 1990.
- Rubin, A. M.**, A comparison of rift-zone tectonics in Iceland and Hawaii. *Bull. Volcanol.* **52**, 302–319, 1990.
- Rubin, A. M.**, Dike-induced faulting and graben subsidence in volcanic rift zones. *J. Geophys. Res.* **97**(B2), 1839–1858, 1992.
- Rubin, A. M.**, Tensile fracture of rock at high confining pressure: implications for dike propagation. *J. Geophys. Res.* **98**(B9), 15,919–15,935, 1993.
- Rubin, A. M. and Pollard, D. D.**, Dike-induced faulting in rift zones of Iceland and Afar. *Geology* **16**, 413–417, 1988.
- Schubert, G., Solomon, S. C., Turcotte, D. L., Drake, M. J. and Sleep, N. H.**, Origin and thermal evolution of Mars, in *Mars* (edited by W. S. Kiefer et al.), pp. 147–183. University of Arizona Press, Tucson, 1992.
- Schultz, P. H.**, *Moon Morphology*, 626 pp. University of Texas Press, Austin, 1972.
- Schultz, P. H. and Glicken, H.**, Impact crater and basin control of igneous processes on Mars. *J. Geophys. Res.* **84**, 8033–8047, 1979.
- Schultz, R. A.**, Assessment of global and regional tectonic models for faulting in the ancient terrains of Mars. *J. Geophys. Res.* **90**(B9), 7849–7860, 1985.
- Schultz, R. A.**, Do pit-crater chain grow up to be Valles Marineris canyons? NASA TM 4130, pp. 539–540, 1988.
- Schultz, R. A.**, Structural development of Coprates Chasma and western Ophir Planum, Valles Marineris Rift, Mars. *J. Geophys. Res.* **96**(E5), 22,777–22,792, 1991.
- Schultz, R. A.**, Studies of faulting on the Earth and other planets. *Trends Geophys. Res.* **1**, 97–111, 1992a.
- Schultz, R. A.**, Limitations on the applicability of Byerlee's law and the Griffith criterion to shallow crustal conditions, *Lunar Planet. Sci. Conf.*, Vol. XXIII, pp. 1239–1240. Lunar and Planetary Institute, Houston, 1992b.
- Schultz, R. A.**, Brittle strength of basaltic rock masses with applications to Venus. *J. Geophys. Res.* **98**(E6), 10,883–10,895, 1993.
- Schultz, R. A.**, Gradients in extension and strain at Valles Marineris, Mars. *Planet. Space Sci.* **43**(12), 1561–1566, 1995.
- Schultz, R. A. and Senske, D. A.**, Uplift and rifting at Valles Marineris, Mars. *Eos 1994 Fall Meeting Abstracts* 413, 1994.
- Schultz, R. A. and Tanaka, K. L.**, Lithospheric-scale buckling and thrust structures on Mars: the Coprates rise and south Tharsis ridge belt. *J. Geophys. Res.* **99**(E4), 8371–8385, 1994.
- Schultz, R. A. and Watters, T. R.**, Elastic buckling of fractured basalt on the Columbia plateau, Washington State, in *Rock Mechanics* (edited by J. J. K. Daemen and R. A. Schultz), pp. 855–860. Proc. 35th U.S. Symposium, Reno, 5–7 June 1995. Balkema, Rotterdam, 1995.
- Schultz, R. A. and Zuber, M. T.**, Why are strike-slip faults that are "predicted" by lithospheric deformation models rarely observed on planetary surfaces? *Lunar Planet. Sci. Conf.*, Vol. XXIII, pp. 1247–1248. Lunar and Planetary Institute, Houston, 1992.
- Schultz, R. A. and Zuber, M. T.**, Observations, models, and mechanisms of failure of surface rocks surrounding planetary loads. *J. Geophys. Res.* **99**(E7), 14,691–14,702, 1994.
- Scott, D. H. and Dohm, J. M.**, Faults and ridges: historical development in Tempe Terra and Ulysses Patera regions of Mars, *Proc. 20th Lunar Planet. Sci. Conf.*, pp. 503–513. Lunar and Planetary Institute, Houston, 1990a.
- Scott, D. H. and Dohm, J. M.**, Chronology and global distribution of fault and ridge systems on Mars, *Proc. 20th Lunar Planet. Sci. Conf.*, pp. 487–501. Lunar and Planetary Institute, Houston, 1990b.
- Scott, D. H. and Tanaka, K. L.**, Mars: paleostratigraphic restoration of buried surfaces in Tharsis Montes. *Icarus* **45**, 304–419, 1981.
- Scott, D. H. and Tanaka, K. L.**, Geologic map of the western equatorial region of Mars (1:15 M). *U.S. Geol. Survey Misc. Invest. Series*, I-1802-A, 1986.
- Segall, P. and Pollard, D. D.**, Nucleation and growth of strike slip faults in granite. *J. Geophys. Res.* **88**(B1), 555–568, 1983.
- Sharp, R. P.**, Mars: troughed terrain. *J. Geophys. Res.* **78**, 4063–4072, 1973.
- Sheridan, M. F. and Wohletz, K. H.**, Hydrovolcanic explosions: the systematics of water-pyroclast equilibration. *Science* **212**, 1387–1389, 1981.
- Sigurdsson, O.**, Surface deformation of the Krafla fissure swarm in two rifting events. *J. Geophys. Res.* **47**, 154–159, 1980.
- Sleep, N. H.**, Martian plate tectonics. *J. Geophys. Res.* **99**(E3), 5639–5655, 1994.
- Sleep, N. H. and Phillips, R. J.**, Gravity and lithospheric stress on the terrestrial planets with reference to the Tharsis region of Mars. *J. Geophys. Res.* **90**(B6), 4469–4489, 1985.
- Smith, D. E., Lerch, F. J., Nerem, R. S., Zuber, M. T., Patel, G. B., Fricke, S. K. and Lemoine, F. G.**, An improved gravity model for Mars: Goddard Mars model 1. *J. Geophys. Res.* **98**(E11), 20,871–20,889, 1993.
- Smith, R. P.**, Dyke emplacement at Spanish Peaks, Colorado, in *Mafic Dyke Swarms* (edited by H. C. Halls and W. F. Fahrig), Sp. Pap. 34, pp. 47–5. Toronto, Proc. Int. Dyke Conf., June 4–7, 1985. Geol. Assoc. Canada, 1987.
- Squyres, S. W., Wilhelms, D. E. and Moosman, A. C.**, Large-scale volcano-ground ice interactions on Mars. *Icarus* **70**, 385–408, 1987.
- Stevenson, D. J. and Bittker, S. S.**, Why existing terrestrial planet thermal history calculations should not be believed (and what to do about it), *Lunar Planet. Sci. Conf.*, Vol. XXI, pp. 1200–1201. Lunar and Planetary Institute, Houston, 1990.
- Suppe, J. and Narr, W.**, Fault-related folding on the Earth with application to wrinkle ridges on Mars and the Moon, in *MEVTV Workshop on Tectonic Features on Mars* (edited by T. R. Watters and M. P. Golombek), LPI Technical Rept 89-06, pp. 55–56. Lunar and Planetary Institute, Houston, 1989.
- Tanaka, K. L. and Chapman, M. G.**, The relation of catastrophic flooding of Mangala Valles, Mars, to faulting of Memnonia Fossae and Tharsis volcanism, *Proc. 4th International Conference on Mars. J. Geophys. Res.* **95**(B9), 14,315–14,323, 1990.
- Tanaka, K. L. and Davis, P. A.**, Tectonic history of the Syria Planum province of Mars. *J. Geophys. Res.* **93**(B12), 14,893–14,917, 1988.
- Tanaka, K. L. and Dohm, J. M.**, Complex structure of the Thaumasia region of Mars, *Lunar Planet. Sci. Conf.*, Vol. XXIV, pp. 1399–1400. Lunar and Planetary Institute, Houston, 1993.
- Tanaka, K. L. and Golombek, M. P.**, Martian tension fractures and the formation of grabens and collapse features at Valles Marineris, *Proc. 19th Lunar Planet. Sci. Conf.*, pp. 383–396. Lunar and Planetary Institute, Houston, 1989.

- Tanaka, K. L., Golombek, M. P. and Banerdt, W. B.**, Reconciliation of stress and structural histories of the Tharsis region of Mars. *J. Geophys. Res.* **96**(E1), 15,617–15,633, 1991.
- Toksöz, M. N. and Hsui, A. T.**, Thermal history and evolution of Mars. *Icarus* **34**, 537–547, 1978.
- Turcotte, D. L. and Schubert, G.**, *Geodynamics — Applications of Continuum Physics to Geological Problems*, 450 pp. Wiley, New York, 1982.
- Turtle, E. P. and Melosh, H. J.**, Stress and flexural modeling of Alba Patera, Mars, *Lunar Planet. Sci. Conf.*, Vol. XXV, pp. 1425–1426. Lunar and Planetary Institute, Houston, 1994.
- U.S. Geological Survey**, Topographic orthophoto mosaic of the Tithonium Chasma region of Mars (1: 500 K). *U.S. Geol. Survey Misc. Invest. Series*, I-1294, 1980.
- U.S. Geological Survey**, Topographic maps of the polar, western, and eastern regions of Mars (1: 15 M). *U.S. Geol. Survey Misc. Invest. Series*, I-2160, 1991.
- Walker, G. P. L.**, Some aspects of quaternary volcanism in Iceland. *Trans. Leicester Lit. Philos. Soc.* **49**, 25–40, 1965.
- Walsh, J. J. and Watterson, J.**, Displacement gradient on fault surfaces. *J. Struct. Geol.* **11**(3), 307–316, 1989.
- Warner, M.**, Basalts, water, or shear zones in the lower continental crust? *Tectonophysics* **173**, 163–174, 1990.
- Watson, S. and McKenzie, D.**, Melt generation by plumes: a study of hawaiian volcanism. *J. Petrol.* **32**(3), 501–537, 1991.
- Watters, T. R.**, The origin of periodically spaced wrinkled ridges on the Tharsis plateau of Mars. *J. Geophys. Res.* **96**(E1), 15,599–15,616, 1991; correction. *J. Geophys. Res.* **96**(E5), 22,829–22,832, 1991.
- Watters, T. R.**, Compressional tectonism on Mars. *J. Geophys. Res.* **98**(E9), 17,049–17,060, 1993.
- Watters, T. R. and Janes, D. M.**, Coronae on Venus and Mars: implications for similar structures on Earth. *Geology* **23**(3), 200–204, 1995.
- Watters, T. R. and Maxwell, T. A.**, Crosscutting relations and relative ages of ridges and faults in the Tharsis region of Mars. *Icarus* **56**, 278–298, 1983.
- Watters, T. R. and Maxwell, T. A.**, Orientation, relative age, and extent of the Tharsis plateau ridge system. *J. Geophys. Res.* **91**, 8113–8125, 1986.
- Watters, T. R. and Schultz, R. A.**, Rock mass strength criterion applied to ridged plains on Mars: implications for elastic buckling, *Lunar Planet. Sci. Conf.*, Vol. XXVI, pp. 1471–1472. Lunar and Planetary Institute, Houston, 1995.
- White, R. and McKenzie, D.**, Magmatism at rift zones: the generation of volcanic continental margins and flood basalts. *J. Geophys. Res.* **94**(B6), 7685–7729, 1989.
- White, R. and McKenzie, D.**, Mantle plumes and flood basalts. *J. Geophys. Res.* **100**(B9), 17,543–17,585, 1995.
- Wilhelms, D. E. and Baldwin, R. J.**, The role of igneous sills in shaping the Martian uplands, *Proc. 19th Lunar Planet. Sci. Conf.*, pp. 355–365. Lunar and Planetary Institute, Houston, 1989.
- Wilson, L. and Head, J. W.**, Mars: volcanic eruption theory and relationships to observed landforms, *Lunar Planet. Sci. Conf.*, Vol. XXV, pp. 1495–1496. Lunar and Planetary Institute, Houston, 1994.
- Wilson, L. and Parfitt, E. A.**, Widths of dikes on Earth and Mars, *Lunar Planet. Sci. Conf.*, Vol. XXI, pp. 1345–1346. Lunar and Planetary Institute, Houston, 1990.
- Wise, D. U.**, Faulting and stress trajectories near Alba volcano, northern Tharsis ridge of Mars, *Proc. Int. Coll. Planet. Geol.*, Rome, Sept. 22–30, 1975. *Geol. Romana XV*, 430–43, 1976.
- Wise, D. U., Golombek, M. P. and McGill, G. E.**, Tectonic evolution of Mars. *J. Geophys. Res.* **84**(B14), 7934–7939, 1979.
- Wohletz, K. H. and Sheridan, M. F.**, Hydrovolcanic explosions, II. Evolution of basaltic tuff rings and tuff cones. *Am. J. Sci.* **283**, 385–413, 1983.
- Zimelman, J. R.**, Noachian faulting in the Memnonia region of Mars, in *MEVTV Workshop on Early Tectonic Features on Mars* (edited by H. V. Frey), LPI Technical Rept 89-04, pp. 94–96. Lunar and Planetary Institute, Houston, 1989.
- Zoback, M. L.**, First- and second-order patterns of stress in the lithosphere: the World Stress Map project. *J. Geophys. Res.* **97**(B8), 11,703–11,728, 1992.
- Zoback, M. L. and Richardson, R. M.**, Stress perturbation and intraplate seismicity associated with ancient continental rifts. *J. Geophys. Res.* 1996 (in press).
- Zoback, M. L., McKee, E. H., Blakely, R. J. and Thompson, G. A.**, The northern Nevada rift: regional tectono-magmatic relations and middle Miocene stress direction. *Geol. Soc. Am. Bull.* **106**, 371–382, 1994.
- Zuber, M. T.**, Wrinkle ridges, reverse faulting, and the depth penetration of lithospheric strain in Lunae Planum, Mars. *Icarus* **114**, 80–92, 1995.
- Zuber, M. T. and Mougins-Mark, P. J.**, Caldera subsidence and magma chamber depth of the Olympus Mons volcano, Mars. *J. Geophys. Res.* **97**(E11), 18,295–18,307, 1992.